THE EFFECTS OF SUBMERGED AQUATIC VEGETATION ON FLOW IN IRRIGATION CANALS

A Dissertation

by

LARRY RALPH DEMICH

Submitted to the Office of Graduate Studies of
Texas A&M University
in partial fulfillment of the requirements for the degree of

DOCTOR OF PHILOSOPHY

August 2008

Major Subject: Biological and Agricultural Engineering

THE EFFECTS OF SUBMERGED AQUATIC VEGETATION ON FLOW IN IRRIGATION CANALS

A Dissertation

by

LARRY RALPH DEMICH

Submitted to the Office of Graduate Studies of
Texas A&M University
in partial fulfillment of the requirements for the degree of

DOCTOR OF PHILOSOPHY

Approved by:

Chair of Committee,	Guy Fipps
Committee Members,	Michael Masser
	Patricia Smith
	Ralph Wurbs
Head of Department,	Gerald Riskowski

August 2008

Major Subject: Biological and Agricultural Engineering

ABSTRACT

The Effects of Submerged Aquatic Vegetation
on Flow in Irrigation Canals. (August 2008)
Larry Ralph Demich, B.S., Washington State University;
M.S., University of California at San Diego
Chair of Advisory Committee: Dr. Guy Fipps

Invasive aquatic species such as *Hydrilla verticillata* (hydrilla) have become a pervasive and nearly ineradicable part of the waterways of the American south. Hydrilla is an aggressive colonizer; grows rapidly and rapidly blocks flow areas, which greatly reduces the capacity of water supply canals. Hydrilla grows up through the water column and is present throughout flow zones that are typically assumed to be free flowing and without resistance, other than that transmitted via the mechanics of a Newtonian fluid. Hydrilla is highly flexible and its morphology in the flow field is dependent on many parameters, including flow, growth stage, cross-section geometry and substrate.

Traditional methods of calculating canal flow capacities assume that resistance to flow originates at the boundary of the channel. These methods typically attempt to account for vegetation by increasing resistance coefficients, which are associated with the boundary of the canal.

A combination of field studies and experimentation in three separate laboratory channels was used to characterize the behavior of hydrilla and its impacts on open-channel flow. This work developed relationships for energy losses of flow within the vegetation, as well as velocity gradients within the vegetation and through the vegetation water interface to the open water.

The information developed in this investigation was used to develop a model of the cross-section of flow with vegetation growing in the center of the channel. The model is based on the Prandtl-von Kármán universal-velocity-distribution law; and uses modifications to the method of calculating the hydraulic radius, to account for the increased frictional elements and reduced

flow areas in the canal cross-section. A simple function was developed to estimate the remaining flow capacity in a canal as a function of the remaining unblocked area.

The Prandtl-von Kármán universal-velocity-distribution law, together with modifications to the method for calculating the hydraulic radius, can improve estimates of the flow in channels impacted by submerged aquatic vegetation. The effects of a broad range of parameters can thus be represented by a relatively simple function, which was developed in this project.

ACKNOWLEDGEMENTS

I would like to take this opportunity to thank the following people without whom this would not have happened. First and foremost I would like to thank Monica, my wife. Without her long-enduring patience and support this effort would have ended long ago.

My sincere thanks to my advisor and committee chair, Professor Guy Fipps, for his willingness to take a chance on a somewhat unusual graduate student and for all his support and guidance.

Immense thanks to Azimjon and Askarali, for work above and beyond the call and immense support and unflinching assistance in the south Texas summer sun. It really wouldn't have happened without you two. My thanks to Nasiba and Guly as well, both for their wonderful hospitality and for their patience when I descended on the Valley and usurped their husbands for weeks at a time. Thanks Eric for your assistance and ideas as well.

I would like to thank the staff and administration at the Texas A&M Agricultural Research and Extension Center in Weslaco, Texas for providing space for my experimental channels, as well as assistance with construction and demolition. I am grateful as well to the Rio Grande Basin Initiative for their support of my work.

Finally I would like to thank Milton Henry and the National Irrigation Commission of Jamaica for providing both access to their canal systems and transport and assistance with data collection, not the least of which was the construction of a bridge from which to collect the data.

NOMENCLATURE

A	Cross-sectional area of flow
f	Darcy-Weisbach resistance coefficient
C	Chézy discharge coefficient
F	Froude number (ratio of inertial forces to gravitational forces in a flow field)
g	Acceleration due to gravity
h	Depth of water in a channel cross-section
h_{veg}	Height of vegetation in a channel cross-section
k	Nikuradse sand roughness coefficient
κ	von Kármán coefficient, commonly assumed to equal 0.40
μ	Dynamic viscosity (N s/m^2)
n	Manning's resistance coefficient
v	Kinematic viscosity (m^2/s)
P	Wetted perimeter of flow
R	Hydraulic radius (A/P)
Re	Reynolds number (ratio of inertial forces to viscous forces in a flow field)
S	Slope
T	Width of channel at the water surface
τ	Shear friction (N/m^2)
U	Flow velocity averaged over the flow cross-section in a channel
u	Point flow velocity at some known point in the flow field
u_i	Velocity vector in the i direction at some known point in the flow field
u_*	Friction or shear velocity
y	Typically treated as the perpendicular distance from a point in the flow field to the nearest static surface

TABLE OF CONTENTS

LIST OF FIGURES

FIGURE Page

FIGURE Page

FIGURE Page

LIST OF TABLES

CHAPTER I

INTRODUCTION

This work extends existing hydraulic engineering methods to the calculation of flow in channels impacted by submerged aquatic vegetation (SAV). The primary SAV of interest for this study is *Hydrilla verticillata* (hydrilla) an invasive species that is having significant impacts on waterways in the American south. The plant is an aggressive propagator and can quickly colonize and clog surface water bodies such as ponds, lakes and channels (both natural and manmade). This work focuses on the interaction of hydrilla with flow in man-made water supply canals.

PROBLEM STATEMENT

- Invasive weeds such as *Hydrilla verticillata* are an effectively ineradicable part of the canal systems of the southern United States.
- Maintenance methods of dealing with this weed are expensive and frequently perpetuate the problem; mechanical removal for example sends fragments downstream, which can then take root and create new plants.
- Without maintenance, plants grow to choke the waterways and greatly reduce the capacity of canals.
- Effective management of flow in infested irrigation canals requires knowledge of the canals' capacity when they are impacted by the weeds.
- Cost effective management of removal efforts—when to remove the weed for maximum cost effectiveness—requires knowledge of levels of impact to canal capacity, based on the level of infestation.
- Existing knowledge on the interaction of aquatic weeds (such as hydrilla) with the flow in canals and the consequences of this interaction to flow characteristics is limited.

This dissertation follows the style of the *Journal of Irrigation and Drainage Engineering.*

PURPOSE

The purpose of this project is to collect empirical data on the interaction of hydrilla with flowing water; and with that data develop methods to predict the effects of hydrilla (and similar vegetation types) on hydraulic processes in water supply canals. Ultimately my goal is to improve the accuracy of flow estimates in vegetated canals, and to develop tools which will assist with the management of this problem.

PROJECT ORGANIZATION

This Chapter introduces the overall project, which included four phases: field observations, laboratory flow experiments, field experiments and analysis.

Field Observations

The field observations included investigation of different types of aquatic vegetation, as well as some flow measurements in existing canals. This work was carried out primarily in canals operated by irrigation districts in the Lower Rio Grande Valley of south Texas. Additional investigation was carried out in irrigation canals operated by the National Irrigation Commission in Jamaica.

However the lack of experimental control over flow conditions in the canals, combined with the variable nature of aquatic vegetation, interfered with the collection of systematic datasets. Nevertheless I was able to develop a working knowledge of both the morphology of vegetation growth in canals, and the types of flow interaction one might expect to see.

Laboratory Flow Experiments

I constructed laboratory flow facilities to aid with the experimental work, specifically the measurement of flow related friction/energy loss in the vegetation and the measurement of flow velocities and distributions around and in the vegetation. Two laboratory channels were designed and constructed for this purpose. The first is a bench channel that is 22 cm wide with an effective test length of approximately 100 cm. Most tests in this channel were run with an

effective flow depth of between 10 and 20 cm. The bench channel was constructed of clear acrylic and was designed to allow visual data collection (video and photographic) from the sides.

Vegetation was cultivated directly in this channel; and flow measurements were made under a range of flow depths and discharges. The vegetative conditions were also varied in terms of density and length of the vegetative mass. The bench channel was used successfully to measure headloss (water surface slope) in very dense vegetation. However the short length of the experimental facilities limited resolution of the water surface slope. This (bench) channel was also used to measure velocity distributions in and above the vegetation.

The second laboratory channel was constructed in Greenhouse 1 at the Texas A&M Agricultural Research and Extension Center in Weslaco, Texas. This channel was approximately 600 cm long and was used to measure energy loss resulting from flow through the vegetative mass. The channel was constructed of plywood and lumber, with a rubber sheet lining (canal/pond liner). A recirculating pump system moves the water from the downstream end of the channel to the upstream. The channel width was approximately 33 cm; and during the experimental process the flow depth was varied between approximately 10 and 50 cm.

The greenhouse channel was originally constructed to provide a controlled environment for growing the hydrilla, a process that was unexpectedly challenging given the reputation of this vegetation. However, as the channel was made just wide enough to accept the trays of growing vegetation, it also made an ideal platform for testing flow through the vegetation. By using this channel to confine flow to the vegetation, we were able to measure headloss as a function of both flow velocity and vegetation density.

Field Experiments

A third channel, also known as the field channel, was constructed at the Extension Center. The field channel was dug into the ground and lined with rubber canal lining material. It was designed to simulate a short length of irrigation canal. The channel consisted of a test section approximately 160 cm wide, 800 cm long and 60 cm deep. A sump downstream of the test section and a stilling basin upstream of the test section were separated from the test section by two concrete control structures. The structures were equipped with stop log dams, which were

used to control the water surface elevation. A pump system was used to move water from the sump up to the stilling basin; from there the water flowed through the test section and back to the sump.

The field channel was significantly wider than the trays in which the vegetation was grown; this channel was designed to measure flow parameters during bypassing conditions. I expected the majority of the flow to bypass the vegetation in this channel. My goal was to measure relative flow in the vegetation and in the channel and to measure velocity distributions between the two flow conditions.

Analysis

The main hypothesis of this work is that submerged aquatic vegetation that reaches up through the water column constitutes both an increase in the wetted perimeter and a decrease in cross-sectional area, and that these changes cannot be effectively accounted for by varying the friction factor in the standard engineering formulations for flow.

I propose a modification to the methodology which incorporates both the area and perimeter of the vegetation into the formula for calculating the hydraulic radius of a canal. The proposed modification is based on the hypothesis that flow in vegetation is significantly slower than that in the open water column and can be effectively ignored. This allows me to assume that (for flexible submerged aquatic vegetation) the perimeter of the submerged vegetative mass is the edge of flow and a no-slip boundary condition can be applied at this perimeter.

The experimental work was designed to test these premises. The greenhouse channel was used to develop data on the resistance to flow within the vegetative mass. The bench channel and the field channel were both designed to measure flow around vegetation for a range of flow conditions. Flow profiles were collected perpendicular to, and on both sides of the vegetation/water boundary.

An additional investigative focus was the response of the vegetation to flow. Some types of submerged aquatic vegetation (SAV) are particularly responsive to flow conditions and will lean over—and move aside—as a result of which they present a reduced obstacle to flow. I used simple bending tests under measured loads to develop the range of response for hydrilla. This

was designed to estimate the response of the vegetation to drag forces, and thus the response of the vegetation to flow.

The analytical section of this work included the development of a methodology for estimating the flow in a vegetated channel. This methodology used the momentum principle, combined with the Prandtl-von Kármán universal-velocity-distribution law and the assumption of steady state conditions, to estimate flow distribution in a channel with a bank[1] of vegetation growing down the centerline of the channel. This ultimately led to a simple function which related the percent reduction in discharge capacity to the percent blockage of the channel.

[1] In this document a bank of vegetation refers to a condition wherein many individual plants are growing closely together and acting as a continuous mass under the influence of flow.

CHAPTER II

EVALUATING FLOW INTERACTIONS WITH AQUATIC VEGETATION

Traditionally, methods for calculating flow in vegetated open channels treated the vegetation as a roughness element on the perimeter of the channel. This is potentially reasonable for a limited set of circumstances, for example where the vegetation is short relative to the water depth or where the vegetation can with confidence be expected to lie over under flow conditions. It may also be reasonable where the vegetation is limited to the banks of the stream. In each of these examples the effects of the vegetation occur in a region closely associated with the boundary of flow, or the wetted perimeter.

However in the situation this project focuses on, aquatic vegetation (hydrilla) grows upward from the channel bottom through the water column to the surface. The vegetation is therefore present in the upper central part of the cross-section of a channel. This is a flow region that is assumed to be both free flowing and the area of maximum velocity (Chow 1959).

Flow velocity at a point in the cross-section of an open channel can also be calculated as a function of the normal distance from the point to the nearest static surface (Chow 1959). As hydrilla is rooted, it does not move downstream with the flow. The velocity of the plant's surface in the stream is therefore zero, discounting any lateral waving of the plant stems. And applying the no-slip condition intrinsic to a Newtonian fluid (Batchelor 1967), the flow velocity at the surface of the plant's stem and leaves must be equal to zero.

The presence of a zero flow condition in the region of the cross-section that has heretofore been assumed to represent the maximum velocity—precisely due to its relative distance from any static surface—can be presumed to have significant effects on the flow field. It is reasonable to conclude therefore, that using a methodology which assumes all drag effects are generated at or by the channel boundary will be problematic in terms of its accurate prediction of flow. This discussion argues against treating this type of vegetation as merely a boundary effect or a friction factor.

The term friction factor is potentially ambiguous and its usage in this document should be clarified. Yen (2002) defines two terms which we will use in lieu of friction factor; they are the roughness factor and the resistance coefficient. He defines the roughness factor to be a geometric measurement of the unevenness of a surface subjected to flow. And he defines the resistance coefficient to be, "*...a measure reflecting the dynamic behavior in terms of momentum or energy, of the boundary in resisting the flow of the fluid*" (Yen 2002). In short a roughness factor represents an actual roughness scale or relief on the channel boundary. The resistance coefficient is a more general parameter; which is used to reflect flow behavior in terms of the boundary conditions.

By this definition the Darcy-Weisbach f, Manning n and Chézy C are all resistance coefficients. The Nikuradse sand roughness k and the roughness value e used in the Moody diagram are roughness factors. However both the resistance coefficients and the roughness factors are defined in terms of the effect that the channel boundary has on the flow (Yen 2002).

The preceding parameters are used to generate estimates for flow resistance in the governing equations of flow. These equations include the following. One is the conservation of mass or the mass balance equation. The next two are the momentum balance equation or the law of conservation of momentum, and the energy conservation equation. A fourth equation that will be used in this work is the Prandtl-von Kármán universal-velocity-distribution law.

Yen's definition of the resistance coefficient includes its applicability to either the energy or momentum equations. Although the energy equation is more commonly used in hydraulic engineering (Yen 2002), my work utilizes the momentum principle, due to the potential for incorporating the vegetation into a modified definition of the channel boundary.

The momentum balance equation is an application of Newton's Second Law (Eq.2.1):

$$F = ma \tag{2.1}$$

where F is the resultant force on an object (or unit of fluid) m is the mass of the object, and a is the acceleration of the object. The right hand term of Eq.2.1 can be read as the rate of change of

velocity of a mass, or the rate of change of momentum, thus the resultant force on the mass equals the rate of change in momentum.

In open channel flow, the resultant force is the sum of two vectors, that of gravity acting on the fluid mass and that of the resisting force created by the channel boundary. In a steady state flow condition, these two forces are balanced, and the change in momentum is zero.

The momentum balance equation can be formulated for individual parcels of fluid, where the resultant force on each parcel is the integral of forces over the surface of the parcel, combined with the gravitational force (weight of the parcel of water). The equation can also be formulated over the cross-section of the channel, with the activating force being the weight of the water in a unit length of the cross-section (times the slope of the channel) and the resisting force being the shear friction on the boundary of the channel, integrated over the boundary of the channel. (Chow 1959 and Yen 2002) The latter formulation will be the primary tool used in this work and is shown as a tensor function in Equations 2.2 and 2.3.

$$S = \frac{-1}{\gamma A}\int_{\sigma}[\tau_{ij}]N_j d\sigma \qquad \text{(Yen 2002)} \qquad (2.2)$$

where S is the slope of the channel (for steady state flow) γ is the unit weight of water, N_j is the unit normal to the channel boundary σ, A is the cross-sectional area of the channel, and τ_{ij} is the shear friction on the boundary of the channel.

$$\tau_{ij} = \mu\left(\frac{\partial u_i}{\partial x_j} + \frac{\partial u_j}{\partial x_i}\right) - \rho\overline{u_i' u_j'} \qquad \text{(Yen 2002)} \qquad (2.3)$$

where μ is the dynamic viscosity, u'_i is the fluctuation in u_i caused by turbulence and ρ is the mass density.

Integrating Eq.2.2 over the channel boundary for a unit length (n_i) of channel and rearranging the terms yields Eq.2.4:

$$F_T = S\gamma A n_i \qquad (2.4)$$

where F_T is the tractive force of the water on a unit length of channel and is equal to:

$$F_T = \int_{\sigma} [\tau_{ij}] N_j d\sigma \tag{2.5}$$

Dividing both sides of Eq.2.4 by the wetted perimeter (P) and the unit length n_i provides a formula for the average tractive or shear stress on a channel boundary (Eq.2.6a).

$$\tau_o = S\gamma \frac{A}{P} \tag{2.6a}$$

Making this substitution and rearranging the terms in Eq.2.6a results in the more familiar form of Eq.2.6b.

$$\frac{\tau_0}{\rho} = gRS \tag{2.6b}$$

The above equation provides the shearing stress at the perimeter of a channel, and essentially constitutes a boundary condition for the analysis. However for the purposes of this project I will require a way to relate the velocity throughout the cross-section, as a function of the boundary. Prandtl (1926)[2] provided a relation for the shear stress in turbulent flow over a solid surface:

$$\tau = \rho \cdot l^2 \left(\frac{du}{dy} \right)^2 \tag{2.7}$$

where ρ is the mass density of water and l is a characteristic length or mixing length. Prandtl assumed that near the flow boundary, the mixing length l is proportional to y the perpendicular distance to the channel boundary and is given by Eq.2.8:

$$l = \kappa y \tag{2.8}$$

where κ is a constant of proportionality known as the von Kármán constant and is experimentally determined to be approximately 0.40 (Bakhmeteff 1936 and Chow 1959). Prandtl also assumed that near the boundary the shear stress is constant, which results in $\tau = \tau_o$. Substituting Eq.2.8 into Eq.2.7 and solving for du gives:

[2] All references to Prandtl and Bakhmeteff in this work were obtained from Chow (1959).

$$du = \sqrt{\frac{\tau_o}{\rho}} \frac{1}{\kappa} \frac{dy}{y} \tag{2.9}$$

Substituting Eq.2.6b into the first factor on the right side of Eq.2.9, Eq.2.10 provides the definition of the shear or friction velocity u_* (Chow 1959).

$$u_* = \sqrt{\frac{\tau_o}{\rho}} = \sqrt{gRS} \tag{2.10}$$

Substituting Eq.2.10 into Eq.2.9 and integrating provides:

$$u = \frac{u_*}{\kappa} \ln\left(\frac{y}{y_o}\right) \tag{2.11}$$

where y_o is a constant of integration, sometimes considered a roughness factor. Eq.2.11 is known as the Prandtl-von Kármán universal-velocity-distribution law.

EMPIRICAL APPROACH TO ESTIMATING FLOW IN CHANNELS

The following material examines the basic (empirical) engineering methods for evaluating flow in channels, as well as the literature which develops modifications to them. The historical development and basic assumptions for the engineering calculation of flow in open channels is reviewed. This is followed by a discussion of flow parameters as they relate to flow in mixed conditions (flow in vegetation and in open water) and of the flow structure in the interface between vegetation and open water.

One of the earliest known methods for estimating flow in open channels was formulated by an 18th century French engineer, Antoine Chézy. In 1768 Chézy was tasked with designing a canal to deliver water to the city of Paris (Rouse and Ince 1963). As part of this work, he was required to both design the cross-section of the canal, and to calculate the flow that the canal would be able to deliver.

Lacking an available methodology, he reasoned that for steady flow in a channel of uniform slope, the velocity of the flow—and thus the discharge—would be proportional to *"...the slope*

of the channel and to gravity, of which the effect is restrained by the resistance of friction against the channel boundaries" (Mouret 1921[3] and Rouse and Ince 1963).

Chézy reasoned that for steady flow the resistance of friction must be equal and opposed to the effects of gravity. He also argued that the resistance to flow would be directly proportional to the square of the flow velocity, *"...because of the number and force of the particules colliding in a given time"* (Mouret 1921). Lastly he reasoned that the resistance to flow would be inversely proportional to the ratio of the area of flow divided by the wetted perimeter.

Chézy formulated a method to estimate the velocity in an unknown or proposed channel section. This method compared conditions in an unknown stream, to conditions in another stream or channel which was similar in nature, and wherein both the flow and stream parameters were known. This formulation is shown in Eq.2.12:

$$U = U_{known}\sqrt{\frac{ASP_{known}}{A_{known}S_{known}P}} \qquad \text{(Rouse and Ince 1963)} \qquad (2.12)$$

where U is the estimated average velocity for the channel being evaluated, A is the cross-sectional area, S is the channel slope and P is the wetted perimeter. The remaining parameters (U_{known}, etc.) represent the same parameters, but for the known section of channel with measured velocity and parameters.

It is worth noting that despite the importance of the friction and the wetted perimeter, Chézy incorporated no specific parameter addressing the friction on (or of) the boundary. Instead, the boundary effects are implicitly accounted for with the requirement that the channels be similar. The reasons for this type of comparative derivation are obvious, given the amount of subsequent work that has gone into developing friction factors. However the potential uncertainties and risks associated with the selection of a 'similar' channel should be equally obvious.

Chézy's original formulation was replaced with the one in use today:

[3] The Mouret references in this document are material that was originally excerpted (by Mr. Mouret) from a manuscript by Mr. Chézy and then quoted in the second reference (Rouse and Ince 1963). The Rouse and Ince reference is the source used in this document.

$$U = C\sqrt{RS} \qquad \text{(Chow 1964)} \qquad (2.13)$$

where C is the *Chézy discharge coefficient* and R and S are the hydraulic radius and channel slope respectively. Substituting Eq.2.13 into Eq.2.12 and solving for C we obtain:

$$C = U_{known}\sqrt{\frac{1}{R_{known}S_{known}}} \qquad (2.14)$$

Equation 2.14 is simply an explicit statement of Chézy's original intent, which was that the necessary information could be developed from conditions in a known stream or channel—*similar* to the channel under investigation—and used to calculate the coefficient C. C is then used to estimate flow conditions in the channel under investigation. Mr. Chézy also cautioned that selecting the similar channel required considerable attention to detail. (Rouse and Ince 1963)

However identifying a similar stream or channel is a cumbersome process at best; and much subsequent effort has gone into developing more versatile methods to calculate C. These methods range from equations that make no explicit assumptions about channel roughness, but are based on a given flow state and assumed velocity distributions, to equations that explicitly incorporate resistance coefficients.

Two equations for C that do not explicitly include roughness information are:

$$\frac{C}{\sqrt{g}} = \sqrt{\frac{\mathrm{Re}}{8}} \text{ ; and} \qquad \text{(Chow 1964)} \qquad (2.15)$$

$$\frac{(u-U)C}{U\sqrt{8g}} = 2\log\frac{y}{y_o} + 0.88 \qquad \text{(Chow 1964)} \qquad (2.16)$$

where u is the point velocity at some distance y from the fixed flow boundary and y_0 is defined variously as a roughness height or a constant of integration. Eq.2.15 represents laminar flow, and assumes a parabolic velocity distribution. Eq.2.16 can be used for turbulent flow, given an

assumed logarithmic velocity distribution. Eq.2.16 is not considered valid at the boundaries (channel bottom or water surface).

Two equations that do relate C to channel roughness are:

$$C = \sqrt{\frac{8g}{f}}\text{; and} \qquad \text{(Chow 1964)} \qquad (2.17)$$

$$C = \frac{R^{1/6}}{n} \qquad \text{(Chow 1964)} \qquad (2.18)$$

where g is the acceleration due to gravity; and f and n are the Darcy-Weisbach and Manning resistance coefficients respectively.

The coefficient f is considered to be a dimensionless parameter (ASCE 1963). The coefficient n is also considered to be dimensionless inasmuch as its use is generally unchanged, whether the calculations are in metric or English units. There has been some discussion as to the validity of this assumption (Chow 1959) however in practice n is treated as being non-dimensional.

The Manning n is also frequently treated in practice as a constant, unaffected by the shape of the channel or the flow conditions. This is not explicitly true except in a restricted range of conditions. If we examine the commonly used form of Manning's equation:

$$U = \frac{1}{n} R^{2/3} S^{1/2} \qquad (2.19)$$

it becomes clear by inspection that Eq.2.18 is generated by replacing the value of U in Eq.2.13 with the right half of Eq.2.19 and solving for C. In addition if we combine Eq.2.17 and Eq.2.18, substituting for C and solving for n, the resulting equation (Eq.2.20) relates Manning's n to the Darcy-Weisbach f.

$$n = R^{1/6}\sqrt{\frac{f}{8g}} \qquad \text{(ASCE 1963)} \qquad (2.20)$$

Eq.2.20 defines n to be a direct function of both f and the hydraulic radius. For both large relative roughness and for large Reynolds number (Re), f is considered constant, for a given relative roughness. As the relative roughness (e/D) varies however n(f) varies also.

Most of the canals we examined in our field work would fall in the fully rough flow regime, when operated under channel control[4]. Thus f and n should be considered a function of the relative roughness for this work. However the relative roughness (e/D) is a function of D, which is equivalent to four times the hydraulic radius R (ASCE 1963). This reiterates that f and thus n will typically vary with the depth of the flow.

The above methodologies for estimating flow (Darcy-Weisbach, Manning and Chézy) are empirical, and as such there is no particular reason to assume that they would be functionally equable. Thus equating one to the other and drawing conclusions based on these solutions potentially provides more insight into their differences than to any intrinsic accuracy that one or the other may have. However, whenever feasible I will use the Darcy-Weisbach f to estimate flow conditions, which is in keeping with the conclusion that f has broader applicability (ASCE 1963). When evaluation of a particular analysis requires use of the Manning's equation, Eq.2.20 will be used to develop the value for Manning's n.

Another issue with the general use of Eq.2.13 is the so-called shape factor or shape function (Strupczewski and Szymkiewicz 1996 and Chow 1959). Neither the Manning equation, nor the Darcy-Weisbach formula contain explicit information about the shape of the channel cross-section—beyond the basic ratio of area to wetted perimeter. One could argue that the Chézy coefficient, with its original requirement of channel similarity, did include some requirement of similar shape. However in its current applications; i.e. using Eqs. 2.15 through 2.18, any original intent to incorporate the shape of the channel has been lost.

It has been argued that in fact the shape of the channel is important to the estimation of flow efficiencies. Although standard practice for calculating flow in channels ignores channel shape

[4] When operating under channel control, the channel slope, resistance factor, cross-sectional parameters and discharge control the average flow velocity and the water depth. Under structural control, typically a downstream structure may be controlling the water surface elevation. Structure control does not typically result in uniform flow, whereas channel control frequently does.

in favor of using the hydraulic radius only, the literature contains numerous references and analyses indicating that channel shape is a factor.

Chow (1959) noted that unusual channel sections—such as river cross-sections with both main channel flow and overbank flow—should not be handled as a single channel calculation. He suggests such channels be handled as compound sections and divided into individual channels with separate flow calculations. In this case the interface between the two channels—essentially a vertical line through the water column—would not be included in the summation of the wetted perimeter.

Later in his book Chow (1959) also develops the theoretical concept of a constant which represents the shape of the channel. Eq.2.13 presents the formula for the mean velocity of uniform flow:

$$U = u_* \left(A_0 + 5.75 \log\left(\frac{mR}{y_0} \right) \right) \qquad \text{(Chow 1959)} \qquad (2.21)$$

where A_0 represents the effect of the shape of the channel; U is the average section flow velocity; u_* is the friction or shear velocity, m is dependent on the roughness of the boundary, and y_0 is a constant of integration resulting from the development of the Prandtl-von Kármán universal-velocity-distribution law (Eq.2.11).

Chow (1959) developed Eq.2.21 by integrating Eq.2.11. And although he describes A_0 as a constant, in the example provided in his text[5] this factor retains a functional dependence on the water depth, the hydraulic radius and the cross-sectional area (Eq.2.22). So it is more of a shape function than a constant or shape factor.

$$A_0 = \frac{1}{\kappa} \ln\left[\frac{h}{mR} \exp\left(-1 - \frac{\gamma_{\text{sec}} h^2}{4A} \right) \right] \qquad (2.22)$$

[5] The example is based on a channel with circular cross-section and the value of A_0 presented in Chow's text is specific to that configuration. Eq.2.21 is derived from the Prandtl-von Karman universal velocity distribution law.

where h is the water depth in the section and γ_{sec} is an unspecified shape function representing the shape of the channel cross-section.

Strupczewski and Szymkiewicz (1996) evaluated two channel sections with equal R but different shapes. They mathematically integrated flow in both a wide rectangular channel and a semi-circular channel flowing full, assuming turbulent flow and a version of the universal velocity distribution law that raises the ratio (y/y_0) to a power rather than calculating its logarithm (Eq.2.23).

$$u = u_* a \left(\frac{y}{y_0} \right)^p \tag{2.23}$$

Strupczewski and Szymkiewicz (1996) define a as a resistance factor (resistance coefficient) and use it in the form of Eq.2.24(a and b):

$$U = a\sqrt{RS} \qquad \text{Chézy} \tag{2.24a}$$

$$U = aR^{2/3}S^{1/2} \qquad \text{Manning} \tag{2.24b}$$

where it would take the place of $1/n$ for the Manning equation or C for the Chézy equation. The exponent p in this method takes the value of 0 for Chézy and 1/6 for Manning. Ignoring the value $p = 0$ for Chézy[6] we examined Eq.2.23 using the Manning formulation. If instead of using $a = 1/n$, we substituted in an additional adjustment factor F_{adj} such that:

$$a = \frac{F_{adj}}{n} \tag{2.25}$$

Then Eq.2.23 can be setup to simulate Eq.2.11. Assuming a rough surface and turbulent flow, y_0 can be replaced with mk, where m takes the value of 1/30 and k is the Nikuradse sand roughness (Chow 1959). We compared results for Eq.2.11 and Eq.2.23 for k values of 0.003, 0.006 and 0.012 (meters) and flow depths up to 2.5 meters, given a wide channel and a channel slope of

[6] The value of $p = 0$ in Eq.2.16 would result in a constant point velocity throughout the water column.

0.0001. Values for F_{red} which provided the best match between the two equations varied according to the value of k and are shown in Table 2.1.

Table 2.1. Adjustment factors used with power law distribution to calibrate results to P-v K law

k	F_{adj}
0.003	0.075
0.006	0.085
0.012	0.096

Strupczewski and Szymkiewicz (1996) integrated Eq.2.23 over two cases, a wide rectangular channel and a semi-circular channel flowing full. The results are shown in Eq.2.26a and Eq.2.26b:

$$U = \frac{aR^p}{(p+1)y_0{}^p}\sqrt{gRS} \tag{2.26a}$$

for the wide rectangular channel; and

$$U = \frac{2^{(p+1)}aR^p}{(p+2)y_0{}^p}\sqrt{gRS} \tag{2.26b}$$

for the semi-circular channel.

Eq.2.26b can be reduced to Eq.2.26a with the additional factor of A_o:

$$U = A_o\frac{aR^p}{(p+1)y_0{}^p}\sqrt{gRS} \tag{2.26c}$$

where A_o represents a shape factor differentiating the two formulations and takes the form:

$$A_o = 2^{(p+1)}\frac{(p+1)}{(p+2)} \tag{2.27}$$

Substituting $p = 1/6$ into Eq.2.19, results in a shape factor of 1.2 indicating a theoretical difference in average velocity of 20%, between a wide rectangular channel and a semi-circular channel, each with the same hydraulic radius and slope.

It is reasonable therefore, based on the evidence presented, to assume that the shape of the channel cross-section can have significant bearing on the estimated velocity in a channel and therefore the capacity of the channel. However, the methodology presented for integrating the velocity distribution to develop shape factors also potentially presents a powerful tool for evaluating the impacts of vegetation masses in a channel.

EVALUATION OF VEGETATED FLOW

Evaluation of the friction effects of vegetation on flow is complicated by the fact that aquatic vegetation takes many forms; and each form may have a radically different impact on flow. In addition there is a range of potential hydraulic regimes that can require evaluation of these flows to consider multi-dimensional and multi-directional analyses. With the advent and ready availability of high speed computers, it has become feasible to model flow in three dimensions and there are a number of models available (Shepsis 2008). However the known 3-D models have not been tested with the scales in mind of modeling flow around vegetation in a large channel. The investigation of scale effects and boundary conditions input for these type of models are a special topic for investigation that is not in the scope of my dissertation.

However even if such a model were developed, a significant limitation that will remain for the foreseeable future is that, in order to accurately construct a 3-D flow model, one must construct an accurate three-dimensional representation of the boundaries of flow. Collecting this type of data for large water bodies or for long and complex canal systems requires considerable resources. And the sedimentation common to many systems would require periodic updating of the three-dimensional channel boundary model. In addition for such a model to be usable, the response of the vegetation to flow would need to be incorporated into the model. So it is unlikely that such a model would see widespread use in practice.

The development of canal network models for canal systems is greatly simplified by the use of one dimensional (1-D) modeling. In addition to this advantage, the general form of canals—that

is a regular simple cross-section that does not vary significantly over a large percentage of the canal's operating length—lends itself admirably to the use of the 1-D equations of flow.

Flow in canals would normally therefore be treated as one-dimensional, if no vegetation were growing in them. Of course the addition of vegetation in the cross-section introduces multi-dimensional aspects, as flow lines part and move around and over the vegetation. Nonetheless the goal of this work is to develop a one-dimensional approach that accounts for the vegetation.

Equations of Flow

There are three basic equations, which are intrinsic to the development of the equations of flow. They are the Continuity Equation, the Momentum Equation and the Energy Equation. Their historical development and application is briefly summarized below.

Continuity Equation

According to Rouse and Ince (1963) the continuity equation was first formalized by Leonardo Da Vinci (1452-1519). Da Vinci noted that, "*A river in each part of its length in an equal time gives passage to an equal quantity of water, whatever the width, the depth, the slope, the roughness, the tortuosity.*" He also noted that for a given discharge at two sections, the ratio of velocity at the two sections was equal to the inverse of the ratio of cross-sectional areas at the sections. The concept seems both obvious and simple in retrospect. However it is one of the basic mathematical elements of most models. The mathematical formulation of the continuity equation provides the basis for the law of conservation of mass.

Momentum Equation

The momentum equation is also known as the Principle of Conservation of Momentum. The principal of conservation of momentum was recognized by René Descartes, a 17th Century French mathematician and philosopher who provided the first known written version in 1629 in a letter to one of his fellows "*I assume that the movement which is once impressed upon a given body is permanently retained, if it is not removed by some other cause; that is, whatever has commenced to move in a vacuum will continue to move indefinitely at the same velocity.*" (Rouse and Ince 1963)

This principle was later formalized by Isaac Newton in the first of his three laws of motion. "*A body in motion tends to stay in motion.*" Newton's second law is more pertinent however. That is, "*The rate of change of momentum for a unit of mass is directly proportional to the net force acting on that unit and inversely proportional to the mass of the unit*."

Energy Equation

Gottfried Wilhelm von Leibniz was credited with first describing what he called "live force" or kinetic energy (Rouse and Ince 1963) although both he and the Dutch philosopher Christian Huygens described the relationship between the energy resulting from a distance of fall of an object and the energy required to return it to its original elevation. Rouse and Ince (1963) describe this as the first explanation of the concept of conservation of energy.

Daniel Bernoulli however is generally credited with developing the theorem or principle that bears his name. This principle equates the "live energy" of an element of fluid to the sum of a function of the velocity (squared) of that element, the pressure in the fluid on the element and the elevation of that element above some datum.

Comparison of Momentum and Energy Approaches

Yen (2002) describes the difference between the momentum approach and the energy approach in evaluating open channel flow. For steady state flows, the momentum resistance slope S_{mi} is the integral of the shear friction over the boundary of the channel section, divided by the weight of the water in the section. This formula provides a basis for applying the conservation of momentum to steady state flows (Eq.2.2).

The energy slope S_e is the, "*gradient of the dissipated mean motion energy*" (Yen 2002). Thus *Smi* provides the losses from the drag on the perimeter of the flow body and S_e represents losses as a function of velocity variations and turbulence within the flow structure.

The momentum equation relates the change of momentum of the fluid (either in a cross-section or water particle) to the sum of the forces on its boundary. The energy equation tracks energy in flow via three elements, the velocity, pressure and elevation. As energy is lost from this system it is assumed that it is converted into heat energy and turbulence. The key difference between

these two for our purposes is that all changes in momentum are assumed to originate on the boundary of flow. Changes in energy can occur throughout the water column, via a number of mechanisms.

In the case of hydrilla and other similar aquatic vegetation, significant losses are occurring in the water column, which would normally require the use of the energy equation. However as mentioned previously, I propose modifications to the basic cross-section parameters; i.e. area and wetted perimeter which will account for the effects in the upper water column and allow the use of the momentum equation.

Compound Channels and Composite Roughness for Use with One-Dimensional Flow Calculations

Composite channels are defined as channels wherein the wall roughness changes from one length of the wetted perimeter to another (Yen 2002). A common example would be a lined channel that has experienced significant sedimentation. The roughness of the side walls of the channel would be dependent upon the nature of the lining material. However the roughness of the channel bottom would be a function of the type and morphology of the sediments. If vegetation has grown in the bottom sediments, this would further differentiate roughness in the areas where the vegetation occurs.

Compound channels are channels that have several different characteristic shapes combined. The classic example is a river with floodplain attached. When flooding occurs, the floodplains are part of the flow channel, however they constitute wide relatively shallow channel section(s), whereas the main channel will generally be deeper and may not be as wide. Flow velocities in the main channel are generally significantly higher than in the floodplain channels.

Yen (2002) lists a range of methods for calculating the composite or compound resistance factor, using Manning's *n* as a basis for calculation. Generally the methods provide equations for weighting the contribution of each section of wetted perimeter and its particular resistance coefficient or roughness factor. Some of the schemes are weighted by the length of the particular section of wetted perimeter. Others are weighted by the contributory area.

To define contributory areas for a geometric channel shape, one method is to draw bisectors at each change in perimeter roughness (Yen 2002). Thus in a trapezoidal channel with a mud bottom and lined sides, a line would be drawn from the juncture of the bottom and a side slope. The line would bisect the angle formed by these two elements. The cross-sectional channel area between the bisecting angle and the side slope would be assigned to the side slope for purposes of weighting the contribution of that side slope, and so on. If two bisecting lines meet under water, a vertical line is drawn to the surface.

Vegetative Interaction with Flowing Water

The hydraulic aspects of flow around vegetation are complicated by the organic and irregular aspects of the vegetation. These aspects represent an array of potential flow parameters to the hydraulic engineer. One dimension of this array is provided by the variety of vegetation types. The other dimension is provided by the range of hydraulic regimes to be evaluated. While this project focused on one type of vegetation and flow regime (hydrilla in manmade water-supply canals) methods developed during the study of other types of aquatic vegetation provided insight for our task. Therefore some review of these other vegetation types and pertinent flow studies is included herein.

Classes of Vegetation Interaction with Flow

Aquatic vegetation takes many forms, and at different times in the growth cycle a given type of vegetation may take different forms. For the purposes of this discussion, I have divided aquatic vegetation into three classes: submerged, floating and emergent. This classification system is based on a given plant's interaction with flow, rather than on a biological basis.

Submerged aquatic vegetation (SAV) is rooted in the substrate and typically has a flexible structure which keeps the vegetation submerged in flowing water, even when the plants are longer than the water depth. Some types of SAV such as eelgrass are relatively low growing (plant height is significantly shorter than the typical water depth). Other plants such as *Hydrilla verticillata* grow through the water column and reach the surface. However they do not typically emerge above the surface. These plants have very flexible stems and when the stem is longer than the water depth, the stem will bend over, keeping the majority of the plant in the water.

Floating vegetation is buoyant and the bulk of the vegetative mass occurs on or at the surface of the water. Floating vegetation can have significant impacts to flow, particularly when there are many plants and they form dense mats on the surface. When they are restrained from moving with the flow (as by a bridge, culvert or siphon) these mats constitute an additional wetted perimeter on the surface, increasing friction. They also reduce the area available for flow. Water hyacinth is one example of this type of plant.

Water hyacinths form dense thick mats which extend down into the water. When these plants float downstream in canals they are blocked by structures across the channel. The trapped plants build up a mass that frequently spans the entire width of the canal. These masses of vegetation have been observed to extend 30 cm down into the water column. This trapped mass therefore both increases friction (on the water surface) and reduces flow area.

Emergent vegetation is rooted in the substrate of the water body and grows through the water column to emerge, with some significant portion of the plant extending into the overlying atmosphere. It is supported structurally by a root system in the substrate and the rigidity of the stems. Examples are cattails, cordgrass and pickleweed.

In some salt marshes the aquatic vegetation is predominantly emergent, with branching (brushy) plant forms and with only the roots and lower stems assumed to be under water most of the time. Pickleweed (*Salicornia virginica*) saltmarshes are an example of the brushy type of vegetation. At low tide the stems and branches of the plant are exposed to air, as the soil around the plant goes dry. As the tide rises the soil is immersed followed by submergence of the plant itself as the tide continues to rise. The wetting and drying cycle may occur completely once to twice per day depending on the tidal regime. The flow regime in this type of marsh is thus cyclical; and over much of the marsh the flows can be characterized more as flooding/draining in overland flow, than as channel flow. Typically this overland flow is collected and consolidated in a network of channels which begin as very small channels that feed into larger channels, etc. (Roig 1994 and Lewandowski 1993)

Another common form of emergent vegetation includes rigid columnar plants. Examples include cattails in freshwater wetlands and cordgrass in saltwater and brackish marshes. These plants are almost never completely immersed--except under flood conditions. The plants

individually rise rigidly from the soil through the water column and emerge into the air as vertical or nearly vertical stems. These plants can form nearly impenetrable masses with very little flow capacity through them. In this case (as in the case of pickleweed) a system of channels may form to facilitate water transport between the vegetative masses. And as with the pickleweed saltmarsh, the marsh acts more as a buffer or storage device than as a channel for flow.

Vegetation as a Roughness Element

Early work analyzing flow in vegetated channels concentrated on developing channel roughness coefficients which incorporated the effect of the vegetation. Some work was conducted by the U.S. Soil Conservation Service, which focused on estimates of flow capacity for flood channels with various types of grassy vegetation growing in them. This work demonstrated that, "*...Manning's n for just one kind of grass varied over a wide range depending on the depth of flow and the shape and slope of the channel. Thus the selection of a design value for n would be nearly impossible.*" (Chow 1959)

However a relationship was identified between Manning's *n* and *UR* (average velocity times the hydraulic radius), which was relatively independent of the channel shape and slope. A series of curves was developed that related *n* to *UR* for five levels of retardance, ranging from Very low to Very high. An accompanying table classified various types of vegetation and their stages of growth in terms of the retardances. The reader is referred to Chow (1959) for details.

Other approaches have been developed to estimate the resistance coefficient as a function of both the vegetations' structure and spacing and the channel boundary. Rigid columnar vegetation has been related to the calculation of resistance coefficients by summing the drag on individual elements and distributing it across the area of the channel boundary.

Thompson and Roberson (1976) calculated the additional bottom shear τ resulting from vertical cylinders for a range of densities and relative depths (water depth/cylinder diameter) The results were presented in terms of the Chézy coefficient $C/(g)^{1/2}$ as a function of the density and relative depths. They also presented a method to estimate the wake behind rigid vegetation. Wu, et al. (2006) used this method together with the spacing and diameter of the vegetation (cylinders) and

the relative height to calculate a modified Darcy-Weisbach *f* for use in the standard flow equations.

In the same paper Wu et al. (2006) presented a method for calculating an effective Manning *n* based on the spacing between cylinders and the relative height (vegetation height/water depth). This method is of interest because it utilized a modified version of the hydraulic radius presented in an earlier paper (Barfield et al. 1979). The hydraulic radius was modified to reflect the flow condition through the vegetation and was calculated by dividing the area between two adjacent cylinders by the wetted perimeter between the two cylinders (distance between the cylinders plus twice the height of the cylinders in the water). This concept—using a hydraulic radius modified to reflect the vegetated conditions—is applied in this project.

Kouwen and Li (1980) demonstrated that the roughness height of the vegetation varied as a function of flow drag and the flexural rigidity of the plant(s). The flexural rigidity as defined therein is a bulk parameter and is calculated as a function of stem density, the modulus of elasticity of the vegetation and the moment of inertia of the stem.

It is generally acknowledged that vegetation growing into and/or through the flow fields in a channel increases the resistance to flow. As discussed above, early hydraulic analysis methods dealt with this by increasing the resistance coefficients. However this is effectively relocating an impact that is occurring in the upper water column (in the case of emergent vegetation or hydrilla) to a parameter that is generally supposed to reflect the impacts of the channel boundary.

And as described above even the grassy plant types which do have a tendency to lie over under flow cannot adequately be addressed using a single resistance coefficient. The value of the resistance coefficient varies with both the velocity and the hydraulic radius. However in practice, the usual methods for estimating flow (e.g. Manning's equation) utilize a single value of the resistance coefficient to account for roughness, irrespective of the depth.

Velocity Distribution Through the Vegetation/Free Water Interface

More recent attempts to evaluate this issue have focused on the flow structure: in the vegetation, above or outside of the vegetation, and in the area at the vegetation free water interface. In fact some of the studies described above used flow structure to approach the problem. Kouwen

(1969) conducted experiments with flexible strips attached vertically to the bottom of an artificial channel, in the manner of individual blades of grass. The vegetative effect appears to have been similar to that of marine eelgrass under a steady unidirectional flow. He postulated a compound velocity distribution curve with the break point or transition at or slightly above the vegetation. The upper portion of the curve was modeled using a function similar to the universal velocity distribution law, namely Eq.2.28:

$$\frac{u}{u_*} = \frac{u_k}{u_*} + \frac{1}{\kappa}\ln\left(\frac{y}{k_{veg}}\right) \tag{2.28}$$

where y is the distance above the channel bottom; u is the point velocity at a distance y above the bottom; k_{veg} is the height of the vegetation above the channel bottom; and u_k is the water velocity at the top of the vegetation.

In Kouwen's work, the lower part of the velocity curve (in the vegetation) is a simple curve which holds the value of u_k at the top of the vegetation and asymptotes to zero velocity at the channel bottom. The two curves join either approximately at or slightly above the level of the vegetation. He does not specify the function of the lower curve; presumably the intent may have been to avoid having to specify this range.

Kouwen conducted a series of experiments in a tilting bed flume with these flexible strips. Parameters that were varied in his experiments included: the slope of the flume, the relative roughness (y_n/k_{veg}), the total discharge and the vegetation height (k_{veg}).

As a result of these experiments Kouwen developed an equation intended for use in vegetated channels:

$$\frac{U}{u_*} = C_1 + C_2 \ln\left(\frac{A}{A_v}\right) \tag{2.29}$$

where U is the average velocity in the channel; A and A_v are the cross-sectional areas of the flow and the vegetation respectively; and C_1 and C_2 are functions of the vegetative density and flexibility respectively. Kouwen provides tabular values of these functions for various types of

vegetation, but states that these values should be determined in the field for each type of vegetation and each "*vegetative climax*". Values were provided for *Elodea canadensis*, a plant which is native to North America and has a similar growth structure to hydrilla. The values given were $C_1 = 0.32$ and $C_2 = 1.61$; however no description was provided of the density or lengths of the plants utilized.

Pressure Gradient vs. Turbulent Mixing

Sustained flow through dense growths of submerged aquatic vegetation can be divided into that which is caused by a pressure gradient through the vegetation and that which is caused by turbulent mixing from flow outside of the vegetation.

Nepf and Vivoni (2000) describe flow conditions for a rectangular channel with wall to wall vegetation. The conditions described ranged from emergent (i.e. flow depth at or below the top of the vegetation) through depth limited or submerged vegetation. With emergent canopy the forcing function for flow through the vegetation is a pressure gradient. In this case the resultant force from the pressure gradient is balanced by wake generation and shear friction within the canopy.

As the ratio of water depth to vegetation height (h/h_{veg}) increases from 1 however, the dominant forcing function for flow in the vegetation changes from the pressure gradient within the vegetation, to the turbulent mixing from the free flow above the vegetation downward into the vegetation.

Further, the concept of a mixing layer is introduced or, "*a free shear layer…characterized by two regions of constant velocity separated by a confined region of shear containing an inflection point.* (Ghisalberti and Nepf 2002) And the concept of a monami is introduced, which is described as, "*large coherent vortices within the mixing layer which dominate the transport of momentum through the mixing layer*". (Ghisalberti and Nepf 2002) These vortices propagate downstream and cause swaying or waving in the top of the vegetation, which motion is called the monami.

Form Drag and Shear Friction on Plants

Work in this area has generally focused on the force or drag on the stem, caused by the water movement around it, rather than the effect of the individual stems on the overall flow field. Borovkov and Yurchuk (1994) equated the drag on the stems to bed shear by summing the drag on individual stems and then distributing the summed drag across the bed area supporting the stems as a shear stress. The actual shear friction from flow along the bottom of the channel was ignored as relatively insignificant. And the bottom shear was equated to the putatively much larger drag on the stems (Eq.2.30):

$$\tau_v = C_D \rho \frac{U_v^2}{2} h_v d_v \frac{1}{M} \tag{2.30}$$

where τ_v is the bottom shear attributed to the stems; C_D is the drag coefficient of the individual stems; ρ is the mass density of water; U_v is the average velocity in the vegetation; h_v and d_v are respectively the height and diameter of the individual stems; and M is the spacing between stems.

By itself, this method would primarily be useful for emergent vegetation or rigid vegetation that maintained a mostly vertical position in the flow. It does not account for drag from viscous shear forces attributable to plant material that is trailing in the flow.

I was unable to identify sources specific to viscous shear forces on trailing plants. And in the case of such plants as hydrilla, much of the plant trails parallel to the flow in the water column. It must therefore constitute a no-slip condition at the location of the trailing plant and both zero flow and the definition of a viscous fluid at the plant surface will be presumed to apply.

The basis for the discussion of viscous shear and velocity distributions is the definition of a Newtonian fluid. Tritton (1988) describes a Newtonian fluid as one in which the shear stress is directly proportional to the velocity gradient, as in Eq.2.31:

$$\tau = \mu \frac{\partial u}{\partial y} \tag{2.31}$$

where τ equals the shear stress along a plane perpendicular to y, μ is the dynamic viscosity of the fluid and $\partial u/\partial y$ is the velocity gradient in the fluid along the direction y. Isaac Newton is credited with first recognizing this relationship, "*The resistance arising from want of lubricity in the parts of a fluid, is, other things being equal, proportional to the velocity with which the parts of the fluid are separated from one another*" (Cajori[7] 1946 and Rouse and Ince 1963). Tritton (1988) also defines a Newtonian fluid to be one of constant viscosity—i.e. one where μ is not a function of the velocity field.

USE OF MODIFIED OR EFFECTIVE PARAMETERS TO MODEL FLOW

I propose to develop modified or effective parameters; i.e. cross-sectional area, wetted perimeter and hydraulic radius. These will be used to account for phenomena which are similar in effect to the basic parameters, but somewhat outside the original definitions. Similar approaches exist in other fields, for example subsurface drainage engineering, wherein an effective radius for subsurface drains is used in place of the actual radius of drainpipes (Moustafa 1997).

SUMMARY

The classical methodology for estimating flow in channels is based on the assumption that most or all of the significant headloss in a channel is a result of friction that occurs on or very near to the wetted perimeter of that channel. This work begins with the premise that this assumption is inaccurate, when applied to channels with aquatic vegetation growing throughout a significant part of the water column.

The material referenced in the preceding sections demonstrates that the shape of the channel—over and above the ratio of the area to the wetted perimeter—has an impact on the energy losses from flow, as well as the effective discharge in the channel. It also suggests that in fact flow structure in the vegetated section of the water column can not be adequately described using only the (standard definition for the) hydraulic radius for the overall channel and a perimeter friction factor. Other references suggest the integration of the universal velocity distribution functions as a means of estimating total discharge in a section and thus the average velocity.

---

[7] The information from Cajori (1946) was obtained from Rouse and Ince (1953).

The concept of incorporating the shape of a vegetated section, by using the integration of the Prandtl-von Kármán universal velocity distribution law, will be useful in terms of both estimating the capacity of vegetated sections and developing ‘effective’ 1-D flow parameters for the practical application to the 1-D flow models.

CHAPTER III

METHODS AND MATERIALS

The methods used to arrive at the goals of this study included:

- Field Investigations;
- Design and construction of artificial (recirculating) canals and pumping systems;
- Cultivation of *Hydrilla verticillata* as an experimental stock of vegetation; and
- Data collection in laboratory and field canals.

FIELD INVESTIGATIONS

My field investigations took place for the most part in two geographic locales. The primary locale was the Lower Rio Grande Valley (LRGV) of south Texas. The second was in Jamaica. In both locations I was provided considerable assistance in terms of both access and data collection, by the National Irrigation Commission (NIC) in Jamaica and by Dr. Fipps's staff in the LRGV.

I was able to take limited velocity measurements in and around vegetation—under field conditions. However collection of a full and sufficient dataset in the field was precluded by the following conditions. First the canals we were working in and around are functioning irrigation canals. This raised two issues. First the type of heavy infestation we needed for our experimental measurements is generally not allowed to persist in working canals. If an irrigation district identified this type of heavy infestation they would be much more likely to call for a backhoe than to notify us.

The second issue is that—because irrigation water is a valuable commodity—we were restricted in the tests we could run. Ideally we would need to be able to vary flow depth and discharge independently, to obtain a sufficiently broad range of conditions. This is theoretically possible because many of the smaller canals in the LRGV have structure control; i.e. the depth of flow is controlled by a downstream structure. However generally both flow depth and discharge are

controlled in a manner that is the most conducive to the canals purpose, which is delivering water to a downstream user.

I did identify one canal in the LRGV, which would have allowed a functional data collection effort. The canal itself was approximately 3 meters wide and 1.5 meters deep. A straight stretch approximately 500 meters long was heavily infested with hydrilla; and depth control via a downstream structure was feasible. During initial discussions with the staff of the District, they indicated that they were amenable to our running tests in the canal; and that they would or could run water through once we were setup. I was granted access, set up a series of staff gages and surveyed them in. Unfortunately the District was then unable to follow through and provide any flow.

Despite the lack of a detailed data set, the overall field efforts provided the opportunity to collect some point velocities in the vicinity of vegetation. Perhaps more importantly, the various site visits provided the opportunity to observe a range of vegetative growth conditions in flowing canals.

Jamaica

I made two trips to Jamaica; the first was a preliminary visit to meet the staff at NIC and familiarize myself with some of their canals. The second involved data collection in one of their larger canals. The NIC provides irrigation water and much of the urban water supplies for the nation of Jamaica. They utilize a range of groundwater and river water sources, with pumps, pipelines and canals to deliver the water. One of their canals was a main water supply canal immediately downstream of a diversion dam. This canal is approximately 13 meters wide and unlined. At the time of my second visit the water depth in the cross-section varied from 0.8 to 1.1 meters. Although the canal is man-made, its cross-section appears somewhat riverine, with deeper areas against one bank and some signs of incipient channel meandering—within the fixed bounds of the canal banks.

The NIC very kindly constructed a footbridge, to allow easy access to the canal and measurement of flow velocities across the cross-section (See Figure 3.1). However at the time of my second and final visit, the vegetation growths in the canal (in the immediate area of the

footbridge) were only moderate and the growth was distributed in a random manner. I collected flow velocities in the channel and around the vegetation; however both the vegetation morphology and the flow structure around it were complex. The structure of the vegetative mass and its dynamic interactions with the flow are discussed further in Chapter IV.

Fig. 3.1. Footbridge placed across canal to enable flow data collection without interfering with flow

---

Lower Rio Grande Valley

Over the course of this project, we observed vegetative conditions in a range of canals in the LRGV. These were primarily lined canals, ranging from 1 meter across to approximately 4 meters across. However to varying degrees, they had all accumulated enough sediment to support some level of vegetation.

As mentioned previously, I was ultimately unable to collect flow data that could be directly used analytically for this project. However I did begin the process on two canals. The procedure used

was fairly straightforward. We first set staff gages in the canal at spacings of approximately 100 meters. We then surveyed the canal and gages. This consisted of running a level loop to tie in the relative elevations of each gage, and measuring the longitudinal distance between each gage. In addition we collected channel cross-sections at each gage. This provided the data required to calculate the water surface slope between the gages and to estimate an energy gradient.

I was interested to note that in the larger of the canals (the one under structure control) the profile of the channel bottom (in the direction of flow along the centerline of the canal) was quite irregular. The channel bottom did not slope generally in the downstream direction. In addition the sediments in the bottom of the canal were very soft and mobilized easily. It appears likely therefore, that the canal is controlled by a downstream structure and operated at low velocities and with deep water. As a result the bottom sediments are undisturbed by the flow.

The next step following the survey would have been to characterize the vegetation in the canal. My proposed method included harvesting and weighing vegetation for a given length of canal, combined with visual observation of the fraction of the surface covered by vegetation at normal still water levels. Ultimately the goal would be to run varying discharges at varying flow depths and measure water surface slope. In an ideal scenario the vegetation would then be removed followed by measurement of discharge, depth and energy slope without the vegetation. This would enable us to compare the energy loss in a vegetated canal with the energy loss in the same canal without the vegetation.

LABORATORY CHANNEL DESIGN AND CONSTRUCTION

Over the course of the field investigation, it became increasingly apparent that I would not be able to collect sufficient data from our efforts in working canals. Therefore I began to develop laboratory tools to facilitate data collection. These tools took the shape of three separate constructed channels with recirculating pumping systems. One of the channels was a small bench scale channel, and was built in Washington State. This channel was constructed of acrylic and was approximately 200 cm long by 22 cm wide. A sump with a recirculating flow system was provided.

The second channel was constructed in Greenhouse #1 at the Extension Center in Weslaco. This channel was constructed of plywood and lumber with a rubber lining. The flow section was approximately 600 cm long and 33 cm wide. Recirculation was accomplished by pumping water out of the (de facto) downstream end and discharging it at the upstream end.

The third channel (field channel) was an in-ground channel which was constructed at the Texas A&M Research and Extension Center in Weslaco, Texas. This channel had a total length of approximately 1800 cm; the test section was approximately 800 cm long and 160 cm wide.

The research goals for each of these channels, together with additional detail regarding their design and construction are provided below.

Bench Channel

This channel was originally referred to as the bench-scale channel. The name was intended to reference the size of the channel and its general configuration, rather than any reference to dimensional scaling of the flow. The experiments conducted herein were not considered to be at a reduced scale in terms of similitude. The vegetation is real and while it is not hydrilla, it is of similar size and structure—as will be discussed further in Chapter IV. The flow in the channel and in the vegetation is referenced to the Reynolds number for comparison to similar flows elsewhere, however it is considered full-scale. Therefore to avoid confusion and misleading nomenclature this channel is referred to as the Bench Channel.

The bench channel was constructed over a sump and was plumbed with two electric pumps that can be used to provide a range of flows. The pumping system can deliver a maximum of approximately 4 liters per second as configured. Discharge is modified by pump selection and by a system of valves and parallel pipes.

The channel is constructed of clear acrylic with a wall thickness of 1.27 cm. The outer dimensions of the channel are 215 cm by 70 cm by 25 cm. The effective test section is approximately 100 cm in length (Figure 3.2). The sump is constructed of lumber and plywood and lined with rubber pond lining.

The channel is constructed so that the substrate could be deposited in the bottom of the channel and the vegetation directly sown. The vegetation was planted full width, initially with 8 plants in each row. The plants were spaced at approximately 2.75 cm in the row, with one half of a space between the plants at each end of the row and the walls of the channel. The half spacing at the walls was intended to minimize flow bypassing. The rows of plants were spaced at 5 cm between each row for the initial set of experiments. In later experiments the spacing between rows was increased to 10 cm and the transverse spacing between plants in the row was increased so that there were 5 to 6 stems in each row.

The channel was constructed with a stilling chamber at the upstream end; and the water left this chamber in an upward directed vertical jet. This tended to set up a vertical eddy, flowing away from the inlet at the surface and returning along the bottom. I tested several means of reducing this effect. However the leading edge of the vegetation proved to be an effective mechanism for reducing the scale of the eddy and turbulence and ultimately this was utilized. Data collection was limited to the area downstream of the leading edge of the vegetation.

At the downstream end of the test section the water flowed over a sharp crested weir, from which it dropped into a sump. Water was recirculated to the stilling chamber at the upstream end of the test section, via a piping system with two in-line pumps. The first pump was a 1/3 horsepower sump pump that was immersed in the sump. The outlet pipe from this pump was routed through a one horsepower irrigation pump. The outlet pipe from the latter pump ran through a 3.8 cm (1.5 inch) pipe to the stilling chamber. An electromagnetic flow meter[8] was installed in this pipe; and provided the flow discharge rate.

[8] Sitrans FM MAGFLO, with a MAG 5000 transmitter and a 1-1/2 inch MAG 5100W sensor; reported discharge was checked against fill and empty times and appeared to be accurate to within approximately 3% for positive flow. Discharge data was recorded on an OWL 500 data logger.

Fig.3.2. Bench channel with vegetation planted. Flow depth is controlled with adjustable downstream sharp edged weir; vegetation is Elodea, a common aquarium plant that serves as an analog for *Hydrilla verticillata*

My purpose in constructing this channel was two-fold. First I used it to estimate energy loss, by measuring the water surface drop, for flow through very dense aquatic vegetation. I did not expect to observe much drop, given the short length of the channel. However this was a necessary precursor to building a larger channel, and was intended to establish the feasibility of measurements in the larger channel. I was in fact able to measure a water surface slope on the order of 1 mm per meter of channel length, given an extremely dense vegetation condition. However the accuracy of visual measurement of water surface elevation was limited by the surface tension of the water and the fact that the water surface and the gages (See Figure 3.2) were on opposite sides of a 1.27 cm acrylic wall. Nevertheless this effort provided sufficient confidence that more accurate measurements could be made over a longer channel length.

The second purpose for the bench channel was to allow visual observation of flow structure both in the vegetation and above the vegetation; and to collect data on the velocity distribution relative to the interface between the vegetation and the free water. I performed these measurements using tracers (dye and particles) and video taping or photographing through the side of the channel. The results of this work are described in Chapter V.

Field Channel

The purpose of this channel was to allow observation and measurement of flow both in and around the vegetation. Initially we also intended to grow the hydrilla in this channel; however due to difficulties described in a subsequent section, we grew the vegetation in trays in the greenhouse channel.

The initial excavation for this channel was made by a backhoe and was approximately 1 meter wide. We used hand tools to lay the sides of the channel back to a slope of approximately 2.5 vertical to 1 horizontal. The sloping of the sidewalls was performed primarily to improve their stability during the experimental process.

The canal was lined with rubber canal/pond lining donated by Hidalgo County Irrigation District #6. Two concrete control structures were built in the length of the experimental channel (Figure 3.3). The structure at the upstream end created a separate section of the channel which acted as a stilling basin. Water from the recirculating pump discharged into the stilling basin and then overflowed at this (upper) structure into the test section of the channel. The downstream control structure was used to control the height of the water surface in the test section. The construction of both control structures was similar and can be seen in Figure 3.3. Standard 3.8 cm (1.5 inch) thick lumber of varying widths was used to create the stop logs.

The channel downstream of the second control structure was widened into a sump to provide more volume and thus greater water surface (elevation) stability during pumping. The sump was approximately 4.5 meters wide by 4 meters long (at ground level). It was originally excavated to a depth of between 1.5 and 2 meters. However the groundwater table was higher than the bottom of the excavation; and the seepage was sufficient that we backfilled the sump until the bottom was above the groundwater level. The bottom of the sump at that point was approximately 0.2 meters below the channel bottom; however this proved more than adequate for the needs of our pumping conditions.

Fig. 3.3 Setting and caulking stop logs for control structures in field channel. Note central slot for placement of trays holding vegetation

There was no electrical power available at the site, so to provide flow we used a gasoline powered 10 cm (4 inch) centrifugal pump. Recirculating flows were conducted via a 10 cm (4") Schedule 40 PVC pipe (Figure 3.4). The intake pipeline utilized two down pipes in the sump, to minimize the risk of air being incorporated into the flow. As configured, the pump was able to generate flows in the pipe of up to 3.4 meters per second, which equates to approximately 27.6 liters per second.

Wooden bridges across the channel were used to support and attach the intake and discharge pipes (Figure 3.4). The large pipe in the lower left hand side of Figure 3.4 is connected via an alfalfa valve to the Extension Center's water supply and was used to fill the channel and sump. The bridge in the foreground of the picture obscures the view of the upper (stilling basin) control structure.

An additional bridge (not shown) was placed across the channel section in approximately the middle of the test section. This was used as a platform for taking flow measurements and videotaping dye tracer studies.

Fig. 3.4. Field channel with pump and piping system in place. Note hydrilla growing in the test section

Greenhouse Channel

The initial purpose of the greenhouse channel was solely to provide a habitat for growth of an experimental stock of hydrilla. The original plan called for testing in the in-ground channel and in an additional above-ground constructed channel. That channel was designed to hold four of the trays at one time. The modules of that experimental channel were constructed, but were never assembled or used. Because I experienced considerable difficulty in actually growing the stocks of hydrilla, the greenhouse channel was constructed and was designed to hold eight trays of vegetation.

Prior to constructing the greenhouse channel we replanted hydrilla over four times, with each 'crop' failing. This effort continued over the course of the summer, fall and winter of 2006 and into the spring of 2007. After the crop failures in the summer and fall, I requested and received

permission to build the channel in Greenhouse 1 at the Extension Center. The channel was constructed and enabled us to continue our attempts to grow hydrilla over the winter.

My attempts to grow the hydrilla were eventually successful. However the greenhouse channel was actually longer and more suitable than the one I had originally intended for the next phase of the experiments. Therefore I used the greenhouse channel; and discarded the components of the other channel.

The "transferred" purpose for the greenhouse channel was the measurement of water surface slope for flow moving through the vegetation. This was achieved with a series of staff gages with millimeter markings suspended from the structure of the channel (Figure 3.5).

The channel itself was constructed of lumber and plywood with a rubber pond/canal lining. It was constructed just wide enough to accommodate the trays the vegetation was grown in (approximately 33 cm) and was approximately 600 cm long. This was long enough to

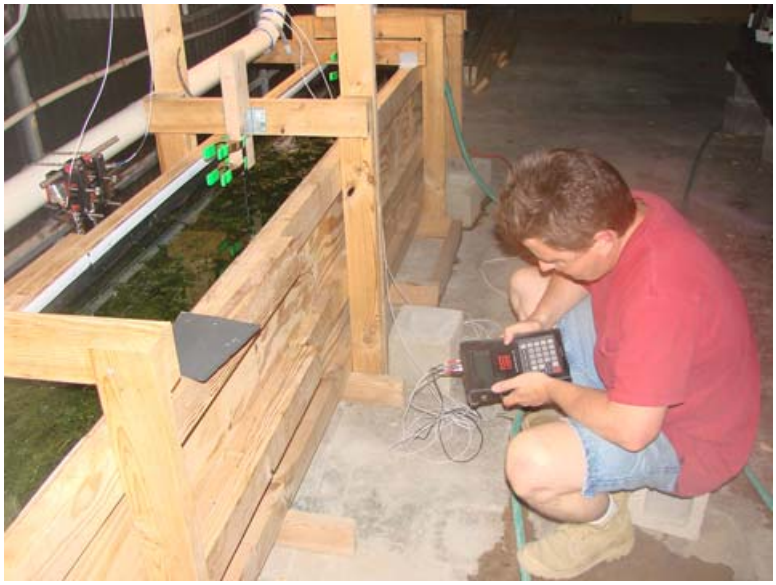

Fig. 3.5. Greenhouse channel showing staff gage setup. Note Panametrix transit time meter clamped to recirculation pipeline

hold the eight vegetation trays, a pump at the downstream end and a short stilling basin upstream of a plastic honeycomb flow straightener. The flow straightener was used both to reduce the scale of the turbulence, and to improve flow distribution across the full cross-section. I used a sump pump with a measured maximum flow rate[9] of approximately 3.6 liters per second. Variations in discharge rate were accomplished with a constricting valve downstream of the pump.

CULTIVATION OF PLANT STOCKS

I experienced considerable difficulty in developing the required stocks of growing hydrilla. The initial research plan called for eight trays of vegetation, divided into two sets of four with a different planting density for each set of four. The variation in density was in the longitudinal direction. The bottom of each tray was cut from standard 2X12 dimensional lumber cut to length (approximately 30 cm). The sides of the trays were made using 1.27 cm plywood.

An array of partial depth holes was drilled into the bottom plank of the tray and nylon wall anchors were then inserted into these holes. These anchors (Figure 3.6) are split on the sides and have a hole in the center of the top which connects down to the split sides. One hydrilla

Fig. 3.6. Planting tray with nylon wall anchors inserted in arrays

[9] Measured maximum flow rate was for the recirculation piping system set up for this channel.

stem was inserted into each anchor, taking care to select a stem that had an unbroken top. Soil was then backfilled around the anchors and the stems to a depth of approximately 5 cm above the top of the anchors (Smart and Barko 1984). See Figure 3.7.

Fig. 3.7. Planting tray with hydrilla inserted and partially backfilled

At the outset I was unsure whether the stem that was actually in the anchors would survive and put out roots, although the anchors were selected for their open sides. However I felt that the 5 cm that was above the anchor and still within the soil would provide ample opportunity for a root system to develop, from which the plants could grow.

Planting

We completed construction of the field channel in early August of 2006. The channel was then filled with water from the reservoir at the Extension Center. On August 10th we collected the initial set of *Hydrilla verticillata* from a canal in Hidalgo County Irrigation District #1. The plants were inserted in the anchors; and the trays were backfilled with soil and placed in the field

channel. Stem lengths above the soil in the trays varied in length between 15 and 25 cm. I expected that the plants would take between one and two months to establish themselves. At the planted lengths we would be able to begin testing once the vegetation had established enough of a root structure to avoid being washed out.

Two days after the initial planting, the site was inspected and it was noted that there were a fair number of plants floating in the channel. This was not surprising, as the process of inserting the stems in the anchors and then backfilling around the stems had a high probability of breaking at least some of the stems. When such an occurrence was observed during the planting process, we went back and replanted in that anchor, either with the same (albeit shorter) plant or with a new one.

However as the days passed after the initial planting, the number of floating plants increased and I decided to retrieve one of the trays and inspect the plantings. The retrieval was necessary primarily because the visibility in the water was extremely poor. In August, the water from the reservoir is well-inoculated with algae; and the water in the in-ground channel had quickly turned green and quite opaque. The retrieved tray was almost completely denuded of hydrilla. The rest of the trays were then recovered and it was clear that the entire planting had failed.

The paw prints of a large dog were noted on the lining above the canal and I suspected that two dogs that had been seen on the Center were playing in the channel, and had thus dislodged the plants. Prior to replanting therefore, we constructed wire mesh covers for the channel and replanted the trays. However even with the covers, the vegetation was again found floating after several days.

At this point I considered the possibility that the soil in the trays (which we had obtained from agricultural fields at the Extension Center) might be contaminated with herbicide or some other chemical inimical to hydrilla. Therefore for the third planting we used clean sand mixed with a commercial fertilizer; but again the planting failed almost immediately.

I had used water from the reservoir at the Center to fill the in-ground channel. As might be expected, the water was well inoculated with algae and other organisms. The second time we planted, we first drained the channel to check for any large animals which might be disturbing

the new plants. We found a small turtle and a number of frogs as well as a large selection of aquatic insects. (Some of the latter were on the order of 5 cm in length.) The amphibians were removed from the channel. However even if they had been burrowing it is unlikely that they would have uniformly removed almost all the plants from 8 trays. In addition it was noted that the lower stems of some of the recovered (floating) plants were brownish and deteriorated.

Despite replacing the water in the channel, in each case the water quickly became green and turbid with suspended algae. After the third failure, I began to consider that water quality might be impacting the growth of the plants. In addition the time period between each of the plantings was 2 to 3 weeks[10], which meant that the days were getting shorter and the growing season was ending. In order to have more control over water quality, water temperature and available light, we constructed the greenhouse channel in mid-October. The channel was sized to hold all eight trays and an array of lights was suspended over the channel (Figure 3.5). A low discharge sump pump recirculated the water and the water was periodically changed using water from the public water supply.

Nevertheless two successive plantings in this facility also failed. In both cases the stems appeared to rot beginning at or near the soil level. When the stem had deteriorated sufficiently the plant would break and float to the surface. Often the upper portion of the plant still appeared healthy and relatively viable.

In early March of 2007 we again planted the vegetation; however a different methodology was used. In all previous plantings I had used the plastic inserts set in the bottom of the tray. One hydrilla stem was inserted in the top of the insert and soil backfilled around it. In each case (it now appears) the stem rotted near the water sediment interface. It is worth noting that some plants, left over from various planting exercises and kept in a tub of clean water—as well as some of the plants which floated to the surface—not only survived, but began putting out roots from the stems.

In the final (successful) effort the plants were attached to the surface of the soil, but not inserted into the soil. We looked for plant fragments which were putting out roots and made some effort

[10] The principal investigator was based in Seattle, WA at this time and was flying back and forth to Texas to conduct the work.

to bury the roots, however the primary focus was to hold the plants at the soil water interface, rather than inserting them into the underlying sediments. This new method was similar to one of the plants' natural method of propagation, which is fragments floating downstream and lodging on the surface of the sediment—from whence roots grow into the soil.

Other changes I made include adding aquarium heaters to the growth tank and adding nutrients to the sediment. I did not have a means for recording water temperature fluctuations; however I did measure a water temperature of around 15ºC (59ºF) during a late morning towards the end of February. When added, the heaters were set to maintain the temperature at 22ºC (72ºF), which is more conducive to aquatic plant growth.

In addition to adding nutrients to the substrate I began adding small quantities of liquid fertilizer to the water in the channel. It has been suggested that hydrilla can absorb nutrients directly from the water column (Masser 2006) and given that the severed stems in our sample tanks could last for weeks if not months, this appears to be borne out.

I also added a type of gravel (fluorite) which is commonly sold as a planting substrate for planted aquaria. This material is a porous clay and is rich in iron. It is purported to support and provide a base for the growth of bacteria which are common to healthy aquatic biological systems.

The number of fertilizer pellets buried in the sediment was also increased. These pellets are designed to release nutrients slowly in an aquarium situation. The use of these had been minimized in earlier efforts, due to a problem with suspended algae. The suspended algae compete with the hydrilla for light as well as CO_2 and (at night) O_2.

The trays also had a tendency to develop mats of green algae on the sediment surface. The trays were monitored and the water was changed regularly to control floating algae. An algaecide that was allegedly safe for aquarium plants was also used in small quantities.

This final planting effort actually occurred in three phases over the course of several weeks. This planting began with two trays, while I was still out of town. When the vegetation in those trays survived and began growing, the remaining trays were planted. The third phase or effort primarily focused on filling in areas where the plants had not survived. This phased planting had

the effect of providing a range of vegetation densities over the eight trays. This allowed me to develop energy loss results that were a function of vegetation density.

The final vegetation density was considerably lower than planned, in terms of stems per square meter. However the vegetation density in the upper water column was sufficient to allow measurable energy loss (water surface slope) in the tests.

*Bench Channel (*Elodea *and* Rotala indica*)*

The bench channel in the Seattle laboratory was planted with species other than hydrilla, primarily because there is no hydrilla currently in Washington State and the relevant agencies were strongly resistant to the suggestion that it be imported. Two other species with a growth structure similar to hydrilla, *Rotala indica* and a member of the *Elodea* family, were used as an analog for hydrilla.

These were somewhat easier to grow. In two plantings of *Elodea* I used the nylon anchors as well. However for these cases the plant stems were inserted into the wall anchor and then the wall anchor was inserted into the gravel. The substrate utilized was a mixture of gravel, sand, peat moss, an organic compost and chicken manure. This worked rather well, but resulted in a strong smell in the lab from the decomposing organic material. In one other planting (the *Rotala indica*) the stems were inserted directly into the substrate and this worked as well, however it is difficult to maintain a tight planting density.

Maintaining Experimental Vegetation Stocks

One constraining factor when using live plant stocks is the relatively short useful life of the experimental stock. The vegetation tends to grow fairly quickly once established. However in a successful biological system, various other epiphytes and algae also tend to grow. In addition it is difficult to establish aquatic vegetation without also establishing a healthy snail population. These reproduce rapidly and can significantly impact plant quality.

Another constraining factor is the variation in plant structure over the stages of vegetation growth. When hydrilla is fairly new, e.g. the distance between the leaf whorls can be quite short, on the order of a few millimeters. As the plant grows, the distance between whorls increases,

presumably due to elongation of the stem between each whorl. This means that over the length of a mature plant, the spacing between leaf whorls varies. The growing end of the stem (with the newest growth) will typically have fairly dense whorl spacing, while the older and lower (in the water column) stem has much more space between whorls.

In addition in deeper water and in conditions where the hydrilla has surfaced and formed a mat, there is limited light reaching the lower water column. It appears that this leads to the loss of leaves in the lower column. This occurred to a certain extent in the greenhouse channel, particularly in the trays with the densest growth. It was also observed in irrigation canals during the field investigation.

In any event we were able to develop the vegetation stocks necessary for the requisite experiments. We experienced both the growth of filamentous algae and a proliferation of snails while the trays were in the greenhouse channel. The snails were controlled by the introduction of *Chromobotia macracanthus* (clown loaches), a species of aquarium fish that feeds on snails. The filamentous algae was controlled by the application of a commercial algaecide whose chief operating ingredient was hydrogen peroxide.

DATA COLLECTION

Three types of data were collected in this project. The first measured friction or energy loss as a function of water flowing through dense vegetation. This work occurred in both the bench channel and the greenhouse channel. The second type was the collection of velocity distribution data. This data was collected in the bench channel and in the field channel. And finally we collected data on the response of vegetation to flow drag. This was collected out of the water and consisted of simple bending tests on the vegetation.

Instrumentation and Methodology

This section describes the instrumentation and methodology used in each channel.

Bench Channel

This channel was setup to collect water surface slope and velocity distribution data, as well as discharge data. Discharge data was collected in the recirculation pipe with a Sitrans FM Magflo MAG 5100W flow meter combined with a Magflo MAG 5000 transmitter. The transmitter was sized for 3.8 cm (1.5 inch) pipe. Data was recorded with an OWL-500 data logger. An adjustable sharp crested weir was installed at the downstream end of the test section. The primary purpose of the weir was to control the water surface level in the test section. We also considered it as a method to test the calibration of the flow meter. However the geometry of the flow section leading to the weir would not have resulted in very accurate measurements with the weir.

Water surface slope was measured by placing acetate overlays on the exterior of the channel's acrylic wall. The overlays were printed with a grid that measured the water surface elevation in millimeters. One of these overlays was placed at each end of the test section. Then with no flow and a level water condition, a relative zero level was marked on each overlay at the water surface elevation. After flow was initiated and sufficient time had passed for the water surface slope to stabilize, the new water surface elevation was marked at each grid, providing the change in water surface elevation at each end of the test section. The difference between the changes in the two water surface measurements divided by the distance between the two overlays (length of the test section) provided a water surface slope.

Water velocity distribution was measured using video, shooting through the side of the acrylic channel. Again a grid was overlaid on the outside of the channel. Then dye or particle tracers were released in the flow. As particles or dye moved past the grid points it was recorded on film. The information on the film was then processed to provide flow velocities at points relative to the vegetation/clear water interface. For higher velocity flows we were able to use a frame by frame advance to measure particle velocity. However some of the smaller particles tended to blur and disappear in the stop frame mode.

Greenhouse Channel

Discharge in this channel was measured in the recirculation pipeline, using a Panametrix PT868 transit time flow meter. Water surface elevations were measured at five stations using stainless steel staff gages (rulers) with millimeter markings. The gages were clamped to cross-pieces attached to the tops of the channel walls.

Measurement of water surface elevation using these gages required use of an angled hand mirror and a flashlight, particularly for the lower water surface elevations in the channel. We built the channel in the greenhouse, so that we could maintain water temperature and provide additional light during the cooler shorter days of the winter. However the actual data collection was conducted during the summer, wherein the daytime air temperature in the greenhouse frequently exceeded 40 degrees Celsius (104 degrees Fahrenheit). For this reason the data collection in this channel was conducted at night, when both the lack of light and the position down inside a narrow (black-lined) channel made reading the gages challenging.

Adjusting for the surface tension was also challenging and potentially contributed to a reduced accuracy. However with the mirror properly angled and positioned it was possible to adjust for surface tension and achieve accuracies within less than a millimeter.

I characterized the vegetation densities using an underwater flash camera and a staff gage, to relate the vegetation to its location in the water column. The material characterizing vegetation is provided in Appendix A.

Field Channel

With the field channel I was primarily interested in measuring flow in the open areas around the vegetation. A schematic layout for the field channel setup is shown in Figure 3.8. The tests typically involved measuring flow velocities in small areas, on the order of 10 to 30 cm in cross-section and/or depth. While any of the available technologies should have been viable in the open flow condition, it appeared that the measuring portions of the instruments took up enough of the available cross-section to disrupt the flow. And the sampling volume of the larger acoustic Doppler hand-helds also made it essentially impracticable to attempt to measure a velocity distribution relative to the vegetation and or channel boundaries.

Two tools were ultimately used for measuring water velocity and distributions. The first was dye tracers and a handheld video camera. The second was a small laboratory scale acoustic Doppler flow meter, the Vectrino Doppler Velocimeter, with a field probe. This flow meter had an extremely high sampling rate; and the sampling volume and head size were small enough to enable measurement of flow velocities relative to the distance from the vegetation and bottom. These results are discussed in Chapter V.

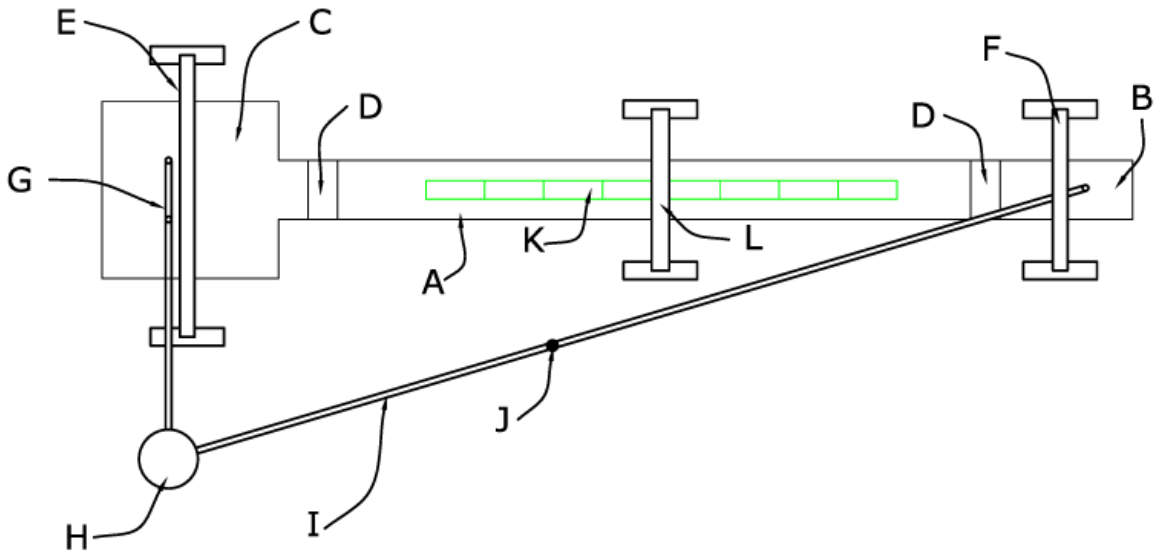

REFERENCE	DESCRIPTION
A	Test section of channel between control structures
B	Stilling basin
C	Sump
D	Control structures (overflow weirs)
E	Intake pipe support structure
F	Discharge pipe support structure
G	Intake pipeline (10 cm Schedule 40 PVC)
H	Recirculation pump (10 cm gasoline powered centrifugal pump)
I	Discharge pipeline (10 cm Schedule 40 PVC)
J	Flow meter (PT868 Panametrix transit time meter)
K	Central slot in bottom of canals sized to hold 8 trays with vegetation growing in them
L	Instrument bridge

Fig. 3.8. Schematic layout of field channel and equipment description

CHAPTER IV

FIELD INVESTIGATION OF AQUATIC VEGETATION

As part of this project I investigated a number of canal sites to investigate aquatic vegetation and its interaction with flowing water. The information collected in this has utility in characterizing field conditions for both flow and vegetation. The bulk of the information provided in this Chapter concerns submerged aquatic vegetation. That is, vegetation that is rooted in the substrate and has flexible stems which trail downstream in the current. However I also had the opportunity to investigate sites that were characterized by floating aquatic vegetation, as well as some with emergent vegetation. The resulting information is described below.

FLOATING AQUATIC VEGETATION

In the early stages of this project we examined flow in channels with one type of floating aquatic vegetation, *Eichhornia crassipes* or water hyacinth. Water hyacinth can have significant impacts on flow in canals. A large plant, it can persist as a free floating plant and will move downstream with currents. As the plants move downstream in flowing canals they are captured by obstructions across the channel such as low bridges, culverts or siphons. The plants tend to form large masses of hundreds or thousands of plants at such obstructions (Figure 4.1).

Water hyacinth starts its life cycle from seed as a rooted plant. The rooted part of the plant sends a thick stem to the surface, where the plant puts out large low density bulbous stems and leaves. The initial stem reaching to the bottom then apparently withers or senesces, after which the plant can break free and continue to thrive as a free floating plant. In flowing canals the plants move downstream with the current until they are stopped by some obstruction.

When the plants accumulate at an obstruction, they create a floating mass of vegetation that does not move with the flow. The plant mass constitutes what could be considered to be a top to the canal—or an additional element in the wetted perimeter.

Fig. 4.1. Hyacinth choked canal with single plant held in foreground. Note structure of plant, this plant would not be stable vertically floating independently of the mass

In addition to plants captured by the structure, the plant mass increases by putting out stolons from which new plants form. See Figure 4.2. As the mass of vegetation grows, the morphology of the individual plant changes to a shape which requires the vegetative mass to be stable. As one can see in Fig. 4.1, the individual plant removed from the canal is quite top heavy and would not float in an upright position by itself. These large vertical stems and leaves are presumably reaching up to maintain the individual plants access to the light. However the resultant of this behavior is that the base of the plants must float lower in the water to provide the additional displacement necessary for the plant to float.

Fig. 4.2. Hyacinth runner (stolon) connecting parent plant and new start. Note feather-like structure to roots

The floating plants extend root systems into the water which resemble broad feathers. These "feather-roots" are semi-rigid and are presumably used to extract nutrients from the water column. From the standpoint of flow evaluation, these roots constitute a roughness element of significant scale. This is in addition to the displacement volume of the plant itself. In the hyacinth colony in Figure 4.1 the vegetation was observed to extend below the water surface approximately 30 cm.

Hydrilla verticillata can also act as primarily a floating plant for some stages of its life cycle. When the length of the vegetation exceeds the water depth of the channel, the vegetation lies over on the surface, where numerous plants can become interlocked and forms mats. This condition greatly reduces light to the lower water column; and the stems—which remain rooted in the bottom—tend to lose their leaves. The result can be a thick mat of vegetation on the surface with very thin individual strands reaching to the bottom. In this situation the dominant impact to flow is probably the surface mat, rather than the stems in the lower water column.

EMERGENT AQUATIC VEGETATION

Emergent vegetation, as described previously, is vegetation that is structurally supported by a root system in the substrate—a foundation—and has a rigid stem or stems which reach through the water column and into the overlying atmosphere. Beyond this definition there are several plant types or categories. As there have been a number of flow studies which used vertical dowels to represent aquatic plants, we should at least consider columnar vegetation as one category. An example of this type of plant is cordgrass or *Spartina alternaflora*. Figure 4.3 shows a stand of this vegetation.

Fig. 4.3. Stand of *Spartina alternaflora*. (Source: USDA 2005)

As shown in Figure 4.3 the stems do for the most part emerge from the water as discrete columns, with leaves growing out from the stem above the water line. If these plants were growing in a channel, there could be some flow between the individual plants. However the water would tend to slow down within the vegetation and this encourages the deposition of any sediment load the flow is carrying. In addition epiphytic communities of algae and other organisms tend to reduce the space between the stems and further retard flow. Any flow occurring in a stand of this type of vegetation will be highly dependent then on both plant spacing and the types of materials that are attached to the plants.

An additional type of emergent aquatic vegetation is typified by the cattail or bulrush. Rather than a single stem with leaves however, this plant has long vertical leaves that emanate from the base of the plant. In the summer the plant also puts up a central stem on which the cattail itself forms. However the form of the plant is more complex than just a simple column. A number of these plants growing close together would generate a complex flow field wherein the water wends its way around and through the mass.

The final type of emergent vegetation considered here would be branched or brushy plants. One example is pickleweed or *Salicornia virginica*. This is a low growing brushy plant that grows in salt marshes. It has very dense growth habits and forms mats and mounds in tidal wetlands. The flow characteristics in the plant masses tend to be slow and more of a flooding and ebbing than a direct throughput. Water is frequently delivered to the vegetation in a series of channels that has been described at times as fractal. At their smallest scale the channels may be nothing more than a slightly greater spacing between plants. Once the water has been delivered to the wetland by the channels however it is more typical of overland flow than channel flow.

SUBMERGED AQUATIC VEGETATION

The type of submerged aquatic vegetation we are considering is rooted in the substrate of the water body and has flexible stems which respond to a velocity field by leaning away from it. The ‘leaning’ results from drag on the plant caused by flowing water moving around and past the stems. This drag is caused by form drag, viscous shear stress or some combination of the two.

Hydrilla verticillata has long thin flexible stems that do branch. However, the plant is completely supported by the water and the stems have little structural rigidity. The soft muds and expansive root systems typical of flowing canals may also aid in the plants leaning away from the flow. A rigid stem in a stiff substrate would tend to come vertically out of the mud. If a long stem were then subjected to flow, as the plant trailed downstream it would be subjected to flexural stresses that approached zero at the downstream end of the plant (the growing tip) and would approach some maximum as one approached the cantilever point where a stiff stem came out of the soil.

This study did not include direct analysis of the structural capability of hydrilla stems. However we did note in our field review that the typical muds were very soft and that in strong flows the stems appeared to exit the sediment at an angle. We also noted during the aforementioned planting exercises that the stems were fairly fragile under certain types of loading. For example when we inserted the stems into the nylon anchors, if we pressed too hard (placing the stem in compression) the stem would snap, presumably due to column buckling. It appears that the main loading on the stem in its natural environment is in tension. However the stems do provide some resistance to bending; and it is likely that there is some flexural loading at the soil water interface.

The morphological structure of the hydrilla plant is a single stem that extends upward from the soil, with small leaves set radially around the stem. These radial clusters of leaves (or whorls) grow at regular intervals along the stem and the individual leaves are usually around one centimeter in length.

There are branchings on hydrilla; and a given plant which has a single stem at the mudline may branch numerous times. Each branch then takes a shape similar to the rooted main plant, which is a long flexible strand trailing in the current. The branchings can be considerable and a mass of trailing stems that is close to a meter in diameter can be depended from a relatively small number of rooted stems (Figure 4.4).

In the case of very dense growth, these submerged plants will sometimes break the surface and some portion of the plant may rise slightly above the surface. However in terms of their interaction with flowing water and for the purpose of this study, these plants are considered to be submerged.

It also appears that hydrilla's tendency to branch is more prevalent in the upper water column, creating the very dense clusters of plant near the surface, while the lower water column is sparsely populated with stems. The branching and plant density may be a function of available light. In deeper canals with a relatively dense plant mass in the upper 30 to 50 cm, the stems in the lower water column appear to be both denuded of leaves and with limited branching. Most of the branching appears in the upper water column.

Fig. 4.4. *Hydrilla verticillata* mass in smaller lined channel. The actual width of sediment in the bottom of the channel was only 1/4 to 1/3 that of the vegetative mass and this mass of vegetation was continuous from the surface to near the bottom

---

In the relatively shallow canal shown in Figure 4.4 light can penetrate to the lower water column on the sides of the vegetation mass. This results from the paraboloid section and the relatively narrow strip of substrate which has collected in the center. Although the plant mass is two to three times the width of the substrate, there is still sufficient space on the sides to allow light penetration. The lower edge of the plant mass in that figure was within five centimeters of the bottom.

The vegetation in this situation was also waving from side to side in the flow. At times the vegetation seemed to wave as a single mass, but this coherent movement would not last long (seconds) before it devolved into individual strand movements. The individual stems did move independently.

Jamaica SAV

The field work in Jamaica involved a different type of submerged aquatic vegetation. This plant had long leaves that were attached to central stems. The leaves and the stems trailed downstream (See Figure 4.5) and moved significantly under the influence of the current.

Fig. 4.5. Aquatic vegetation in NIC canal in Jamaica. (This photo was selected for plant visibility, however much of the canal vegetation was closer to that shown in the bottom left of this photo)

I was able to collect point velocities around the vegetation. The surface velocities in the channel cross-section—away from the vegetation—varied from approximately 0.3 meters per second near the bank to approximately 0.8 meters per second near the center of the channel and at least 1 meter away from the nearest vegetation mass. An approximate section of the canal and the flow data are included in Appendix B.

Velocities closer to the vegetation were on the order of 0.2 meters per second. If the instrument[11] was placed at the very edge of the vegetation or within it however, the data reading invariably indicated no velocity. This vegetation was moving significantly—including waving back and forth—under the influence of flow. The attempt to keep the flow probe on the edge of the moving vegetation required moving it laterally across the flow. This lateral movement no doubt affected the flow through the tube that delivers flow to the measurement probe. The combination of the moving vegetation, the sampling time for the instrument and low resolution precluded collection of a flow profile around the vegetation. However two videos were collected which allow qualitative review of the flow state. And visual evidence from these videos indicates that there is significant velocity very close to and—at least at times—within the vegetation.

The first video was collected of a section of vegetation that was near the surface. The vegetation in this canal is flexible and in this case was on the order of two meters long, from the rooted base to the ends of the fronds. The plant mass consists of many rooted stems and each stem has multiple branches. The leaves on the branches tended to be 2-3 cm wide and between 10 and 30 cm long.

The vegetation tended to wave back and forth in the current; however attempts to measure a frequency of oscillation were generally not successful. The mass of the vegetation appears at first to move as one unit. Observed in plan view from the surface, the vegetation waves back and forth about a central axis, presumably defined by a stem or a locus of individual stems. Observed from within the water column, there is also vertical movement of individual plants in the plant mass, as well as occasional movements that imply rotation of the plant mass relative to the central axis of the stem. These rotational movements, if they are such, are short lived, with durations of less than a second. They are followed not so much by a reversal or relaxation of the rotation, as might be expected, as by a dissolution of the vegetative mass as a coherent element.

It is as if the flow periodically treats the vegetal mass as a single coherent structure. But when the mass is rotated beyond a stable condition, the mass devolves into individual elements which then return to a (presumably) more stable orientation.

---

[11] Global Water Flow Probe FP101

Observation of floating debris moving across the top of the vegetation yields an approximate Reynolds number of 10^4, which indicates that the flow is in the turbulent range. The video also shows variations of velocity both in magnitude and direction in the same area and same time period indicating complex flow fields.

I was able to collect a very brief dataset in one other canal in the NIC system. This canal was smaller—approximately 3.0 meters across from top of bank to top of bank (Figure 4.6). The canal sides were lined and sloped at approximately 1:1. This canal had dense growths of hydrilla covering the entire bottom of the canal to a depth of approximately 0.4 meters. The flow in the canal was sufficiently fast, so that the vegetation laid over along the bottom, rather than extending into the upper water column.

Fig. 4.6. *Hydrilla verticillata* in NIC canal in Jamaica

The cross-section of this canal is shown in Figure 4.7 along with the approximate locations of the four points at which flow velocities were collected. We were at this canal briefly; and I made two sets of measurements, which are shown in Table 4.1.

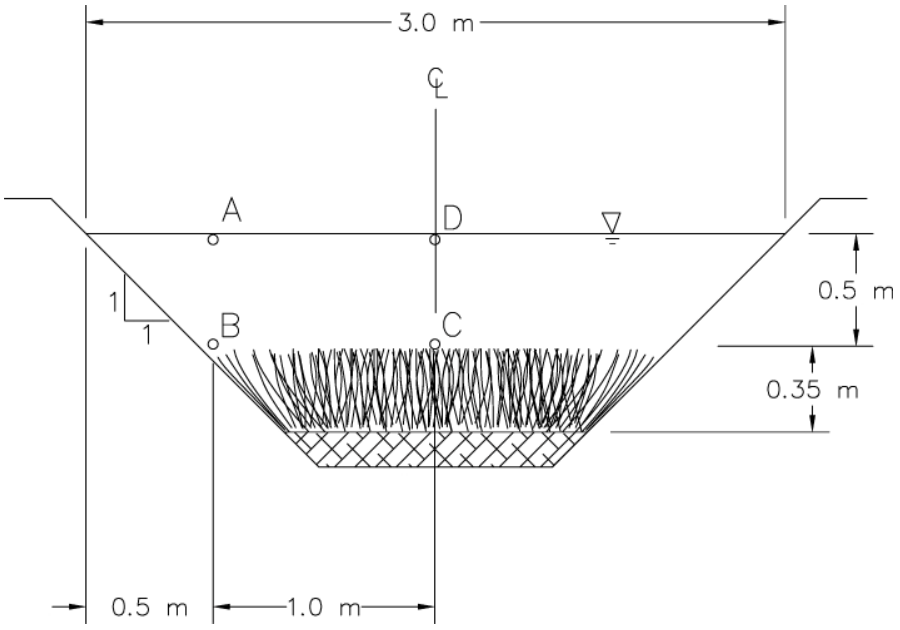

Fig. 4.7. Cross-section of canal in Jamaica shown in Fig. 4.6

Table 4.1. Measurement of flow velocities around hydrilla in NIC canal in Jamaica. See Fig.4.7 for location of measurement points.

Measurement Point	Measurement Set 1 (meters/sec)	Measurement Set 2 (meters/sec)
A	0.5	0.4
B	0.1	0.2
C	0.2	0.2
D	0.3	0.3
In vegetation	0	

Lower Rio Grande Valley

The following is a brief summary of the canals we visited and the overall vegetative hydraulic conditions.

Hidalgo County Irrigation District #1 – East Main 3

This was a seemingly ideal canal for testing. The canal alignment was straight for approximately 500 meters; and the cross-section was approximately 4 meters wide at the top of bank (Figure 4.8). Although the cross-section was lined, up to 30 cm of sediment was recorded in the canal at the center of the section.

Vegetation densities varied over the length of the proposed test segment, but overall the vegetation was substantial. The variation would have allowed us to test the effects of vegetation as a function of the density. Water surface elevation in the canal was controlled by a downstream structure, which would potentially have allowed us to test at different depths and discharges. However after we had installed a series of staff gages and surveyed their locations, the district determined that they would not run water through the canal and directed us to remove the staff gages.

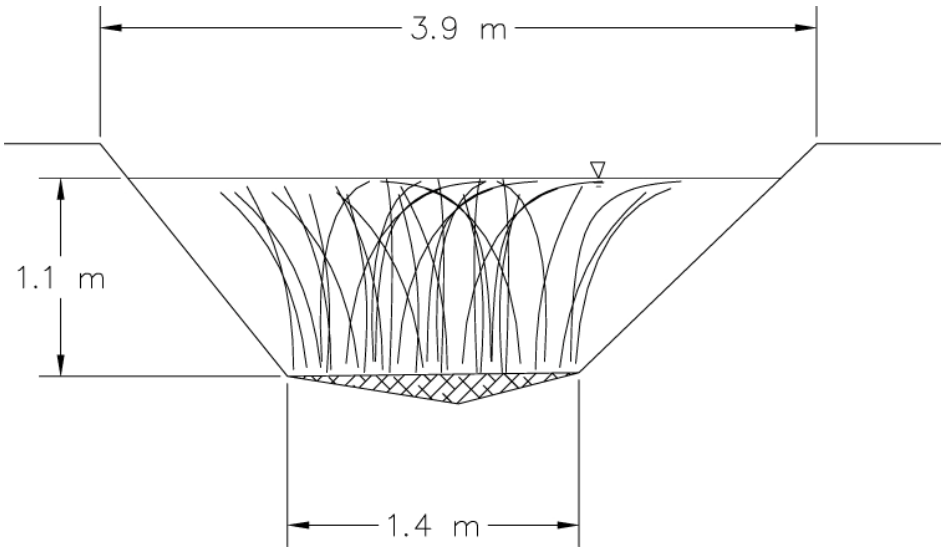

Fig. 4.8. Cross-section of canal in Hidalgo County Irrigation District (HCID) #1. Depicted vegetation is schematic

The sides of the canal were relatively steep (approximately 1.25 vertical to 1 horizontal). The width of the sediment in the bottom of the canal was approximately 1.4 meters, for a channel wherein the width of the channel at the water surface was approximately 3.9 meters. Nevertheless the canal when observed appeared in places to have surface vegetation from one bank to the other.

This was probably due to two factors. When we observed the canal it was not flowing; and the water level appeared to be lower than the normal level. Both of these factors would have contributed to an increase in observed surface coverage as follows. When the canal was flowing at any appreciable velocity, the vegetation would have streamed downstream with the current. This would thus tend to restrict the observed vegetation to above the suitable substrate. In addition the lowered water surface would also increase the amount of the vegetation that reached the surface; and as observed elsewhere in this document, after the stem of the vegetation reaches the surface, the plant lies over and has more relative surface coverage.

Two other factors are also worth noting for future data collection exercises. First, the profile of the bottom mud appeared quite irregular when related from section to section. The material was a very soft anaerobic mud and when it was disturbed stayed in suspension for some minutes. The water surface elevation in this channel is apparently controlled by a downstream structure and it appears likely that even when flowing, the water is held deep enough so that the flow velocities have little effect on the bottom configuration. This implies that the slope of the canal bottom (over short distances) can be independent of the actual capacity.

The remaining factor is that the depth at which the canal is typically maintained has an impact on both the structure of the vegetation and its potential reaction to flow. A canal that is kept in a state with fairly deep water will tend to accommodate and grow longer individual strands of vegetation. However when the vegetation does surface and ‘top out’ it still can form mats on the surface. This will eventually contribute to a thinning of vegetation in the lower water column, primarily because the stems in the deeper water lose their leaves (presumably due to a lack of light for photosynthesis).

Prior to learning that we wouldn’t be able to collect flow data in this canal, we had begun some efforts to characterize the vegetation, including removing vegetation from a known length of

canal and weighing it. In each of two separate sections, we removed all vegetation for a length of canal equal to approximately 1.5 meters. The vegetation was roughly rinsed, bagged and the bags were then drained.

One section yielded 22 kilograms of plant material; the other 24. Prior to removal, the vegetation in each section covered between 50 and 75% of the water surface. We also brought some of the plant material back to the lab (in water) and weighed a sample of individual strands after patting them dry. The average mass per length of stem for the sample was 0.046 gm/cm. Given an average mass (per section) of 23,000 grams of hydrilla, this would lead to a total length of vegetation in each section of 500,000 cm or 5 kilometers of vegetation in a 1.5 meter section. If we assumed an average length of 2 meters per stem, this would imply that there were 2,500 stems of hydrilla in a section of canal 4 meters wide and 1.5 meters long.

Figure 4.9 depicts the mass per length data, arranged in order of stem length.

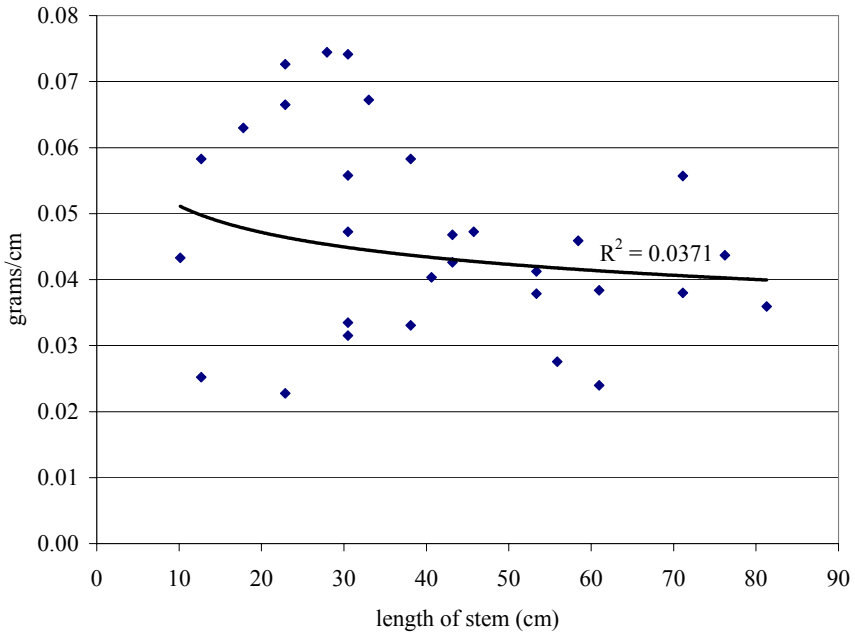

Fig. 4.9. *Hydrilla verticillata* mass per unit length. Plotted as a function of the stem length from the sample

The longer stems in this sample tended to have less leaves in the lower parts of the stem. It could be argued therefore, that the trend line shown in the graph would ultimately asymptote at the weight per unit length of the stem itself (without leaves). That value is estimated here to be 0.038 grams per cm. Stem diameters were also measured from photographic samples (See Appendix B) and these range from 1.4 to 3.0 millimeters. However the majority of the stems appeared to range from 1.8 to 2.2 millimeters in diameter.

Delta Lake

This was a small canal, approximately 1.5 meters across, with a total depth of 0.8 meters from the top of bank to the bottom in the centerline. It was lined, but had accumulated approximately 10 cm of sediment in the bottom. The canal supported a substantial growth of hydrilla.

The canal also had a sharp 90 degree bend to the right (facing downstream) approximately in the middle of the section we were observing. There was a control structure approximately 190 meters upstream of this bend. Approximately 400 meters downstream of the bend the canal dropped into an underground pipe, as a result of which the flow in the downstream leg of the canal eventually became supercritical. This rendered the canal useless for this project, as this work is focused on subcritical steady state flow.

Nevertheless the flow conditions were worth noting. Upstream of the channel bend, the water was deeper and slower (subcritical) and the vegetation was only intermittently visible. Downstream of the bend the water accelerated and appeared to be flowing over the banks of hydrilla which were pressed to the bottom of the channel by the flow. The flow over the top of the hydrilla was on the order of 10-15 cm in depth. The surface of the water was wavy and gave the appearance of nearing critical flow. However, further downstream where there was less vegetation this semblance of critical flow lessened.

This was the first clearly visible case we viewed where the vegetation had been pressed down by the water, with flow primarily over the top. This could be attributable at least partially to the downstream drop, both through the mechanism of lowering the downstream water surface and through increasing the velocity of the flow. However, at no time on this project did I observe

canals that had both significant flow velocities and significant amounts of vegetation at the surface of the water.

General Observations

Based on my observations, the following are conditions which have significant impacts on the way that hydrilla interacts with flow in a given canal. They include:

1. Flow conditions at the time flow is being evaluated;
2. Growth stage of the hydrilla;
3. Flow conditions over the period in which the hydrilla has been growing.
4. Channel cross-section and available growth media (substrate); and

These conditions are not independent; however the following discussion treats each separately for clarity's sake.

Flow Conditions at Time of Evaluation

The vegetation responds to certain levels of flow conditions. If the flow is high enough, vegetation will lie over, which allows the water to flow over the top of it. If the mass or density of vegetation is low relative to the channel cross-section, the vegetation can also be compressed or compacted by the flow. This allows the flow to bypass the vegetation to an extent, which would result in a lower expenditure of energy. If the flow is relatively low, the water may follow a sinuous path around individual vegetation masses and/or depending on the density and condition of the vegetation it can flow through the vegetative masses. This latter condition was observed on the Rio Grande River during the summer low flow period.

Growth Stage

The effect or relative impact of the vegetation on the flow is also dependent on the phase of the growing season. Even in lower latitudes in the United States, hydrilla will go through a winter phase, wherein it is at least not growing aggressively. For the purposes of this discussion, we will assume that for the most part the overwintered plants have been removed or have senesced, leaving their root systems and turions in the canal substrates.

In the spring the plants begin to grow again. The new stems are of course short; and the new growth has dense whorls of new leaves. At this stage of their growth they are confined to the lower water column and could reasonably be treated as a friction effect on the wetted perimeter.

However growth rates for hydrilla are on the order of 2.5 cm (1 inch) per day (Langeland 1996). For the depths of water in the typical canal, well established vegetation can reach the surface and top out within a month of the start of the growing season. But this description implies a static water condition.

Flow Conditions During Growth Period

In canals with regular water flow, the vegetation grows upwards but trails downstream in the direction of flow. So a canal with flow of less than a meter depth may have plants up to several meters long. If the flow is continuous and at a high enough velocity the plants may still not reach the surface (Figure 4.4).

If the canal only flows intermittently, but water is maintained in the canal, the type of condition shown in Figure 4.10 is obtained. The vegetation grows upward, and when the water is static—without the drag of the flow—assumes a near vertical position in the water column, until it tops out. As the stem reaches the surface, it bends and lies over along the surface. If many individual plants are growing they form a mat on the surface. In this situation most of the branching and resultant biomass occurs in the top 0.5 meters of the water column (Langeland 1996).

Fig. 4.10. *Hydrilla verticillata* growing in a channel with maintained water depth and no flow. (at time of photo)

If the water in the canal remains static or at low velocity for a sufficient period, the mass of hydrilla at or near the surface will become a host to filamentous algae and other epiphytes which can cause it to act as a solid mass. In this case water flow within the vegetation is probably quite low and the vegetation becomes a significant obstruction to flow.

However if flow in the canal is maintained at a sufficient level, the vegetation tends to move freely and lean over under the drag of the water. This can result in a situation where a canal that appears heavily infested under static conditions, has little visible vegetation when the water is flowing. The vegetation is of course still there, and it can still have significant impacts on flow.

Figure 4.4 shows an example of vegetation that is much longer than the water is deep. The vegetation in this picture is 1-2 meters long and the water is about 0.8 meters deep. However the canal presumably is operated regularly as there is no buildup of filamentous algae or other detritus in the vegetation. Nevertheless the vegetation in this figure takes up between 25 and 50% of the channel cross-section and significantly reduces the canal's capacity.

Substrate and Cross-Section

Figure 4.10 also demonstrates the impact of the canal substrate and cross-section. This canal is lined; however sediment has accumulated in approximately the central third of the bottom of the canal. The vegetation grows in the sediment and given sufficient time with no flow, it will spread out to cover the whole surface. However this canal has been in recent use, as evidenced by the cleared areas in the surface of the vegetation and on the sides.

Given sufficient energy, the flowing water will move vegetation to the side and create channels in the vegetation. When this channel is flowing, water is probably flowing over the top of the vegetative mass and on the sides where the sloping lining has prevented sedimentation. The water marks on the side of the channel indicate that the water surface was higher and that flow was recent.

The filamentous algae and other detritus visible in this figure probably serve to tie the vegetation together which can cause it to act as a continuous mass, rather than individual plants moving independently. This would explain the vegetations tendency to retain the form visible in the figure, rather than return to the dispersed form of individual plants.

CHAPTER V

EXPERIMENTAL RESULTS

Analytically, my initial step in approaching the problem of vegetation in flowing water considers the definition of a Newtonian fluid (Eq.2.20) which is that the shear stress in a fluid near the boundary is proportional to the rate of change of velocity along a normal to that boundary[12]. As discussed previously, one of the resultants of the definition of the Newtonian fluid is the no-slip condition at a static boundary.

I submit however that in addition to the fixed channel boundary, each vegetal surface projecting into the flow field constitutes a flow boundary with the same no-slip condition. Therefore there are a myriad of locations within what is normally considered the main flow field, where the flow velocity is zero. In each of these locations the resisting force from Newton's 2nd Law—normally ascribed only to the channel boundary—is applied to the flow by the vegetation.

However the effects of the individual stems and leaves can be simplified. Under certain sets of vegetative conditions, I submit that the vegetative mass acts as a coherent unit; and that in fact the boundary of the vegetative mass can be treated as an extension of the boundary of the channel. A corollary to this assertion is that the interior of the vegetative mass is effectively removed from the field of flow.

This chapter includes the results of three separate experimental efforts. The first effort consisted of flow studies wherein water was forced to flow through masses of submerged aquatic vegetation and the energy slope was measured. This work provided an estimate of energy loss as a function of vegetation density and flow velocity. The second effort developed data depicting the flow structure around and within a variety of submerged aquatic vegetations. And the third effort developed baseline information on the morphological response of hydrilla to drag forces. The goal of this work was to quantify the effects of vegetation on the flow and vice versa.

---

[12] The definition of a Newtonian fluid is not limited to being near a boundary. However it is applicable as described and is described so herein for succinctness.

ENERGY LOSS IN FLOW THROUGH SUBMERGED AQUATIC VEGETATION

One of the basic questions in the effort to evaluate flow in vegetated channels is how much flow is occurring within the vegetation itself? I suggest that flow through aquatic vegetation with any significant density requires a much higher expenditure of energy than flow in an open channel, which is resisted primarily by friction on the wetted perimeter.

Measurement of Headloss in Bench Channel

I began this project with work in a small channel. The bench channel was designed to allow me to grow vegetation in the channel and then conduct flow experiments. Due to legal issues with growing hydrilla in Washington State, I used several common aquarium plants which are approximate analogs to hydrilla. For each plant type, individual leaves grow in whorls at intervals along flexible stems. The leaves for all types are approximately 1 cm long.

My goal for this channel in this phase of the research was two-fold. First I wanted to establish that measurement of energy slope across a short length of plant mass was feasible. And second I needed to be able to observe flow within the matrix of the vegetation. Both efforts were successful.

The measured surface slope was on the order of 0.5 to 1.0 mm per meter, when forcing water through very dense vegetation at approximately 2 to 3 cm/sec. The slope data was collected by measuring the water surface elevations at two stations, one at the beginning of the vegetative mass and the second at the end of the vegetative mass. Water surface elevations were first marked under zero flow conditions; then with water flowing through the vegetation the water level at both stations was marked and the change in elevation at each station was measured. The difference between the two stations (change in water surface elevation through the vegetation) was then divided by the distance between the stations to calculate slope. This test was conducted twice for the compacted (very dense) vegetation conditions, which was the only condition which yielded a detectable slope.

During these tests, the water surface elevation was slightly less than the height of the vegetation, with the vegetation lying firmly over on the substrate. Under these conditions the vegetation density is characterized as “compacted.” That is, rather than the vegetation being supported by

buoyancy, it is supported by the substrate from below and weighed down by the only partially supported (by buoyancy) weight of the vegetation above.

This is not a particularly common flow scenario in working canals. Presumably the only time you would see this condition is when flow was just being initiated in a canal that has been drawn down temporarily. Nevertheless it provided a first data point and established that measurement of energy loss was in fact feasible. For additional data that provided more resolution, we turned to investigations in the greenhouse channel.

Measurement of Headloss in Greenhouse Channel

The test section of the greenhouse channel is approximately 600 cm long, ranging from Station 1—which is 37 cm from the pump intake—to Station 6, which is 634 cm from the pump intake. A flow straightener was used immediately upstream of Station 6 to reduce the scale of turbulence in the test section.

The vegetation (hydrilla) in this channel varied in density from one end of the test section to the other, ranging from sparse at Station 1 to dense at Station 6. Appendix A provides a pictorial characterization of the vegetation density used in this work.

Table 5.1 characterizes the vegetation along the segments of the test section. Each segment encompasses the area between two stations. Thus segment 1-3 consists of the length of test section between Station 1 and Station 3[13].

The vegetation also varied in density according to its position in the water column, with the greatest density being at the top. The vegetation characterization given in Table 5.1 is based on a water depth of 45 cm and provides density estimates based on this depth.

[13] Station 2 was established at the beginning of the data collection effort, but was not used for water surface slope data collection.

Table 5.1. Vegetation densities by depth in the greenhouse channel. Water depth of approximately 45 cm

	Depth Block (Distances from Bottom)		
Segment	0-15 cm Bottom	15-30 cm Mid-Depth	30-45 cm Surface
1-3	sparse	light	medium
3-4	sparse	light	dense
4-5	sparse	light	dense
5-6	light	medium	dense

Figures 5.1a through 5.1d show the measured water surface slope, for each segment and for a range of discharges and water depths.

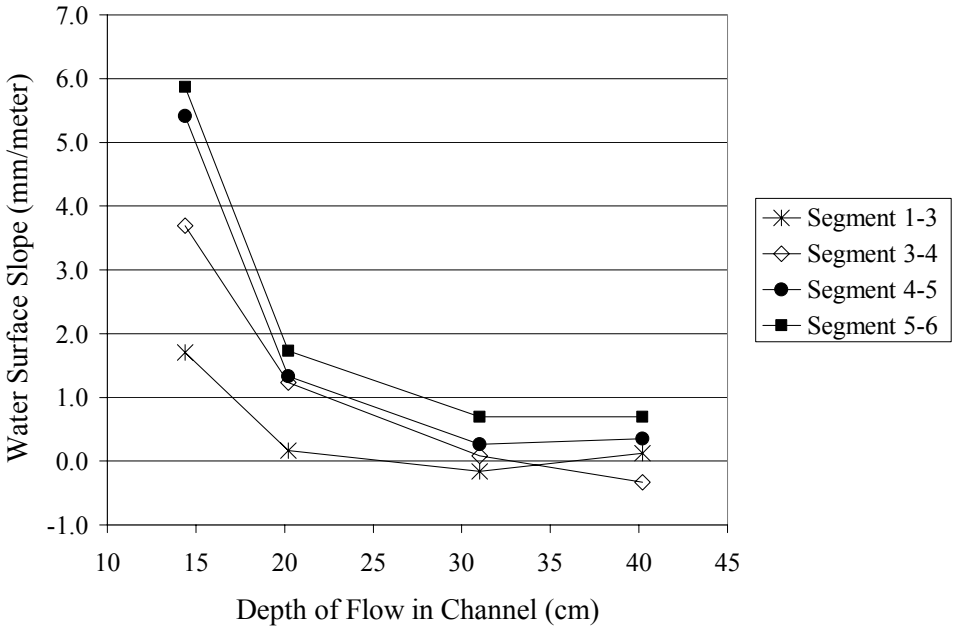

Fig. 5.1a. Water surface slope as function of depth; Q = 3.8 l/sec. See Table 5.1 for vegetation densities corresponding to segments

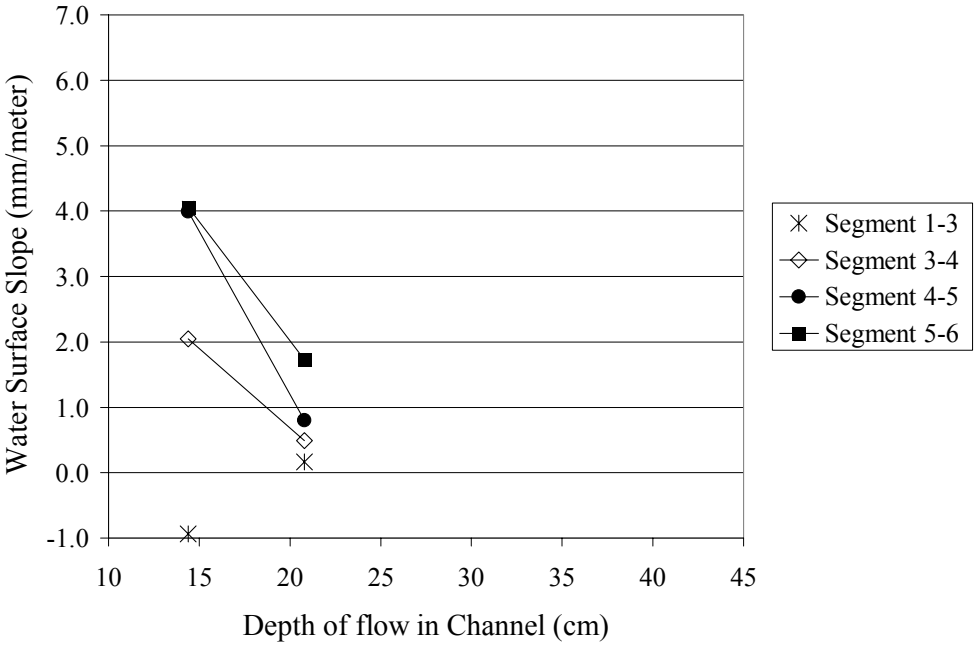

Fig. 5.1b. Water surface slope as function of depth; Q = 3.1 l/sec. See Table 5.1 for vegetation densities corresponding to segments

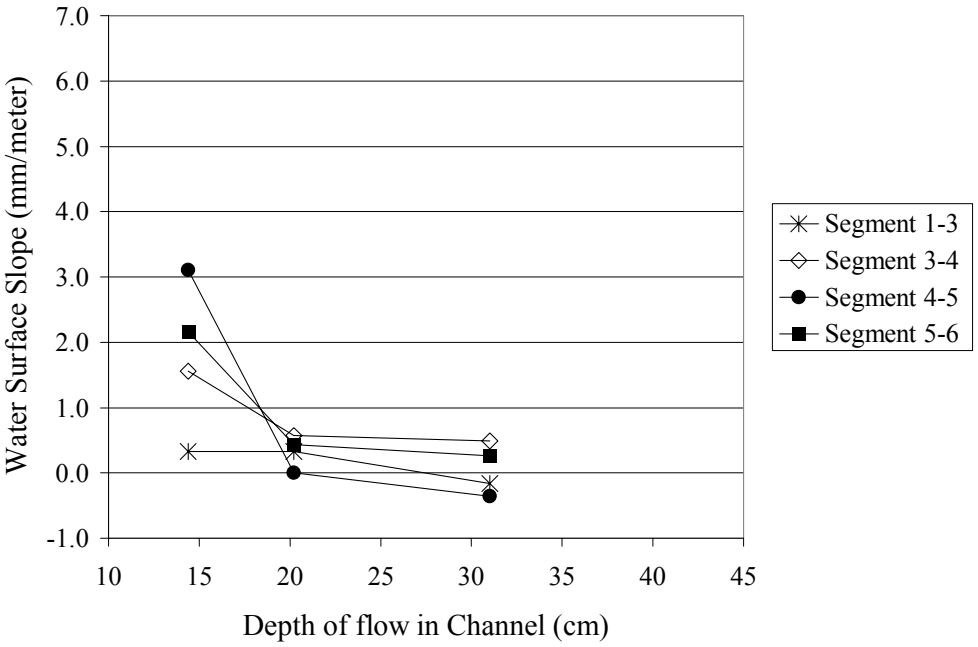

Fig. 5.1c. Water surface slope as function of depth; Q = 2.2 l/sec. See Table 5.1 for vegetation densities corresponding to segments

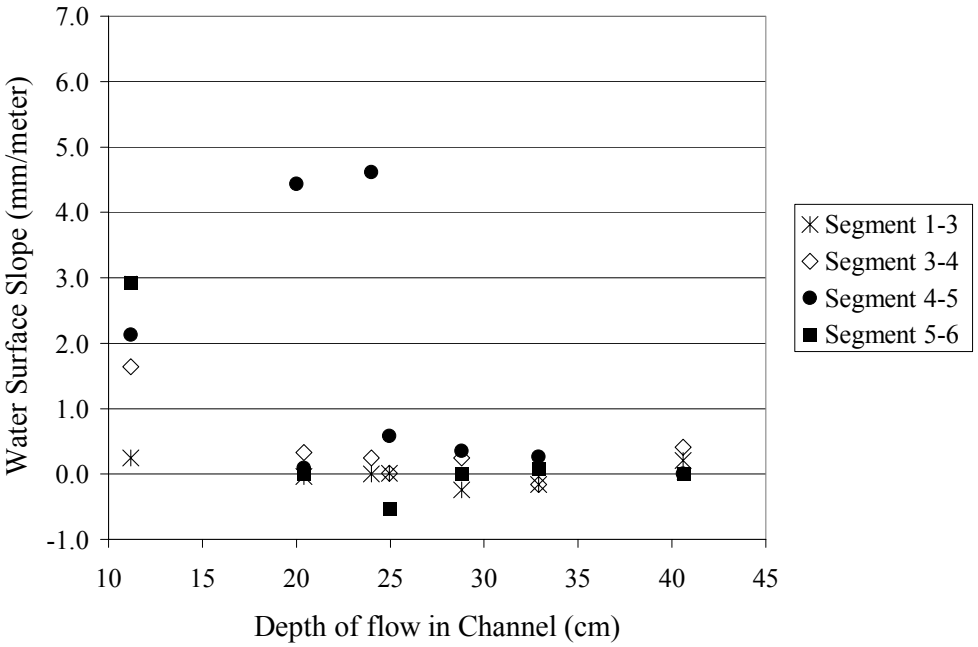

Fig. 5.1d. Water surface slope as function of depth; Q = 1.4 l/sec. See Table 5.1 for vegetation densities corresponding to segments

---

The negative values in the above graphs resulted from inaccuracies in the data collection process. Measurement of the water surface elevation involved use of an angled mirror and a flashlight and also required some interpretation of the meniscus associated with surface tension. The negative data points were included here for completeness, but are not included in the analysis. In addition the lines connecting the data points were removed from Figure 5.1d for clarity.

The above graphs do not fully describe the vegetation density however, as for greater water depths the water can bypass the dense vegetation and flow along the bottom of the channel where the vegetation is less dense. When the water depths were greater, I did in fact observe higher flow velocities in the lower water column, combined with near zero flow in the surface (dense) vegetation.

To address this issue, the next step uses data drawn only from the tests with lower water surfaces (depth of flow reduced). In addition the data was graphed in terms of the calculated flow velocity instead of the discharge. And finally the vegetation was characterized in terms of three densities, light, dense and compacted. The latter occurs when vegetation is so dense that it supports some vegetation in the air column above the water surface. The (compacted) density occurred in our tests in the upper part of the channel (segments 4-5 and 5-6) when the water depth was at or below 15 cm. Figure 5.2 shows the results for all three types of density.

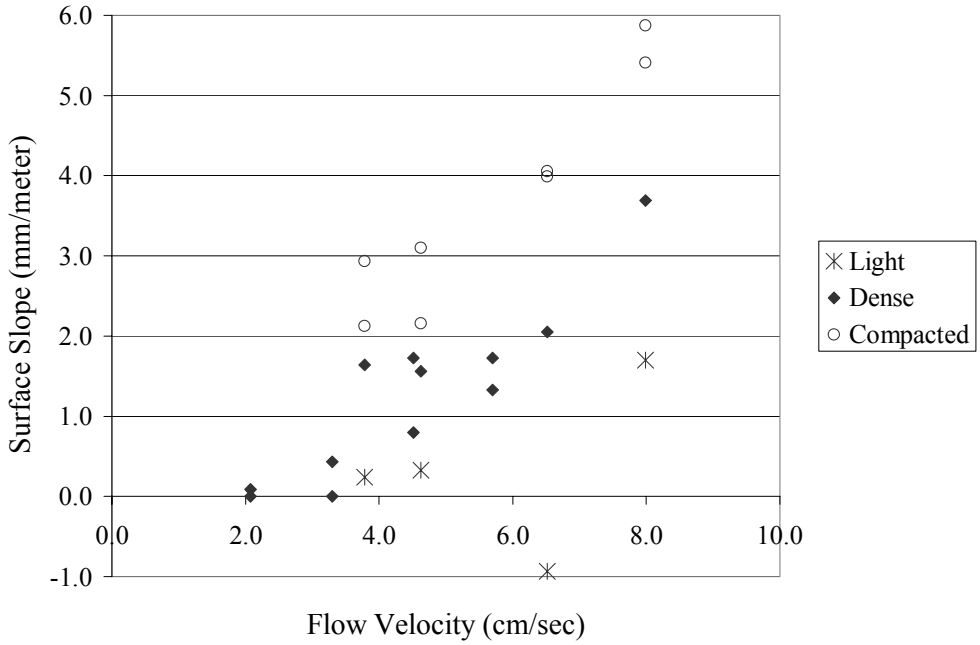

Fig. 5.2. Water surface slope as a function of flow velocity and vegetation density

Figures 5.3a through 5.3c show each of the vegetation densities separately. Each figure also shows a function, which approximates the surface slope as a function of flow velocity for each density. These functions are estimated visually, assuming a paraboloid shape which has a zero y-intercept.

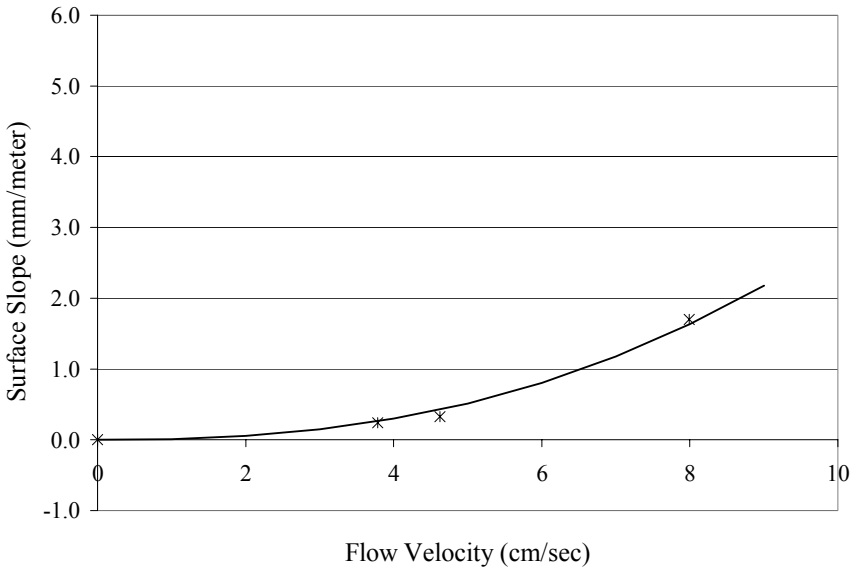

Fig. 5.3a. Water surface slope as a function of velocity; vegetation is light. (density)

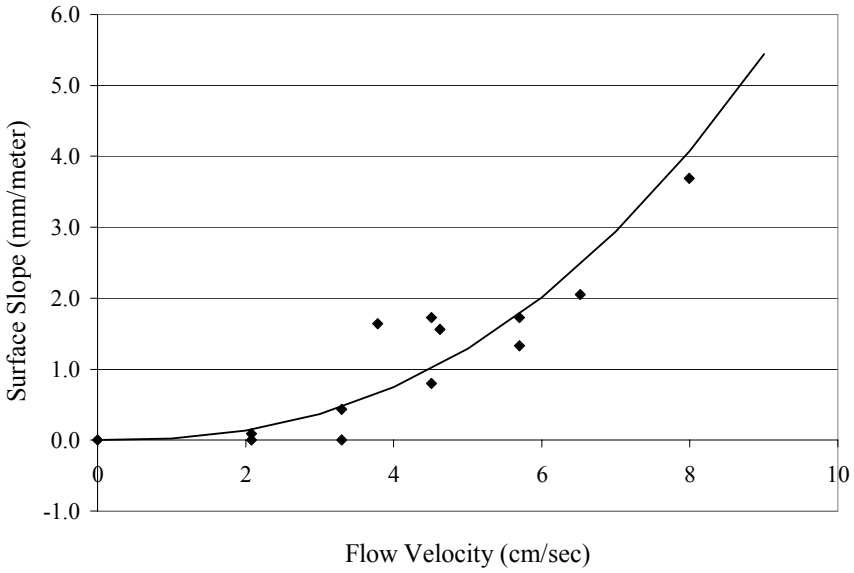

Fig. 5.3b. Water surface slope as a function of velocity; vegetation is dense

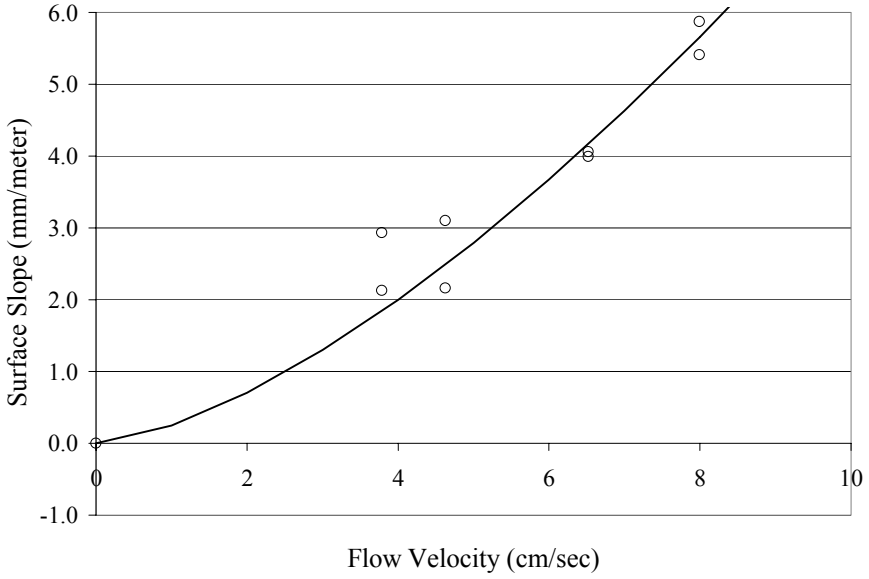

Fig. 5.3c. Water surface slope as a function of velocity; vegetation is compacted. (vegetation is dense enough that some protrudes above the water)

The functions shown in the above graphs are all of the form:

$$S = aU^r \qquad (5.1)$$

where:

S = water surface slope or energy loss (mm/meter);

U = the average flow velocity (cm/sec); and

a and r are fitting parameters.

The values of a and r for the above three examples are shown in Table 5.2.

Table 5.2. Fitting parameters for estimating water surface slope as a function of flow velocity and vegetation density

	Values for three vegetation states		
Parameter	**Light Density**	**High Density**	**Compacted**
a	0.01	0.025	.25
r	2.45	2.45	1.5

Solving Eq.5.1 for flow velocity or *U* yields Eq.5.2:

$$U = \left(\frac{S}{a}\right)^{\left(\frac{1}{r}\right)} \tag{5.2}$$

The values in Table 5.2 are empirical parameters developed from the measured data shown in Figures 5.1(a-d) and 5.3(a-c). Charting Eq.5.2 with the values provided in Table 5.2 for the three types of vegetation, yields the lower three lines in Figure 5.4.

For comparison to the empirical functions (lower three lines) we have also charted representative functions for two canal sections (Channels A and B) using the Manning equation (n = 0.02). Channel A is a rectangular channel that is 2.5 meters wide with a flow depth of 1 meter.

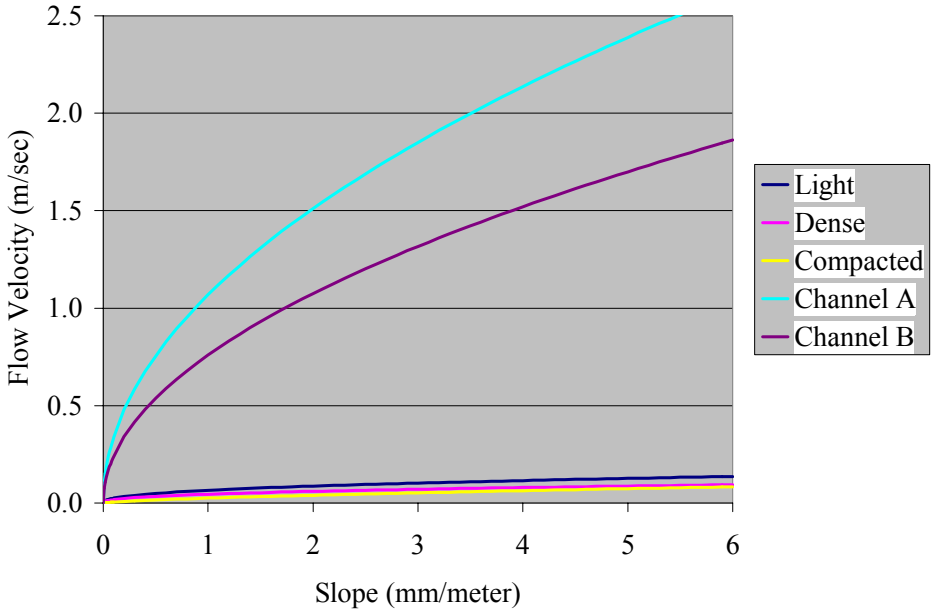

Fig. 5.4. Flow velocity as a function of energy loss. Cases include vegetation characterized as light, dense and compacted and two small irrigation canals with typical parameters

Channel B is the same channel with a 0.5 meter wide section taken out of the center (to represent a central mass of vegetation. Channel B is then treated as the sum of two independent channels; each 1 meter wide and 1 meter deep. The vegetation that makes up one side of the two sub-canals is assumed to have the same roughness coefficient as the channel boundaries. Channel B is intended to approximate Channel A with the central 0.5 meter occupied by vegetation.

As Figure 5.4 shows, the flow velocity in the free water flowing area of the canal will be significantly higher than the flow velocity in the vegetation. This is the case even for vegetation characterized as light density.

VELOCITY GRADIENTS IN AND AROUND SUBMERGED AQUATIC VEGETATION

The goal of the effort discussed in this section was to develop information about the structure of flow velocities in and around submerged aquatic vegetation. To achieve this, I collected data in

two environments; the bench channel in my Seattle lab and the field channel at the Extension Center in Weslaco, Texas.

As described previously, the bench channel was constructed of acrylic, which allowed visual observation of flow patterns, both within the vegetation and above it. Acetate sheets with 1 cm grids printed on them were attached to the side of the channel. A video camera was set up approximately 1.5 meters away from the channel and focused through the grid to a point in the middle of the channel. During flow tests I introduced particles into the flow to act as tracers. A variety of materials were tested, but sawdust proved the most effective. Sawdust is typically composed of a large range of particle sizes and while some were too large or small, there were generally enough that were both large enough to see on the video tape and small enough to track the flow.

The field channel was constructed to allow study of flow both around the vegetation masses and over the top. During the initial data collection effort in July of 2007, the vegetation was confined to a strip down the center of the channel; and flow velocities were collected in the free-water areas to either side of the vegetation mass.

By the time of the final data collection effort in October, 2007 rooted vegetation had spread to the full width of the channel. During the October effort the initial flow configuration was similar to that in the bench channel. That is, there was flow within a continuous vegetative mass and a shallow flow over the top of the mass.

However during the October tests in the field channel, the flowing water quickly established a channel within the vegetation by forcing the vegetation to either side. The flow that was observed in this "induced" channel is discussed herein. The resulting data and the analysis for each channel are described in the following sections.

Bench Channel

The bench channel was transparent, with walls constructed of 12.7 mm (0.5 inch) acrylic. The flow channel within the structure was approximately 22 cm wide. The length of the planting section in the channel can be as long as 150 cm; however the effective length for most of this work was approximately 90 cm. The vegetation was planted full width, initially with 8 plants in

each row. The plants were spaced at approximately 2.75 cm in the row, with one half of a space between the plants at each end of the row and the walls of the channel.

Primary data collection consisted of videotaping particle motions in the flow through and above the vegetation. Post processing involved tracking individual particles as they moved past the grid on the tank wall. This method was used to produce the data shown in this section.

I developed velocity profiles through and above the vegetation for the two sets of vegetation density parameters. In the case of the dense vegetation (8 plants per row and 5 cm between rows) the vegetation mass was continuous for approximately 90 cm (Fig. 3.2). In this case we tested the velocity distribution at two different locations. The first location was 15 cm downstream of the leading edge of the vegetation and the second was 50 cm downstream.

The two tested locations (15 and 50 cm) were selected to allow evaluation of how the velocity distribution changes as it moves through the bank of vegetation. The two locations were also tested with multiple water depths and discharge rates, to evaluate how these parameters affected the velocity distribution.

I collected a second set of data for the less dense set of vegetation (5 to 6 plants per row at 10 cm between rows). This clump of vegetation was also shorter in the direction of flow. That is the length of the bank of vegetation was approximately 40 cm from leading edge to trailing edge. The data in this test provided comparisons with the first dataset. The evaluations in the two vegetation setups are discussed further below.

Velocity Distribution in Dense Continuous Vegetation

For this set of tests the bank of vegetation was relatively dense and continuous for approximately 90 cm. The plants were arranged in rows of eight plants with 5 cm between each row. The vegetation was approximately 14 cm high (h_{veg}).

Two test sites at 15 cm and 50 cm downstream of the leading edge of vegetation were studied at several different combinations of flow rate and water depth. For the initial effort, the flow was set at 0.54 liters per second, with a water depth of 16 cm, or approximately 2 cm above the top of the vegetation. The resulting velocity distributions are shown in Figures 5.5 and 5.6.

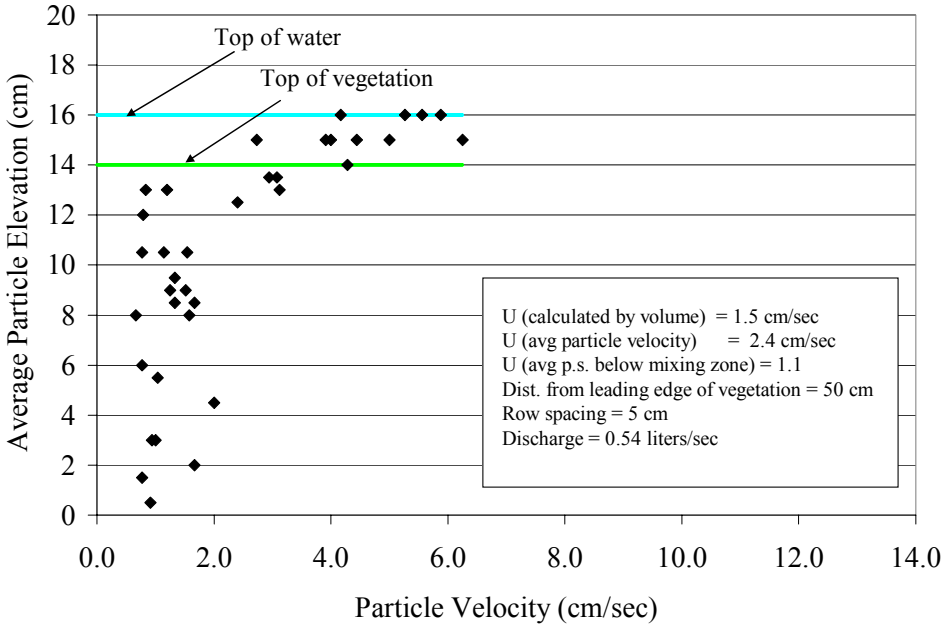

Fig. 5.5. Velocity distribution 50cm downstream of leading edge of vegetation (Q=0.54 cm). Note nearly vertical or constant velocity within the lower vegetation and a mixing zone in the upper two cm of vegetation

It should be noted that the velocities shown in the graph are one dimensional in the x direction (main direction of flow). The particles frequently had a measurable vertical velocity, as well (presumably) as a cross-channel velocity that would not have been detectable with the measurement method. However the cross-channel velocities as well as the vertical velocities must necessarily have averaged out to zero. In addition the vertical velocity information would have been compromised by the density of the tracer particles. Sawdust has a range of densities. Some of the particles sank to the bottom and stayed. However, the smaller particles appeared to track well and any vertical motions were excluded from the dataset.

Figure 5.5 shows a nearly constant velocity in the lower part of the vegetated water column. The velocity range increases in the upper part of the vegetation. This supports the hypothesis wherein flow in the lower vegetative mass is controlled by the pressure gradient along the canal; while the flow in the upper vegetation is defined by a mixing zone (Nepf and Vivoni 2000). This mixing zone transitions between flow velocities in the free water column above the vegetation and velocities in the pressure gradient-driven flow in the lower vegetation. The

mixing in the upper vegetation is driven by turbulent mixing from the higher energy flows in the free water column.

In Figure 5.6 below, higher velocities are distributed much more deeply into the vegetation. This dataset was collected upstream of the dataset in Figure 5.5 (approximately 15 cm downstream of the leading edge of the vegetation). The water column at the leading edge of the vegetation would have turbulence and higher velocities in the lower water column. These would impact the leading edge of the vegetation and some of the higher velocity water particles would propagate into the vegetation—including in the lower water column. However the higher velocities and larger scale turbulence would tend to be damped or filtered out by the greater resistance of the vegetation. As the observer proceeded downstream therefore, the higher velocities would be filtered from the lower water column, leaving only the velocities that continued to be supported by the pressure gradient.

Figure 5.7 again shows flow conditions at the 50 cm station. However the flow has been increased from 0.54 liters/sec to 1.23 liters/sec. Comparison with Figure 6.1 shows significantly higher flow velocities in the lower vegetation. However, once again the average velocity appears roughly constant—with respect to depth—when below the mixing zone.

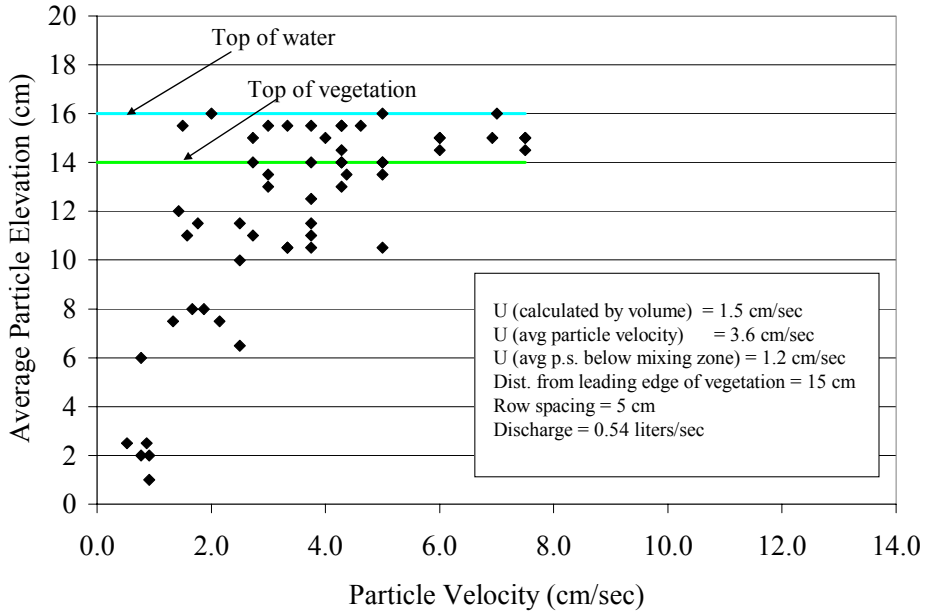

Fig. 5.6. Velocity distribution 15 cm downstream of leading edge of vegetation (Q = 0.54 l/s)

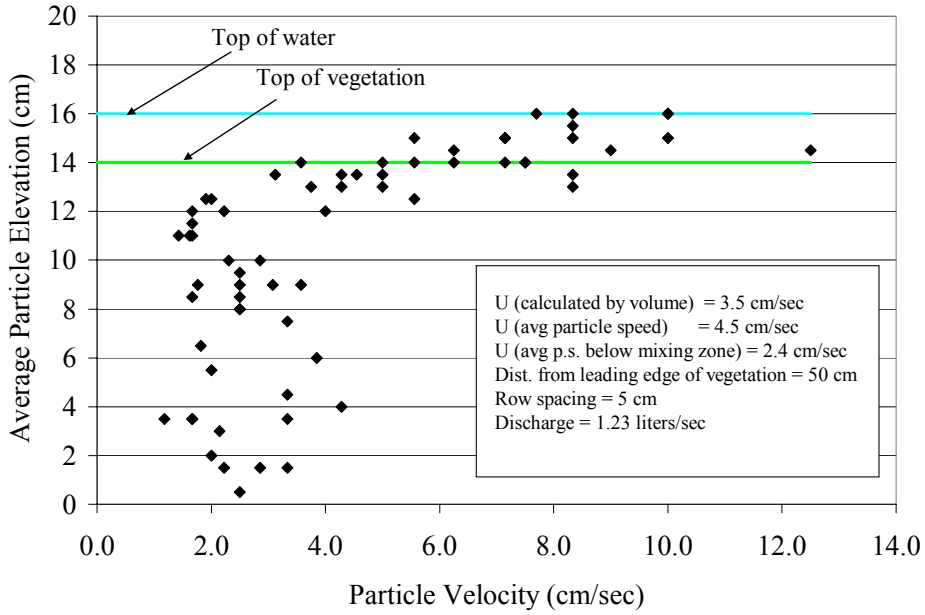

Fig. 5.7. Velocity distribution 50 cm downstream of leading edge of vegetation (Q = 1.23 l/s)

Figure 5.8 shows test results with the water surface level dropped to a depth of 8 cm. The top of the vegetation dropped with the water surface, so vegetation that had previously been distributed over a 14 cm depth was now confined to 8 cm. The primary purpose of this test was the previously described measurement of water surface slope in "compacted" vegetation. Figure 5.8 depicts the velocity distribution with this setup and a reduced discharge of 0.36 liters per second.

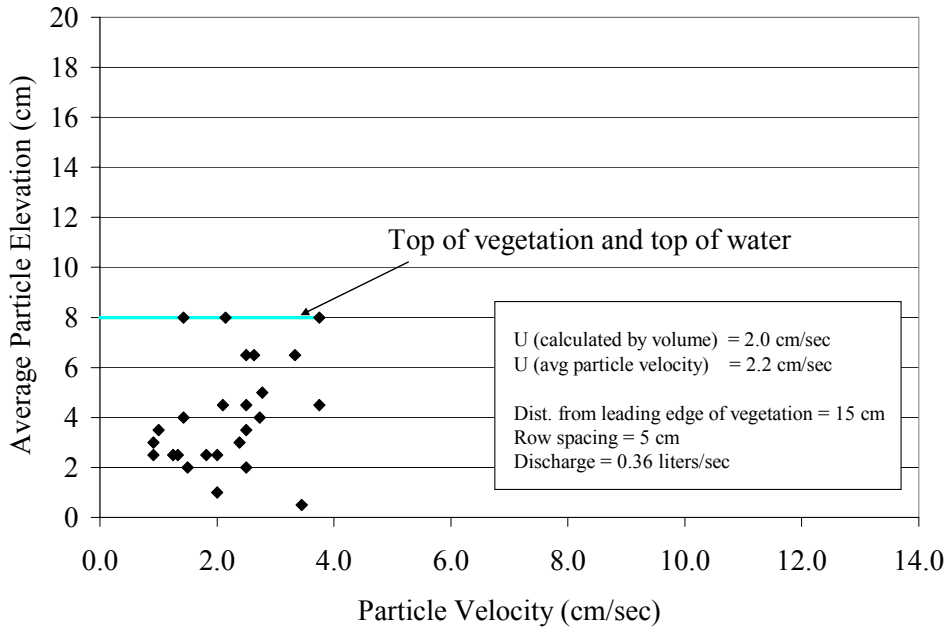

Fig. 5.8. Velocity distribution in compacted vegetation

One interesting aspect of this data set was the comparatively broad range of velocities in the confined space. One additional factor that is not demonstrated by the graph is that the streamline tracks were highly irregular. This indicates that the water was wending its way through the vegetation mass. This phenomenon was much more pronounced than in the previous tests.

And it should be noted that the average particle velocity is greater than the average velocity would be (discharge/total cross-sectional area) if there were no vegetation. This infers that a porosity parameter K_p would be required, if particle tracks were used to establish average flow

velocities. Because the average particle velocity is slightly larger than the average velocity U (calculated volumetrically), one could infer a porosity $K_p = U_{vol}/U_{vel}$. Where U_{vol} is the average velocity by volume (Q/A) and U_{vel} is the average particle velocity.

Velocity Distribution in Patchy Vegetation

This set of tests was run using the less dense growth of vegetation (5 to 6 plants per row at 10 cm between rows). In addition to being less dense, the bed of vegetation was approximately 40 cm long and the vegetation was only approximately 10 cm high. Measurements were taken in the center of the bed, or approximately 20 cm downstream of the leading edge of vegetation.

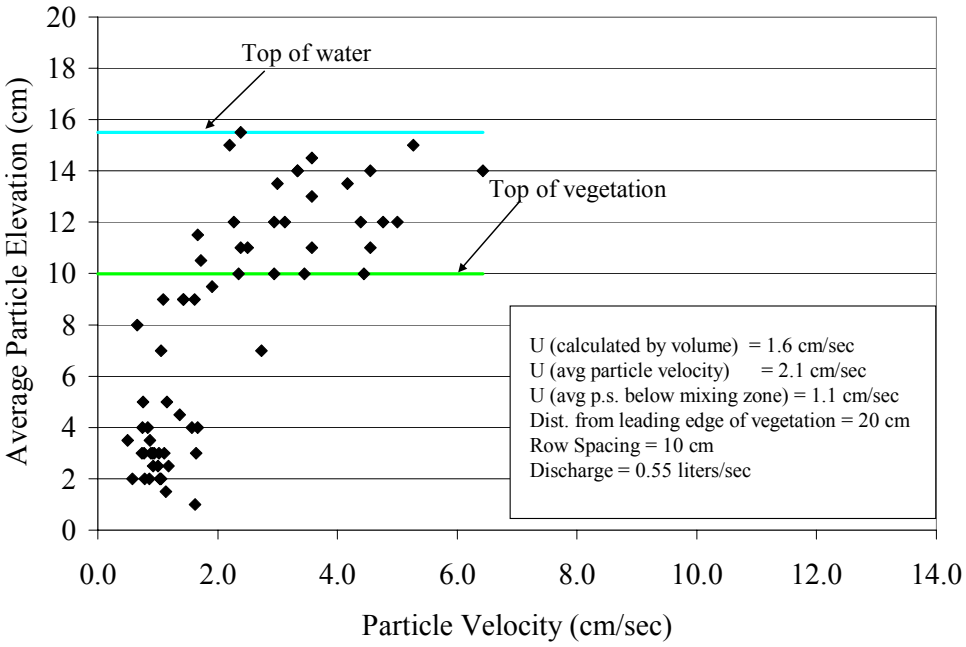

Fig. 5.9. Velocity distribution 20 cm downstream of leading edge of lower density vegetation (Q = 0.55 l/s)

For the lower discharge (0.55 liters/sec) Figure 5.9 still shows a relatively steady velocity in the lower vegetation. In fact the calculated average velocity below the mixing zone is the same in Figure 5.5 and Figure 5.9, although the former has the higher planting density. This may be due

to the fact that in the flow studies represented by Figure 5.9 the vegetation leaned over more, primarily due to the lesser amount of vegetation and its ability to move more. So in fact the vegetation in the latter case may approach the density of the vegetation in the earlier more dense plantings.

Figure 5.10 shows the test in the lower density vegetation at a higher flow rate of 1.29 liters/sec. This figure still shows higher flows in the free water column, lower flows in the lower vegetation and a mixing regime in the upper vegetation. However the flows in the lower vegetation are clearly higher than in Fig 5.7 (note change in horizontal scale of graph) which had similar flow depths and discharge. This vegetation bed is both shorter and less dense and the observation point is closer to the leading edge of the vegetation. Therefore the higher velocity fluids as well as the turbulence from the open water—which were dissipated by the longer denser bed of vegetation in the earlier figures—is propagating further into and through the lower vegetation.

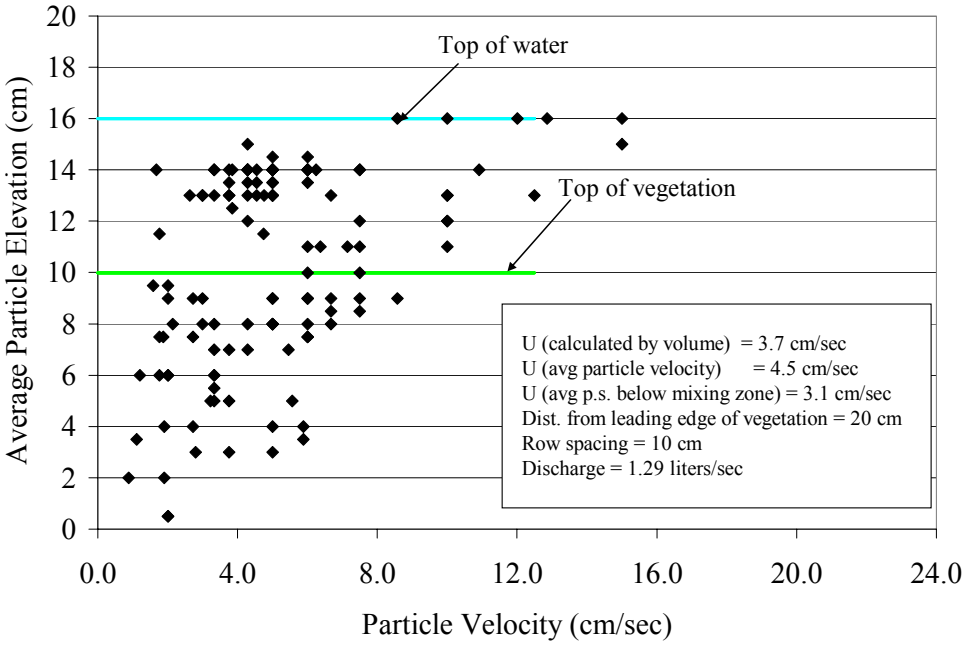

Fig. 5.10. Velocity distribution 20 cm downstream of leading edge of lower density vegetation (Q = 1.29 l/s)

Some discussion of the data collection methodology used herein (visual recording of particle velocities from videotape) is appropriate. First of all the selection of particle tracks is not necessarily random, primarily because we do not have visual access to the full study area. Second the vegetation is not heterogeneous and where there are significant masses of vegetation against the side of the channel, there may be less particles available for viewing and recording.

In addition, the sampling is going to be weighted more towards the viewing side. To reduce this effect, the video camera was deliberately focused on the center of the channel, which is relatively narrow. This combined with the uniform planting should reduce the impact of this issue.

The third issue with the sampling is that the higher velocity particles were more difficult to record. The video equipment allowed a frame by frame advance (30 frames per second). This allowed the viewer to count the number of frames it took a particle to cross a known distance, providing a calculated velocity. However in frame advance mode, the small particles tended to blur and become less visible. The tendency therefore may have been to select more of the slower particles. This is indicated in the upper 6 cm of flow in Figure 5.10, where there are many more records in the 3 to 7 cm/sec range than in the upper velocity ranges (8 to 16 cm/sec).

Therefore I retained the presentation of actual data, rather than presenting the more traditional mean and range type data. This presentation provides the actual range of the data, without making any judgments regarding the distribution. Meanwhile the fact that there is a wide range of velocities at the same elevation infers information about the stability of flow and the level of turbulence in the flow.

Summary Conclusions from Bench Channel Data

The data supports the hypothesis that there are two forcing mechanisms for flow in aquatic vegetation. One forcing mechanism is the traditional pressure gradient associated with flow in any channel and which must pertain in the vegetation as well. The other mechanism is turbulent mixing into the vegetation from flow outside the vegetated area. This mechanism is limited to a mixing zone that reaches into the vegetation, from the interface between the vegetation and the open water. The size of this mixing zone (how far it intrudes into the vegetation) is a function of

vegetation density, flow velocities or energy and the scale of the turbulence. As will be discussed later in this document the ability of the vegetation to move and respond to the flow also can have a significant impact.

At or near the leading edge of a bank of vegetation, it appears that turbulent mixing into the vegetation occurs over nearly the full depth of the vegetation. The data suggests that as one moves downstream in the vegetation bank, turbulent mixing and higher velocities are filtered or damped out and become restricted to the areas of vegetation nearest to open water flow. For the conditions studied, the elimination of the higher energy flows associated with turbulence and open water occurred within the first 40 cm of the vegetative mass.

The separation of flow regimes would also presumably extend to open water flow on either side of a bank of vegetation as well. If as proposed previously and shown in Figure 5.11, the vegetation is limited to the center of the canal, with open water flow above the vegetation and on both sides, then flow in the center of the mass of vegetation could be driven by a pressure gradient roughly equivalent to the slope of the main channel. There would be a mixing zone around the perimeter of the vegetative mass, which would transition average flow velocities from the pressure gradient flow in the center of the vegetation to the pressure gradient flow in the open water column.

It is reasonable to postulate that, given a steady state condition such as the one represented by Figure 5.11, the pressure gradient driving the flow in the vegetation would be equivalent to the slope of the channel itself, as well as to the pressure gradient driving the flow in the free water zone. The transition zone between the two regions would be governed by the difference between the two and by the scale of the turbulence in the outer free water zone.

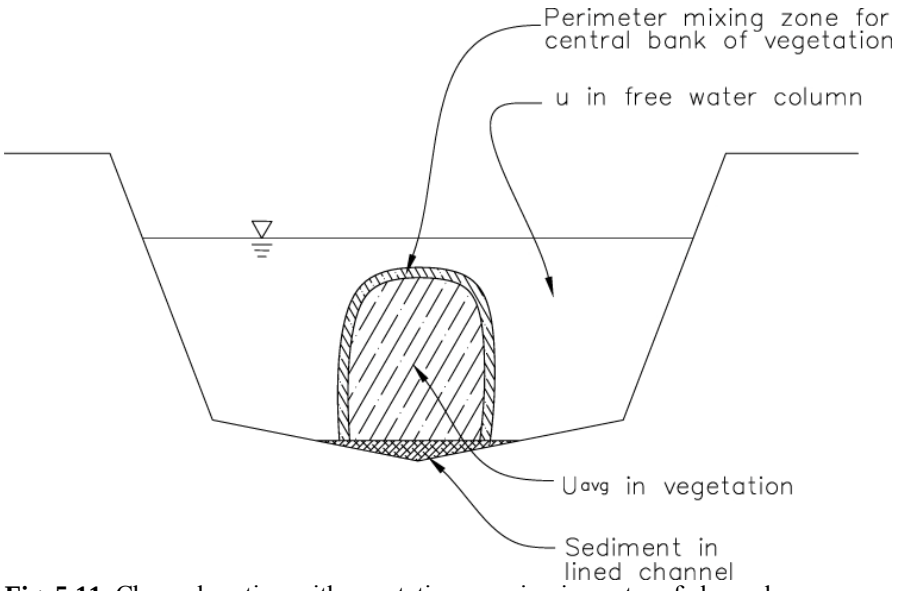

Fig. 5.11. Channel section with vegetation growing in center of channel

Field Channel

The field channel was designed to allow examination of flow around vegetative masses, both flow along the sides and flow over the top of the vegetation. As has been discussed previously, the process of developing the vegetation stocks for the flow studies was much more challenging than anticipated. Nevertheless we were ultimately able to develop the necessary stocks of vegetation and conduct the requisite flow studies.

There were two distinct episodes of data collection. The first was in July, 2007 and the second was in October of the same year. In the first episode the channel and vegetation morphology was similar to that shown in Figure 5.11. That is vegetation was growing in the center of the channel, with open water on either side of the vegetation.

By the time of the second data collection episode in October, the vegetation had spread throughout the channel cross-section and was growing essentially, “wall-to-wall”. During this episode, we observed the formation of an induced channel in the vegetation. That is an open channel formed approximately in the center of the vegetation. This channel was apparently

formed by flowing water moving the vegetation out of the way, which would allow flow to occur in a lower resistance regime.

Flow with Vegetation Restricted to the Center of the Channel

During this data collection episode I tested a range of instruments for measuring flow velocity. However the combination of very low flow velocities and small flow areas rendered most of them unusable. Ultimately the data was collected using dye tracers. This section briefly describes the issues associated with the instruments; then describes the data obtained from the dye studies.

This effort included testing a Flow Tracker Handheld ADV, a Price Type-AA propeller meter and an Argonaut SW, but I was unable to collect useful datasets from any of the three. There were three main issues associated with this. The first was the relatively low flows being examined in the tests. The tests resulted in water velocities on the order of 0.1 meters per second, which was at the lower end of the detection range for all three instruments. In addition, in the case of the two handheld instruments the submersed part of the instruments took up a significant portion of the flow cross-section. It appeared that the instruments themselves disrupted the flow, perhaps further reducing the velocities in the area of the instrument heads.

Acoustic Doppler instruments are known to be sensitive to interference from aquatic vegetation, which tends to absorb the acoustic signal, rather than reflect it back. The field channel was approximately 120 cm wide at the base and the central 30 to 40 cm of this channel was taken up by vegetation. The two acoustic instruments were unavoidably in proximity to the vegetation, so there may have been some interference there. I was unable to collect a useful electronic dataset from these instruments and instead used video equipment and dye tracers. While this did not provide information on the flow structure in the lower water column, the data provided comparison of flow in the vegetation with flow in the free water—at the water's surface.

The data was collected with two different water depths in the channel and is presented in Table 5.3. With the vegetation in the center of the channel, the flow occurred in two side passages which formed two separate channels. During the first set of tests the downstream control structure was set so the water was flowing through the test section at a depth of 20 cm. In this

case the vegetation was surfaced in the center and formed a surface mat. During this test the surface velocities in the vegetation was zero.

The average velocities in the side channels were calculated as follows. After measuring the cross-section of each side channel, the areas of the two channels were found to be within 2 percent of the average. The discharge was assumed therefore to be assigned to each side channel proportional to its cross-sectional area. Flow throughout the vegetation was assumed to be zero. Average velocities (U_{avg}) were calculated by dividing the attributed discharge by the measured area. Table 5.3 compares the calculated average velocities for each side channel to the measured surface velocities in the same channel.

Table 5.3. Water velocity measurements during tests in field channel. Vegetation is growing in center of the channel. Channel segments include a left channel, right channel and the center strip with the vegetation to the surface of the water.

Flow Depth	Position of Velocity Measurement in Channel	Measured Surface U_{surf} (cm/sec)	Calculated U_{avg} (cm/sec)	U_{surf}/U_{avg}
The following measurements were taken at a total discharge of 29 liters per second				
20	center of left channel	16	16	1.0
20	left channel 10 cm to left of vegetation	4	16	0.25
20	center of right channel	20	16	1.3
20	center of vegetation	0		
The following measurements were taken at a total discharge of 10 liters per second				
20	center of left channel	7	6	1.2
20	center of right channel	8	6	1.4
20	center of vegetation	0		
The following measurements were taken at a total discharge of 28 liters per second				
35	center of left channel	12	8	1.6
35	center of right channel	11	8	1.4
35	center of vegetation	~1		

During the flow test at the greater depth (35 cm) there was some water above the vegetation, and some very minor flow. Individual stems of vegetation still broke the surface and there were substantial additional areas of vegetation within 10 cm of the surface, however there was not a surface mat. In this situation the flow above the vegetation was on the order of 1 cm/sec. It was

not feasible to determine the vertical structure within the vegetation, due to the opacity of the water and the aforementioned instrument limitations.

Surface velocities were measured with dye tracers and video equipment. Surface velocity measurements were taken in the center of each side channel and in the center of the vegetation. Velocities were measured at an additional point very close to the edge of the vegetation, yet still in the open water. Due to the rapid diffusion of the dye tracer, it was impractical to use this to measure a precise velocity distribution relative to the flow. However, the flow in the vegetation was zero; the flow approximately 10 cm away from the edge of the vegetation was 4 cm per second; and the flow in the center of the left channel (approximately 24 cm from the vegetation) was 16 cm per second. This relation is shown in Figure 5.12.

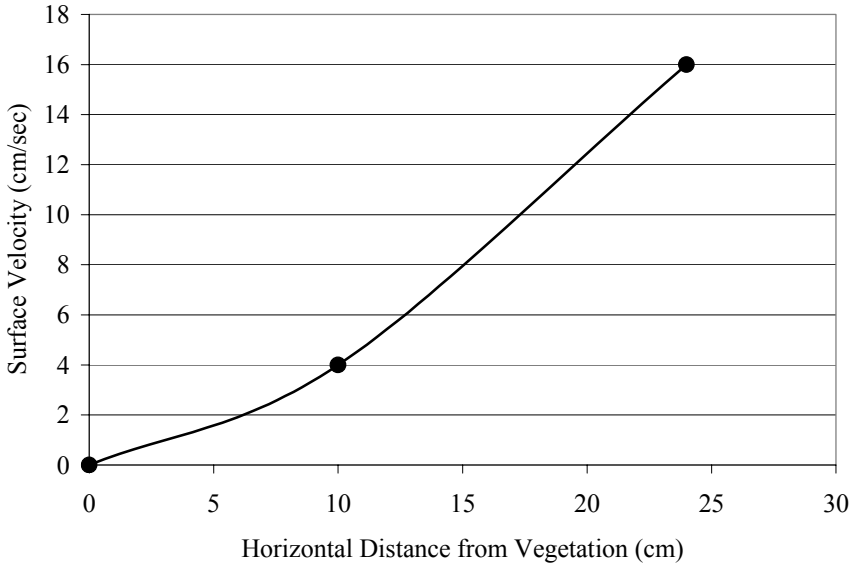

Fig. 5.12. Approximate surface velocity distribution in field channel. Surface flow distribution in side channel along a normal to the edge of the vegetation

The relation shown in Fig. 5.12 is problematic as one generally expects the velocity to asymptote to some maximum central velocity. However in this figure the velocity gradient remains nearly constant. This figure should not be utilized for evaluating velocity gradients.

Flow with Induced Channel in Center of Vegetative Mass

After concluding the data collection effort in July of 2007, I identified an alternate instrument which was expected to provide a more detailed picture of the flow in the vegetation. The instrument identified is a *Vectrino high resolution acoustic velocimeter* and provides 3-dimensional flow data from a relatively small sampling volume. I rented the instrument from the manufacturer[14] and scheduled an additional data collection episode in October.

By the time I returned to the site in October however the vegetation morphology had changed substantially. The hydrilla had spread until there were plants growing in the substrate for the full width of the channel. The water in the channel had been maintained at a depth of approximately 30 cm and the vegetation appeared to have grown to somewhat higher than this height and lain partially over (Figure 5.13). The channel was completely full of vegetation.

Fig. 5.13. *Hydrilla verticillata* growth in field channel (October 2007). The thinner more yellow plants are probably from the original plantings in the trays, whereas the fuller green plants are newly grown

[14] NortekUSA

However, almost immediately after we began pumping water through the field channel, the flow created a secondary channel in the surface of the vegetation. This secondary channel was induced by the flow—approximately in the center of the vegetation. The induced channel formed as the flow worked through the vegetation, moving it aside to create a continuous opening through the vegetation.

The induced channel began at the water surface, approximately in the center of the main channel, with its main axis parallel to the axis of the main channel. This channel was approximately 27 cm deep and 20 cm wide; and it appeared to be shaped roughly like a parabola. See Figure 5.14.

Two smaller channels were also formed along the sides of the field channel. These formed against the slope of the channel side, where the lining on one side and the lack of suitable substrate immediately below provide a local minimum in the flow resistance. They approximate a triangular shaped channel with one side being the water surface, one side being the lined (and sloped) side of the channel and the third side formed by the edge of the vegetation.

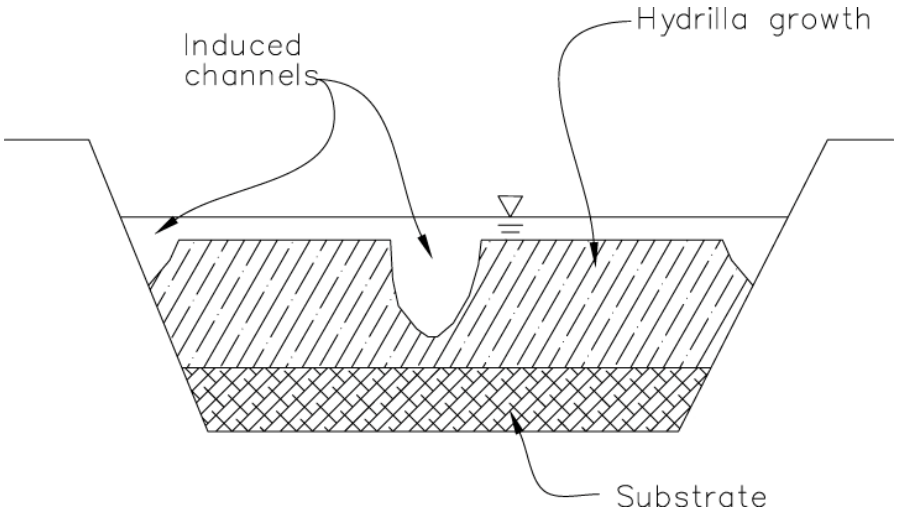

Fig. 5.14. Field channel cross-section showing vegetation morphology for October data collection effort. Note induced channel in the center of the vegetation and side channels associated with the sloping sides of the lined canal

Flow Tests

The flow tests during this episode were collected at a constant discharge rate of approximately 28 liters per second. The discharge was recorded using a transit time meter on the pipeline sampling at 10 second intervals. The resulting data is shown in Figure 5.15.

Flow velocity data in the channel was collected using the Vectrino velocimeter. The data was collected at a sampling rate of 200 samples per second. The data shown herein has been averaged using a running one second average. The instrument collects velocities in three dimensions (x, y and z). Horizontal flow along the main axis of the channel is in the x direction. The y direction is horizontal and perpendicular to the x direction and the z direction is vertical.

The velocimeter was used as a handheld instrument. This would result in some errors in positioning and axis definition, however the positional accuracy was adequate for its use in this project. In a permanent setup, we would mount this instrument on an adjustable base.

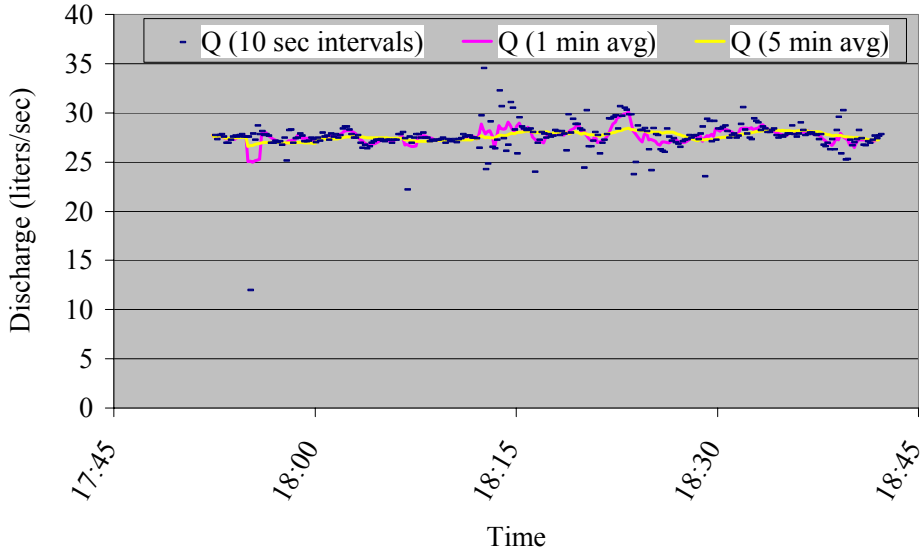

Fig. 5.15. Recirculating discharge rate for field channel during October test. Average discharge =27.7 liters per second, data collected with a Panametrix PT868 transit time flow meter; blue dashes represent individual readings at 10 second intervals, magenta and yellow lines represent 1 minute and 5 minute running averages respectively

The velocimeter was used to collect flow velocities at three points on the vertical centerline of the induced channel, at 2 cm, 9 cm and 16 cm from the approximate bottom of the induced channel. In addition data was collected approximately 8 cm to either side of the centerline and approximately 16 cm above the bottom. The resulting data on the centerline of the channel is shown in Figures 5.16 through 5.18.

Flow velocities in the central induced channel were also collected at the surface using a dye tracer. These measurements were made by first noting the point that the dye was dropped onto the water surface. The dye diffuses rapidly however and there was typically a significant difference between the time that the leading edge of the dye passed the downstream mark and the time that the trailing edge passed the same mark. I therefore measured the time required for both the leading and trailing edges to pass the mark; and used the average of the two times to estimate surface velocities. The surface velocities in the center of the induced channel were measured using dye tracers and estimated at an average of 15 cm/sec.

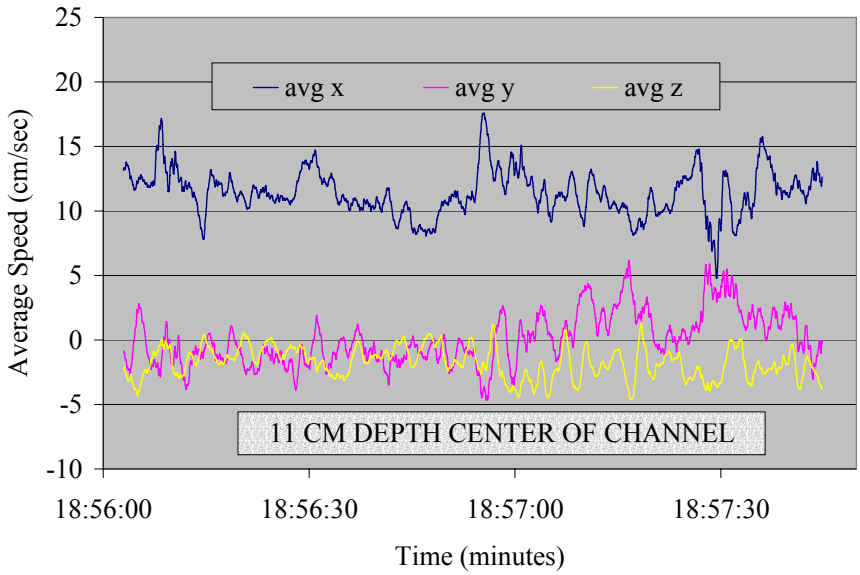

Fig. 5.16. Velocity data collection, center of induced channel, depth = 11 cm. (Approximately 16 cm above the bottom of the induced channel)

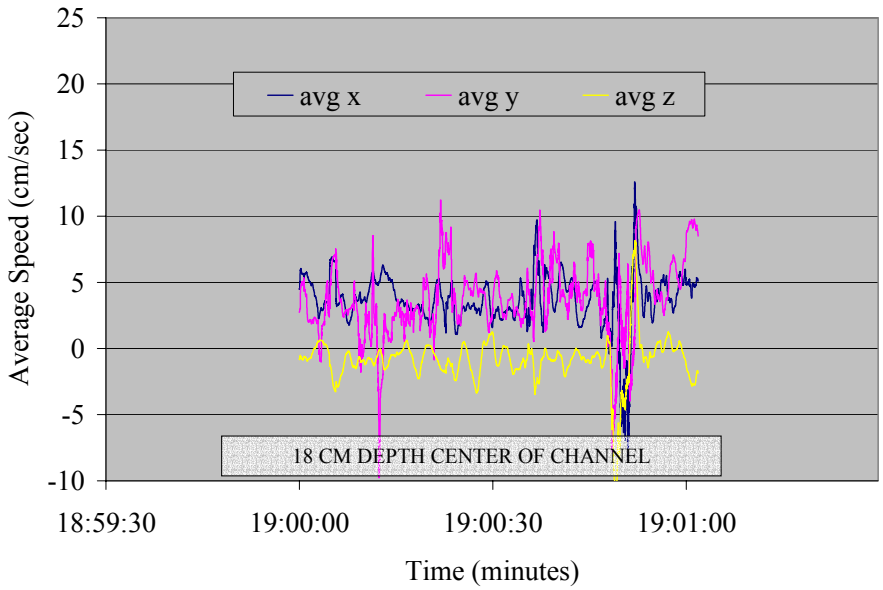

Fig. 5.17. Velocity data collection, center of induced channel, depth = 18 cm. (Approximately 9 cm above the bottom of the induced channel)

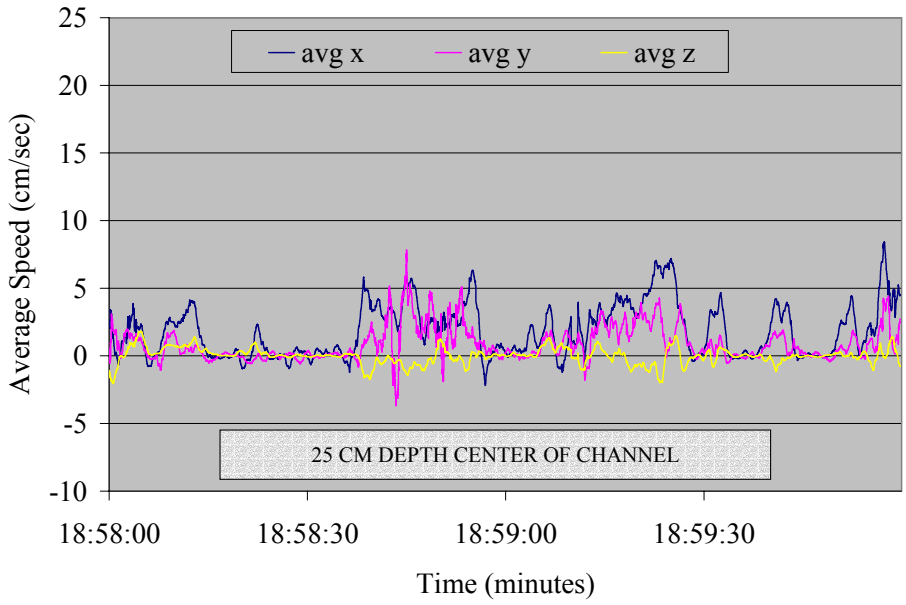

Fig. 5.18. Velocity data collection, center of induced channel, depth = 25 cm. (Approximately 2 cm above the bottom of the induced channel)

Evaluation of the above figures shows the trend in average velocities which is described in Figure 5.19. Turbulence of a relatively large scale, in terms of variation in flow velocities relative to the mean flow velocities, is also a dominant feature. This turbulence retains its scale even near the bottom of the induced channel, where the velocities are nearly zero in absence of the turbulent bursts (Figure 5.18).

Negative velocities are frequently evidenced in the above figures. In some cases the negative velocities are relatively steady and appear to be associated with flow structure at the particular location. In Figure 5.16 for example much of the data shows negative vertical velocity. This is presumed to be a local trend in the flow, probably mediated by the morphology of the vegetation which forms the channel sides.

Some of the negative velocity data appears to be associated with the turbulent 'bursts' as they move through the test area. These bursts are at times associated with large variations in all three dimensions, which implies a structure to the turbulence.[15]

The turbulence in Figure 5.17 is much 'denser' with nearly continuous rapid variations in velocity. This sampling point is fairly low in the induced channel, at a point where the walls of vegetation are probably as close as or closer than the bottom of the channel. This combined with the potential for movement in the walls of vegetation probably explains the somewhat irregular nature of the data—when compared to the other figures.

The data also indicates that flow in this channel is typified by a base flow that increases in magnitude as one moves away from the vegetative walls combined with turbulent bursts whose magnitude is less dependent on the proximity to, or distance from, vegetative walls.

---

[15] It is instructive to view turbulence in and around flexible vegetation. As part of both this data set and my field investigation I collected video footage of both hydrilla and other types of flexible vegetation. The level of movement and interaction by the vegetation can be quite impressive. However it also demonstrates the large variations in fluid movement that can occur.

And finally it is worth noting that in close proximity to the vegetation the velocity is essentially zero, except when a turbulent burst moves through. In addition these turbulent bursts have a positive net velocity; which is to say that they contribute to the net positive flow in the channel.

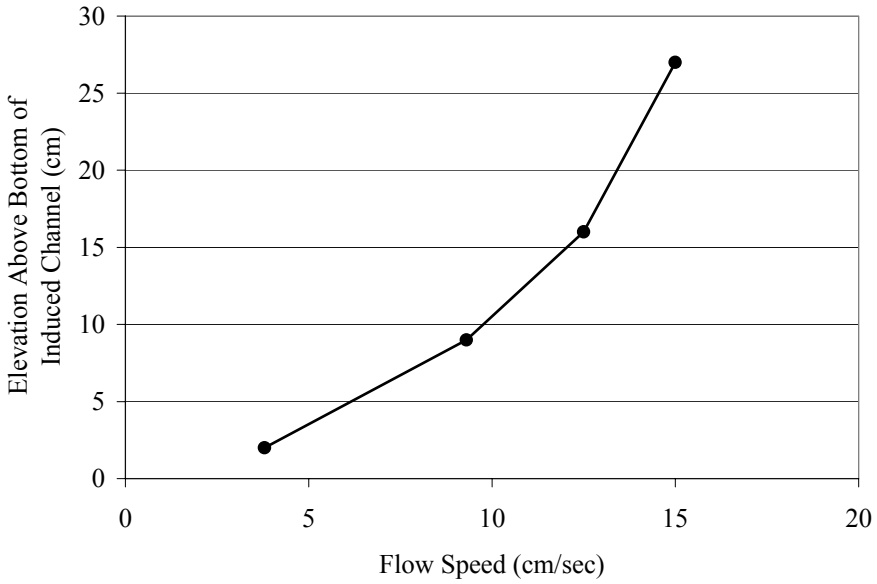

Fig. 5.19. Vertical velocity gradient along center of induced channel. The data in this graph represents the amplitude of the vectoral sum of the x and y velocities

Figures 5.20 and 5.21 below represent flow conditions near the side walls of the induced channel in the upper portions. The instrument was positioned 8 cm to the left and right of the induced channel centerline, which would place it within 2 cm of the vegetative walls in each case. As the figures show, the velocities in these locations are nearly zero for much of the time with occasional bursts of turbulence moving a net flow through the sampling volume. These samples were taken at approximately 11 cm of depth, or 16 cm above the bottom of the induced channel.

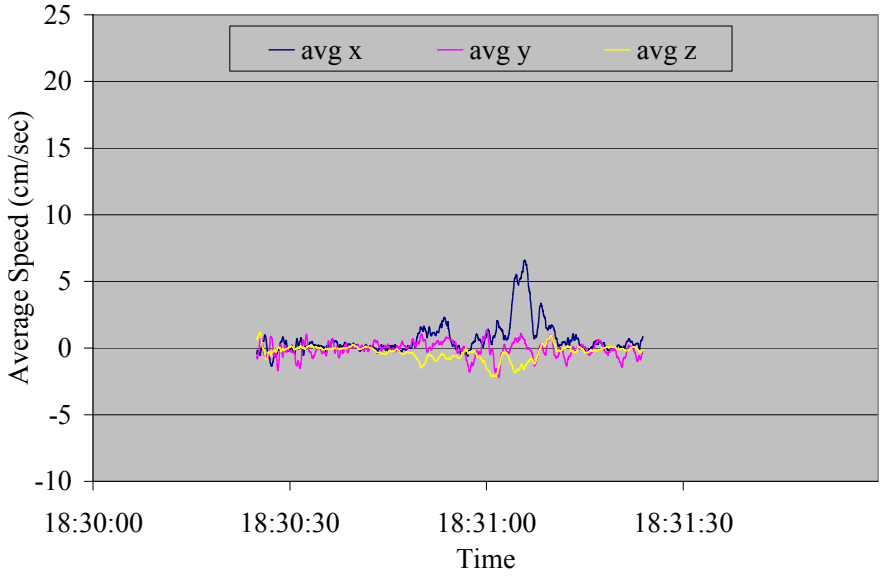

Fig. 5.20. Velocity data, 8 cm left of center of induced channel, depth = 11 cm. Sampling volume was at or near the edge of the vegetation

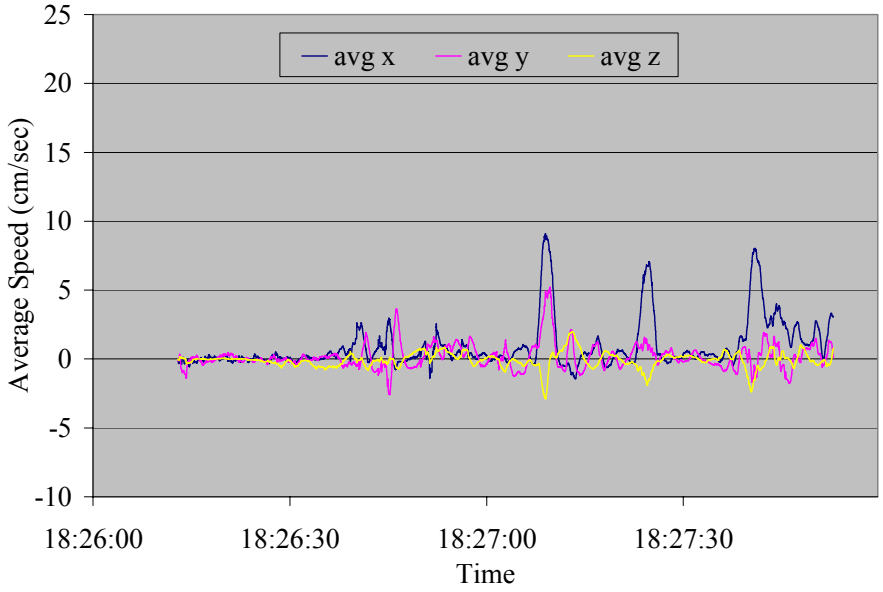

Fig. 5.21. Velocity data, 8 cm right of center of induced channel, depth = 11 cm. Sampling volume was at or near the edge of the vegetation

The near-zero base velocities at the bottom and sides of this induced channel strongly imply that there is no base velocity within the vegetation itself. This combined with the knowledge that the flow itself created the induced channels implies that a balance is struck between the flow in the vegetation and the flow in the channel.

Table 5.4 provides estimated cross-sectional areas for the five flow areas or parts of the channel cross-section (Figure 5.22) as well as measured flow velocities. The cross-sectional areas of each individual component are approximate, due to the general movement and unfixed nature of the medium.

Table 5.4. Estimated flows in field channel by cross-section segment. Assumes a total water depth of approximately 45 cm and flow over the top of the vegetation of approximately 13 cm

Area	Segment Description	Area cm^2	Velocity (cm/sec)	Discharge (liters/sec)	Percent of Total Flow
A	Top Left Edge Channel	300	13	3.9	14%
B	Left Top of Vegetation	500	9	4.5	16%
C	Center Induced Channel	500	13	6.5	23%
D	Right Top of Vegetation	500	9	4.5	16%
E	Top Right Edge Channel	300	13	3.9	14%
Subtotal Open Water Flow		2,100		23.3	83%
Total Area & Discharge		6,000		28	
Remaining Assigned to Vegetation		3,900		4.7	
Calculated Velocity in Vegetation			1.2 cm/sec		

The flow in the induced channel is a relatively small proportion of the total flow, on the order of 23%. The sum of the measured/estimated open water flow was approximately 83% of the total flow, leaving 17% unaccounted for. Table 5.4 provides an estimate for average flow through the vegetation, based on the assumption that all unaccounted for flow occurred in the vegetation. It is more likely however, that there were flows beneath the bulk of the vegetation.

If for example a 5 cm layer in the bottom of the channel (120 cm wide) were flowing at 6 cm/sec, this would result in a flow of 3.6 liters per second, which would account for most of the remaining unassigned flow. As noted previously the flow at the immediate boundary of the vegetation appears to be nearly equal to zero. It is improbable that the flow would asymptote to

zero at the edge of the vegetation and then increase as one moves into the vegetation. It is probable therefore that the flow in the vegetation was very minor and that most of the flow occurred in the open water column.

In any event it seems clear that where aquatic vegetation is sufficiently flexible, flowing water will move it aside to create channels. This will presumably occur until the vegetation reaches some maximum density that is constrained by the structure of the leaves and stems. At this point the vegetation will still have some capacity to transmit fluid, but it will be significantly less than the open channel.

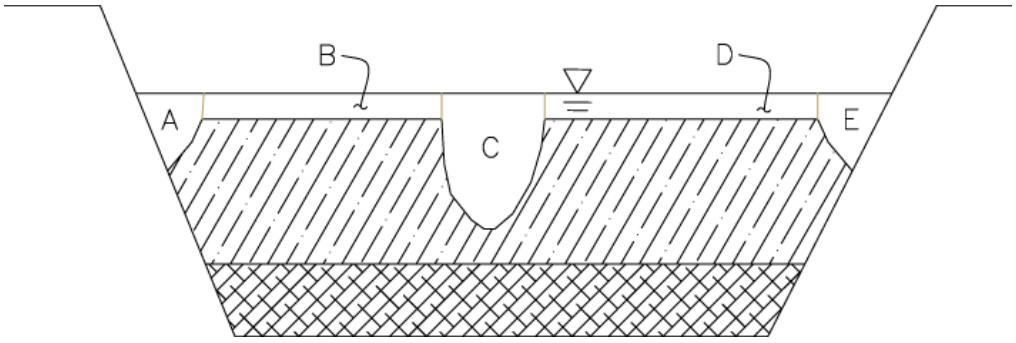

Fig. 5.22. Areas of bypassing flow in field channel cross-section. (correspond to areas in Table 5.4)

RESPONSE OF AQUATIC VEGETATION TO FLOW REGIMES

This section develops basic information on the response of hydrilla to bending loads. This includes analysis of both the plant's flexibility and its flotation characteristics.

Without undertaking a detailed analysis of the plant's internal structure it would be difficult to discuss hydrilla's flexibility in terms of typical engineering parameters such as the moment of inertia and the modulus of elasticity. In addition the standard equations for structural deflection are not applicable, as most engineering formulations begin with the assumption of minimal deflection (and thus minimal change in section properties) as well as the assumption of continuous properties for a structural element.

It becomes immediately obvious upon picking up a length of hydrilla stem, that the plant will bend to a very high rate of curvature, without apparent harm. In addition, the individual stems appear to be structurally discontinuous at the leaf nodes, as they are able to sustain angle points at the leaf joints under loading, followed by recovery after the load is removed.

I conducted simple experiments wherein hydrilla stems were placed in bending, under a range of loadings. The range of response of the stems under these loadings, together with other approximations, helped characterize the basic plant responses, as they might be affected by the flow.

Bending of Hydrilla Stems

Freshly harvested hydrilla stems were taken out of the water and subjected to bending by their own weight. The loading was varied by the simple expedient of cutting off sections of the hydrilla, weighing them and observing the stem's response to the reduced weight. Figures 5.23a through 5.23c show one such experiment in progress. The grid shown in the figures is on a spacing of 1 cm per square.

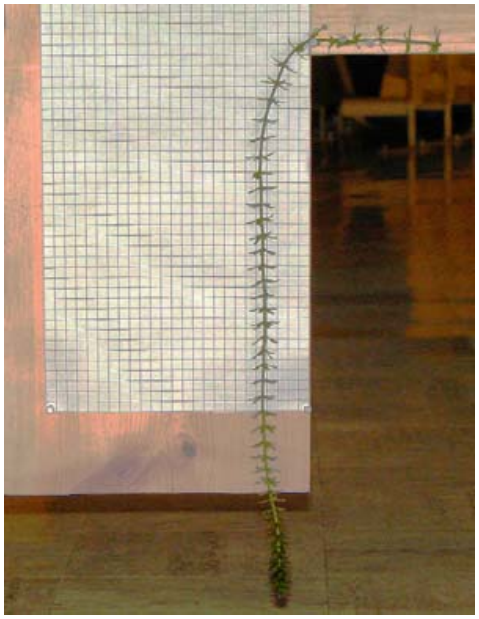

Fig. 5.23a. Bending of hydrilla stem under its own weight

Fig. 5.23b. Bending of same hydrilla stem with 2.9 grams removed from end. (stem and leaves removed)

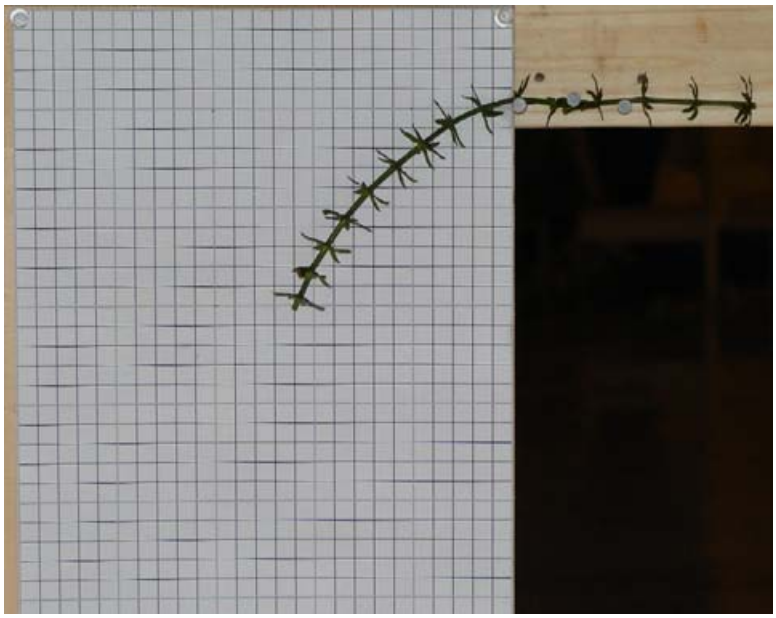

Fig. 5.23c. Bending of same hydrilla stem with 3.9 grams removed from end

---

This experiment was repeated for a number of stems and the resulting curves were captured in Figure 5.24.

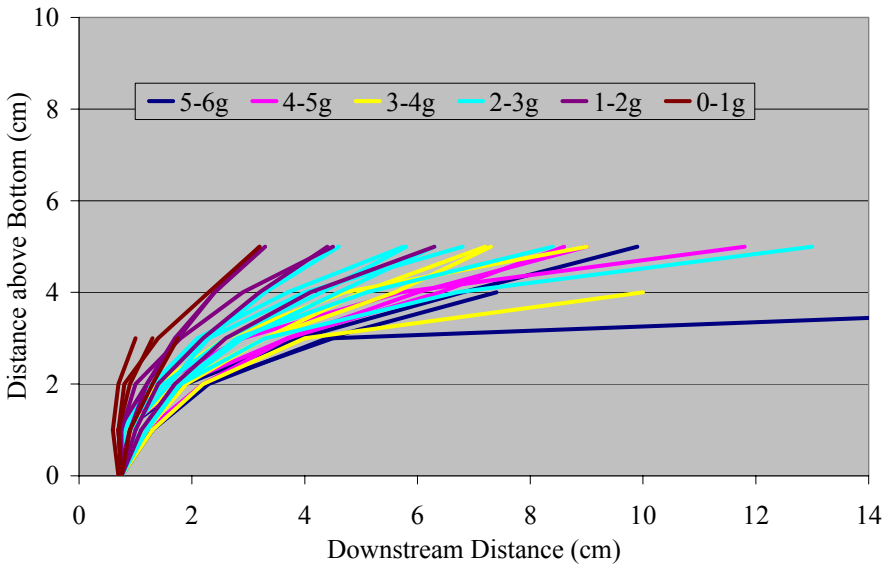

Fig. 5.24. Range of bending for hydrilla stems based on total force applied. Applied forces equal to the listed weights in the downstream direction, e.g. the dark blue lines represent plants subjected to a force in the right direction equivalent to the weight of 5 to 6 grams

The experiments were conducted using a vertical arrangement, in which the plant's own weight provided the loading (Figures 5.23a through 5.23c). However the axes in Figure 5.24 were rotated graphically to demonstrate bending as if the plant stems were emerging vertically from the substrate and the bending was the result of drag from the flow in a channel.

Figure 5.24 combines the results of the experiments and plots the configuration of the stems growing out of a hypothetical channel bottom (growing vertically out of the substrate). In reality in soft unconsolidated mud (most channel bottoms) the stems are probably not constrained to leave the bottom vertically. For the purpose of simplification of this experiment however, this phenomenon is neglected.

Figure 5.24 graphically demonstrates that hydrilla stems are highly flexible. This is further demonstrated in Figure 5.25, where the stem with the least bending (from Figure 5.24) is shown in a hypothetical flow situation. The loading for this condition is approximately 0.01 Newtons (1 gram). Even with the stem (artificially) constrained to emerge vertically from the substrate, if there is a drag force equivalent to at least 0.01 N on the plant, the plant stem can bend to fully horizontal by the time that it is 10 cm above the channel bottom.

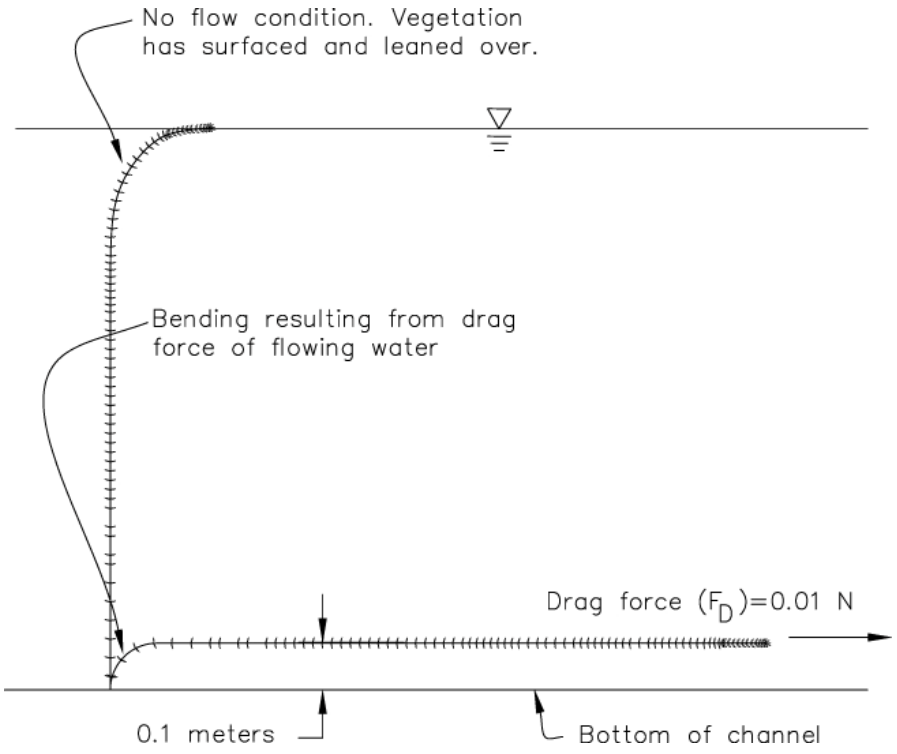

Fig. 5.25. Hydrilla deflection for smallest loading tested

Specific Gravity of Hydrilla

The primary force that is available to counter drag forces from the flow is the natural buoyancy of the plant.[16] The buoyancy of the plant is a vertical force which can counter the drag's tendency to pull the vegetation downstream. In order to estimate the significance of this countering force, we developed estimates of the buoyancy. The small size and nonuniform shape of the individual plant elements would have made it difficult to calculate the density of plant elements by measurement of volume. However the density can be estimated by examining the vertical acceleration of submersed plant elements.

We video taped the under water release of a sample of plant segments from freshly harvested hydrilla plants, and then tracked the change in their vertical velocities. This turned out to be a very approximate estimate, because the vegetation reached its maximum velocity in approximately 1/5th of a second. We used the stop frame capacity of the video camera, from which it was possible to measure an averaged peak acceleration of approximately 1.8 meters per second squared, or approximately 18% of the acceleration of gravity. Applying Newton's second law, this translated to a specific gravity of approximately 0.85 for the stems[17].

$$g\left(V\rho_w - V\rho_{veg}\right) = V\rho_{veg}a \text{ , (Newton's 2}^{nd}\text{ Law) and} \tag{5.3}$$

$$SG_{veg} = \frac{\rho_{veg}}{\rho_w} \tag{5.4}$$

where g is the acceleration due to gravity, V is the volume of the plant element, ρ_w and ρ_{veg} are the mass density of water and the vegetation respectively, a is the measured acceleration of the plant element when released in water and SG_{veg} is the specific gravity of the vegetation.

The leaves of hydrilla however were significantly denser than the stems; and had a specific gravity that was slightly greater than 1. Their rate of sinking was very slow however and I was

[16] Turbulence also affects the morphology of the plants, causing waving of individual stems or entire masses of vegetation. For the purposes of this study however, we will assume that in a steady state situation the net impact of turbulence on the average static shape of the vegetation is zero.

[17] Two decimal places of accuracy are not really justified for this measurement. However the calculated value was nearly exactly 0.85 and rounding it to 0.8 or 0.9 would eliminate some available information.

unable to refine enough information to calculate a value for acceleration. For the purposes of this evaluation I assumed a specific gravity of approximately 1.0+.

The fact that hydrilla stems are buoyant and leaves are not is interesting from the standpoint of a potential discussion on adaptive growth patterns. As previously noted, the portion of the hydrilla plant in the lower water column tends to lose its leaves. I have speculated that this is due to the lack of available sunlight beneath large surfaced masses of hydrilla. However the lack of leaves in the lower water column also results in two additional benefits that would help the plant reach the upper water column. First of all, the loss of leaves reduces the flow drag on that portion of the stem, which would help the plant maintain a more vertical position (i.e. reaching for the sunlight). Second the lack of leaves increases the average buoyancy of that segment of the plant, which also improves the plants surfacing tendency.

The growing tip of the plant on the other hand, has a much denser arrangement of leaves (See Figure 5.23a), which would tend to both increase drag and bring the average buoyancy of that portion of the plant closer to neutral. This would keep the tip of the plant parallel to the flow at whatever level it was at; and would reduce the likelihood that the plant would actually surface. The growing tip of the plant would remain in the water, which it is reasonable to assume would be an advantage for an aquatic species.

Flow Impacts on Hydrilla

The force effects from flowing water on vegetation can be divided into two categories. The first is form drag; this effect has typically been treated as the most relevant for vertical stems and emergent vegetation such as reeds.

Form drag is created by a pressure differential around the boundary of a vertical cylinder or stem. For higher Reynolds number flows—such as those in typical canals—the flow on the downstream face of the stem separates from the face, generating turbulent eddies which propagate downstream with the current. The effect of the flow separation and eddies is to reduce the pressure on the downstream face. The differential in force between the upstream face and the downstream face causes the drag force on the stem.

The second applicable category of force that flowing water exerts is viscous shear friction, often referred to as viscous drag or skin-friction drag (Roberson 1970). In open channel flow, this effect is primarily considered in terms of the force exerted by the flow on the wetted perimeter. In this case drag force is caused by a viscous fluid flowing parallel to the fixed surface of the wetted perimeter. Flow velocity at the fixed surface is zero, because of the no-slip condition. From the zero flow at the fixed surface, velocities increase as one moves away from the surface along a normal to the surface, transitioning up to the maximum flow in the channel. By the definition of a Newtonian fluid, the velocity gradient causes (or is caused by) the shear stress in the fluid and on the boundary (Eq.2.31).

This shear stress is also applicable on rooted vegetation that is trailing downstream in the flow, for example trailing strands of hydrilla. Because the plants are rooted, the stems do not move downstream with the flow. Aside from lateral motions associated with swaying (which are ignored in this study) the vegetation presents a fixed surface in the center of the water column. Therefore we have a no-slip or no flow condition in the middle of the water column—in addition to that which is on the wetted perimeter. And this stem, with its no-slip condition in the middle of the water column, is subjected to the same conditions which result in shear stress at the wetted perimeter.

This shear stress is a function of the dynamic viscosity μ and the rate of change of fluid velocity along some vector normal to the surface—in this case the surface of the vegetation. In most cases of vegetative drag studied to date, this form was considered to be small relative to the form drag. This may have been due to the fact that, even though the vegetation was leaning with the current, it was still primarily upright.

Hydrilla however is potentially influenced by both types of flow effects. If one assumes a viewpoint wherein the viewer is in the channel cross-section and facing downstream, the stem would rise vertically out of the mud for some distance before it bends away from the viewer (looking downstream). This vertical portion of the plant is the part that would be subject to form drag.

However for the majority of hydrilla's 'presence' in the flow, the stem is trailing downstream and is parallel to the direction of flow. In the trailing portion of the stem, the form drag is

effectively zero. But the stem trailing downstream parallel to the flow is subject to viscous shear along its entire surface; and it is reasonable to pursue the assumption that this will be a significant contributing load.

This project did not collect data specific to either of these effects. Nevertheless, we have sufficient information from our observations and from the literature to warrant a brief investigation of the potential range of forces that flow could exert on a stem of hydrilla.

Form Drag on a Hydrilla Stem

A common formulation for form drag on a cylinder in flow is:

$$F_D = h_{veg} d_{veg} C_D \frac{\rho U^2}{2} \tag{5.5}$$

where: F_D is the drag on the cylinder or stem; h_{veg} and d_{veg} the stem height and diameter respectively have been substituted for their counterparts on a cylinder; C_D is the drag coefficient; ρ is the density of water; and U is the average flow velocity in the channel section. For Reynolds number values between 10^3 and 10^5 a single cylinder in a steady flow yields an approximate drag coefficient of $C_D = 1$ (Roberson and Crowe 1980). However for a very rough cylinder ($k/d \approx 0.06$) and Re ranging from 4.0×10^4 to 10^6, C_D falls between 1.2 and 1.3. This is not a significant difference for the order of magnitude estimates we are making, however we used the value of 1.2 in the upper ranges and interpolated for the lower range. Eq.5.6 provides the Reynolds number:

$$\mathrm{Re} = \frac{U d_{veg}}{\nu} \tag{5.6}$$

where ν is the kinematic viscosity of water (m^2/sec). The diameter of the actual hydrilla stem is approximately 0.002 meters; the diameter from leaf tip to leaf tip (across the stem) is approximately 0.02 meters. It is likely that the 'effective' diameter would fall between these two limits. Lacking a method for estimating the effective diameter, I initially proceeded by using both limits and assuming that the results lie somewhere between the two bounds. As the two

limits provided significantly disparate results, I also added a third analysis based on an averaged diameter.

I assumed that for a given 0.012 meter long stem segment, approximately .004 meters was represented by the larger 0.02 meter diameter. The remainder was represented by the smaller 0.002 meter diameter. This resulted in a 'weighted' diameter of 0.008 meters. Figure 5.26 shows the resulting form drag in Newtons per meter of standing stem, as a function of the flow velocity in meters per second.

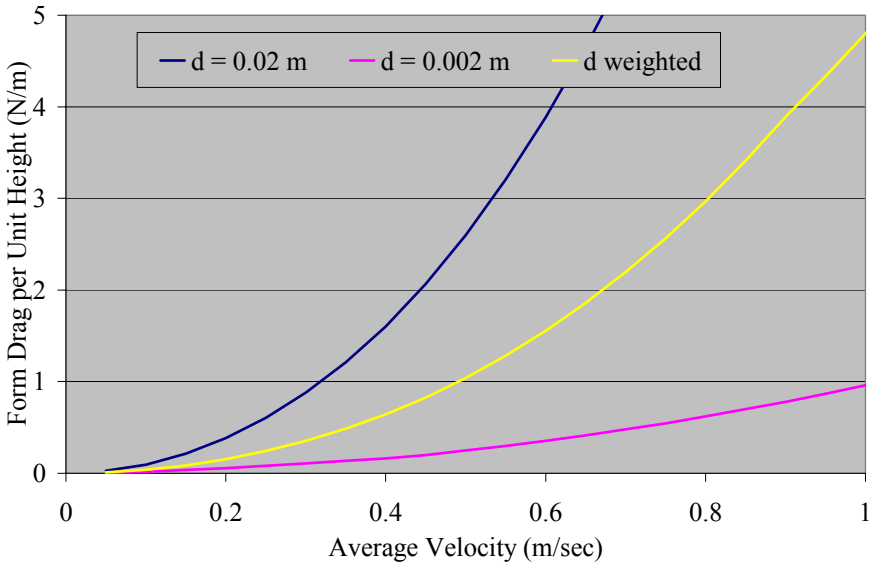

Fig. 5.26. Estimated form drag per meter of erect stem. Calculations are based on three stem diameters, the diameter from outer leaf tip to outer leaf tip (0.02 m), the diameter of the stem itself (0.002 m) and a weighted diameter of approximately 0.008 meters

Again assuming a flow velocity of 0.5 m/sec and starting with the larger vegetation diameter (0.02 meters for leaf tip to leaf tip) the drag on a single hydrilla stem from Figure 5.26 would be F_D = 2.5 Newtons per meter of plant height. Referring to Figure 5.24, the largest weight applied to the vegetation was equivalent to approximately 5 grams or 0.05 Newtons which resulted in

complete deflection of the stem within 4 cm of the fixing medium (channel bottom). The calculated drag force for a plant 1 meter tall is therefore 50 times that required to cause the maximum deflection we measured.

Of course as the plant deflects, the overall height and thus the form drag decreases. If we arbitrarily assume that the plant deflects until it exposes a total height of 0.1 meters to the flow, the total form drag would only be 0.25 N (assuming the larger diameter). The resultant of the form drag would be at one half the distance from the bottom or 0.05 meters. By our graphical exercise (Figures 5.24 and 5.25) we determined that the plant would have to be subjected to .01 N of force at 0.10 meters above the bottom (or a calculated moment of 1.0×10^{-3} N-meters) to achieve full deflection at 0.1 meters from the bottom. Our calculated form drag of 0.25 N applied 0.05 meters above the bottom still provides a significantly greater moment (12.5×10^{-3} N-meters) at the mudline.

Examining the lower limit for diameter as well, we use the lowest line in Figure 5.26, which shows a total drag force of $F_D = 0.25$ N/meter. Applying this to the deflected plant height (0.10 meters, resultant force applied at 0.05 meters) the total moment at the mud line becomes 1.25×10^{-3} N-meters, which is only slightly higher than the moment required to achieve the bending.

It is likely that the effective value for the diameter of the stem should be somewhere between the leaf tip to leaf tip diameter and the stem diameter. Visual examination of the plant structure (Figures 5.23a through 5.23c) suggests that neither diameter would be completely dominant. There is sufficient space between the individual leaf whorls that—when the stem is vertical—flow will occur between the leaves in such a manner that the stem diameter will be a relevant scale. However the spacing of the leaf whorls is not so large that the whorls can be ignored as contributing to the form drag.

Therefore as described above we used a weighted diameter of 0.008 meters. This resulted in the central line in Figure 5.26. The weighted diameter resulted in a total moment—as calculated above—of 5.0×10^{-3} N-meters or roughly five times that required to achieve the deflection.

It appears that form drag alone could provide for the complete deflection of the hydrilla stem, in terms of overcoming the bending resistance provided by the stem. However it also seems likely

that the shear friction resulting from fluid flow parallel to the trailing stem will contribute a complementary loading.

Viscous Drag on a Hydrilla Stem

We identified no studies which specifically addressed the viscous drag on long trailing stems or leaves in flowing water. Therefore the following assumptions have been made:

- The condition under discussion is defined to be steady state flow; and the flow treats the vegetation as a minor obstruction. This implies that the flow accelerates in the immediate vicinity of the vegetation to maintain continuity around the partial blockage, but that a single stem does not significantly change the flow beyond the immediate vicinity of the vegetation;
- The portion of the stem being considered is positioned horizontally in the water column with its long dimension parallel to the main axis of flow; and
- As the stems are horizontal, the arrangement of the leaf whorls act as a shield and prevent significant flow from occurring within the diameter of their tips, that is the no-slip condition, applies at an outer diameter of approximately 0.02 meters.

Further we will assume that the range of influence (from the no-slip condition at the outer edge of the leaves to the point where flow is unaffected by the stem) is relatively small. This assumption is based partly on the first assumption, wherein the fluid is assumed to accelerate around the outer edge of the stem. It is also based on observations of flow in the bench channel, wherein flow in the immediate vicinity of the vegetation at times appeared higher than further away in the open water. Observations of this type of events are in keeping with the premise that water will accelerate around a short-term obstacle to maintain continuity of flow.

Given the above assumptions, the flow velocity at the edge of the vegetation would still be zero (no-slip). Moving away from the edge of the vegetation along a normal, the velocity would increase rapidly to some magnitude that is greater than the average velocity in the section (to maintain continuity). It would then decrease to the average velocity in the flow.

Using the definition of a Newtonian fluid (Eq.2.31):

$$\tau = \mu \frac{du}{dy} \tag{2.31}$$

and the following inputs, I developed an initial estimate of the shear friction loading on a hydrilla stem.

The diameter of the hydrilla from leaf tip to leaf tip is approximately 0.02 meters. We will consider a length of hydrilla that is oriented in a horizontal position, parallel to the flow, so that the flow 'sees' the end of a horizontal cylinder. We assume that as the water impinges on the leading end of the cylinder, it splits and flows around the plant. We further assume that the stem is treated as a short term obstruction in the flow, which is to say that the flow accelerates around the vegetation in order to maintain continuity.

Therefore, the velocity immediately adjacent the vegetation will be greater than the velocity of the flow in which the vegetation is embedded. This velocity is assumed to peak some distance away from the vegetation stem and then reduce to the average velocity in the section. Figure 5.27 shows two velocity curves that could represent such a distribution. The velocity starts at zero on the edge of the vegetation (also zero on the y axis). From there it accelerates quickly to some peak and then decreases.

The shape of these curves is arbitrarily parabolic; however they are constrained in two ways. The first is that the distance that the modified velocity has expanded from the edge of the vegetation is 1 stem diameter in the case of the first or blue line. For the second line the zone of influence has expanded to two stem diameters. The second constraint is that the area under the velocity curves in the zone of influence is summed up to be equal to the unit discharge if the vegetation were not there. In other words continuity is maintained.

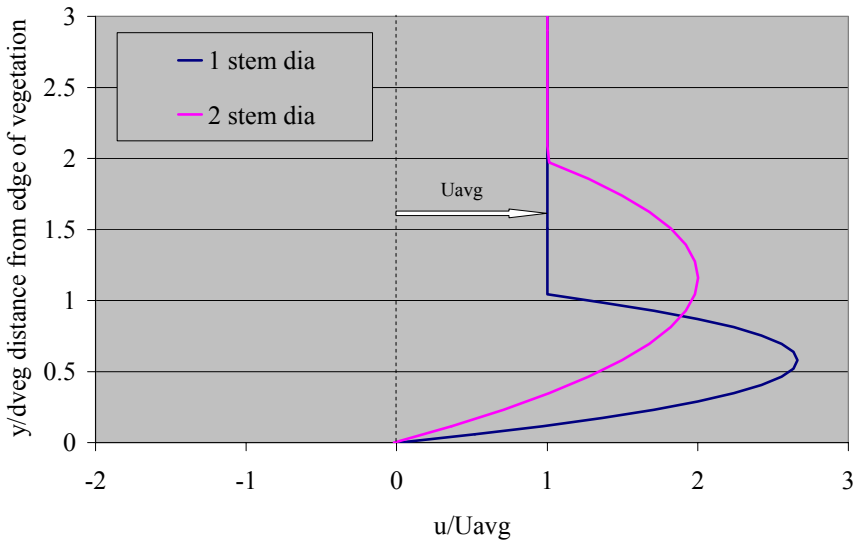

Fig. 5.27. Hypothetical velocity distribution from edge of trailing hydrilla stem. Assumes area under velocity curves is equal to sum of flow displaced by hydrilla and in affected region at U_{avg}

Given these two curves I can make the additional observation that—given the assumptions up to this point—the curve with the smaller zone of influence and the larger peak velocity would be closer to the upstream end of the vegetation under consideration. As an observer progressed downstream along the edge of the hydrilla, the high narrow velocity peak that would occur at the leading edge of the vegetation would gradually expand and dissipate both through friction on the vegetation and through diffusion of momentum outward from the stem.

Therefore if I assume that the shear stress on the edge of the stem is a function of the rate of change of flow velocity closest to the stem, I can calculate a shear stress using Eq.2.31. Given these assumptions, the viscous drag for the two curves shown in Figure 5.27 is plotted as a function of velocity in Figure 5.28.

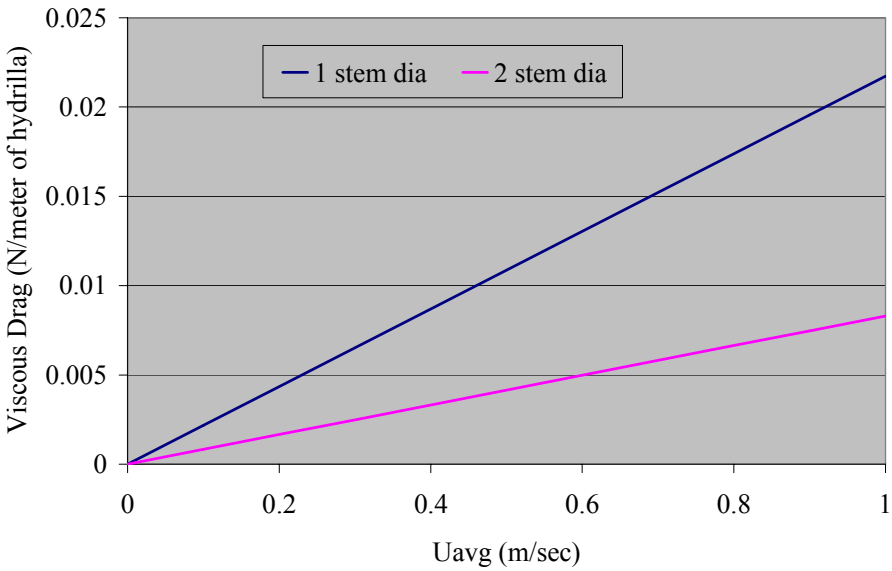

Fig. 5.28. Estimated viscous shear drag on trailing hydrilla stem. Assumes stem is parallel to the flow, given the flow distribution plotted in Figure 5.27

The curve representing drag based on a zone of influence equal to one stem diameter is, presumed to be the more upstream of the two curves. The exact location is of course unknown, however this curve is used to provide the comparison with the loading from the form drag and the buoyancy.

As the resulting comparison in Figure 5.29 shows, the form drag provides a much higher loading per a given length of hydrilla. However this figure can be misinterpreted, because the form drag is a function of the vertical length of hydrilla in the flow, whereas the viscous drag is a function of the horizontal length of hydrilla.

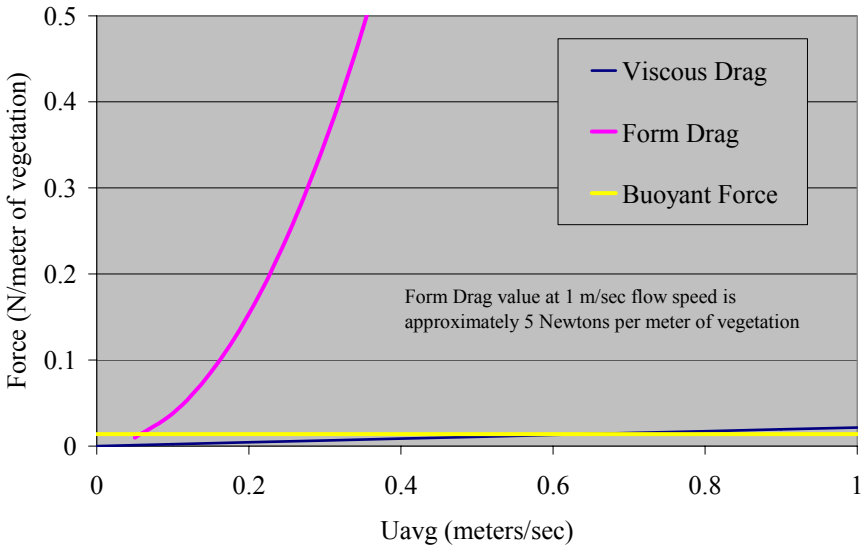

Fig. 5.29. Comparison of form drag, shear drag and buoyancy. Forces acting on hydrilla stems in flowing water, given the results for the weighted diameter in Figure 5.26, the upstream or 1 stem diameter influence in Figure 5.28 and a calculated buoyancy of 0.014 N/meter

---

To provide a more reasonable comparison I applied these values to the deflected scenario from Figure 5.25. I assumed that the hydrilla was deflected and that the exposed height for form drag was 0.1 meters. The trailing length of hydrilla stem was set at 2 meters. The buoyancy was calculated assuming a total length of 2.1 meters; and the resulting comparison is shown in Figure 5.30.

This figure and the assumptions built into it provide a very general estimate of the relative magnitude of forces acting on a single hydrilla stem. At velocities of less than 0.2 meters per second, the buoyant force of the vegetation will have an impact on the plant's position in the

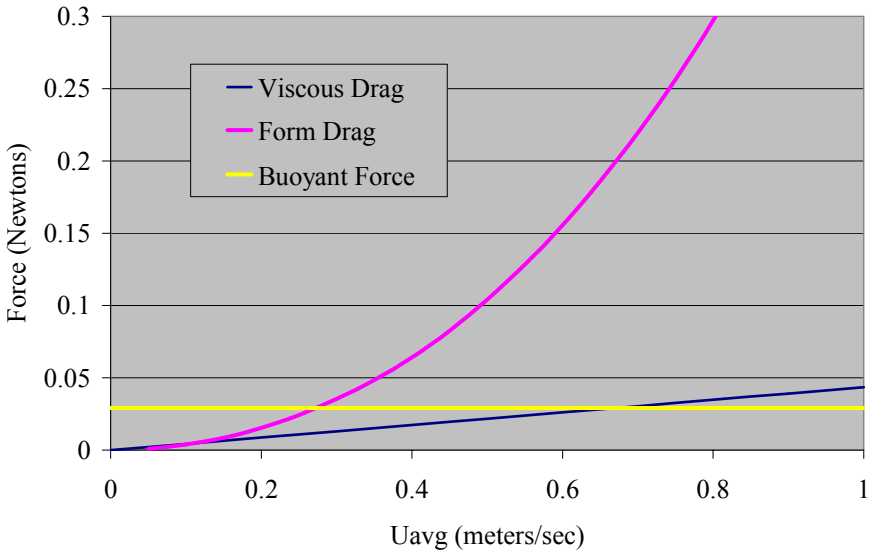

Fig. 5.30. Comparison of form and shear drag and buoyancy on deflected stem. Based on a 2.1 meter hydrilla stem in flowing water, assuming 0.1 meters is vertical and 2.0 meters is trailing in the current[18]

water column. Beyond about 0.4 meters per second, form drag becomes the dominant force. It appears that viscous shear on a single plant generally has a lesser effect. The values for viscous drag remain significantly lower than form drag for most of the range of velocities examined. The viscous drag forces should probably in fact be lower, as this curve was obtained by applying a drag rate we have assumed is only applicable in the upstream part of the trailing vegetation. It appears that for an investigation of this type, the viscous drag on a single plant can be ignored. This analysis does not however apply to large masses of the plant in the water column.

Based on the evaluations in this section, we can assume that hydrilla is very flexible longitudinally, relative to the forces that are applied in a flowing canal. The hydrilla stem will rapidly respond to a bending moment by deflecting through the necessary angle in a short distance from the bottom. We also found that the structure of the stem appears to be discontinuous and under bending is capable of sustaining angle points at the leaf nodes. Finally

[18] Note that the viscous drag was calculated by applying the larger drag force from Figure 5.28, this drag should probably be further reduced.

we found that the buoyancy in hydrilla is limited to the stem. The leaves are slightly denser than water and the stems have an estimated specific gravity of between 0.8 and 0.9.

SUMMARY OF EXPERIMENTAL RESULTS

The bench channel and the field channel may be regarded as having approximately opposed conditions. The vegetation in the bench channel was relatively inflexible as the individual stems were short and the planting density was high. The stems were constrained from moving, both by the planting density and the fact that they were planted in a narrow channel. Flow in this channel was constrained to pass through the vegetation. Flow in the field channel on the other hand was not so constrained. The vegetation in this channel was free to move and the level of flow was low enough so that the water could largely bypass the vegetation.

In the greenhouse channel the hydrilla was also much more flexible than the vegetation in the bench channel. However the experimental conditions were controlled to force flow through the vegetation and provide estimates of energy loss under these conditions.

This results in the conclusion that aquatic vegetation—hydrilla in particular—will move aside and the flow will bypass it. However if the flow is high enough relative to the available space, flow can still occur within the hydrilla. Given water flowing through the hydrilla, I have developed estimates of the relative energy losses caused within the flow. Conversely for an assumed energy slope and a given vegetation density, I have developed estimates of the flow velocities within the vegetation for a range of densities (Fig. 5.4). For an arbitrary rectangular channel section, flow velocities in the vegetation were between 5 and 10% of those in the free water column.

During our experiments in the field channel there was sufficient space available for the water to bypass the vegetation and the vegetation was free to move, thus there was very little or no flow through the vegetation. Presumably if the discharge through this channel were increased sufficiently, the vegetation would reach some maximum density and as the flow continued to increase, sufficient potential would then develop to begin to force some water through the vegetation. However based on this work, it is reasonable to assume that the flow in the vegetation would not be a significant contributing factor to the channel's discharge.

CHAPTER VI

ANALYSIS OF HYDRILLA IMPACTS ON OPEN CHANNEL FLOW

Hydrilla is highly flexible; and will tend to follow the streamlines of the flow. At lower flow velocities the buoyancy of the plant will have more of an effect and the plant will maintain a higher position in the water column. However hydrilla grows in large multiple plant masses such that, even when it is lying over completely, the volume of horizontal and parallel stems can still take up a significant portion of the cross-section of a channel.

Chapter V established that even if water is constrained to flow through hydrilla, the relative energy losses are such that the flow velocities in the vegetation are much smaller than those in the free water column. It also established that due to the flexibility and morphology of hydrilla in particular, the vegetation mass can compress and move aside to provide more space for flow. Flowing water can form induced channels through the vegetation, which allows flow to bypass the vegetation. I observed that even at relatively low flows, the vegetation will compress sufficiently that flow in the vegetation drops essentially to zero. Extending this phenomenon to the case of hydrilla growing down the center of the channel—with flow bypassing on either side and above—I assume for the purposes and conditions considered in this investigation that the vegetation in this condition will also be compressed so that flow will bypass it and therefore flow in the hydrilla will be effectively zero.

In addition to the experimental data, I have observed flow conditions in active irrigation channels where the vegetation has been compressed to allow flow bypassing (Fig. 4.10). In the field review of flowing canals I have observed cases wherein the vegetation was limited to a bank of vegetation along the centerline of the canal, with significant flow occurring both above and on either side of the vegetation bank. This is by no means the only morphological condition in which hydrilla grows. However it is a common one and it provides a simplified system which can be readily modeled. This is the condition that the ensuing analysis addresses.

For the purposes of this analysis, I assume a channel configuration similar to that shown in Figure 6.1, which is a trapezoidal channel with a single continuous mass of vegetation growing down the center. Analysis will be further limited to the condition wherein the banks of vegetation are continuous along the centerline of the channel. This allows the assumption that flow conditions around the vegetation have reached steady state.

The analysis is also limited to flow conditions wherein the vegetation is static. That is this study will not consider the dynamics of hydrilla movement due to interactions with the flow in canals. And the banks of hydrilla will be presumed to have already responded to the flow and been displaced, such that there is essentially no flow in the vegetation. These conditions and assumptions allow application of the no-slip condition at the perimeter of the vegetation.

The bank of vegetation in the center of the channel is therefore treated as an extension of the wetted perimeter. And the area within the vegetation is removed from the cross-section of flow. And finally for simplicity's sake I will assume that the effective cross-sectional shape of the vegetation is as shown in Figure 6.1. The width of the vegetation (B_{veg}) and the height of the vegetation (h_{veg}) will be varied experimentally.

This Chapter contains the results of two analyses or cases. In the first case, a computer model was developed and tested against the standard Chézy method for calculating flow in a canal. In the second case the computer model was used to estimate the impacts of the vegetation configuration shown in Fig.6.1.

The computer model used in both cases is based on the Prandtl-von Kármán universal velocity distribution law (P-v K law) using the form of the law shown in Eq.6.1.

$$u = \frac{1}{\kappa} u_* \ln\left(\frac{y}{mk}\right) \qquad \text{(Chow 1959)} \qquad (6.1)$$

where u is the point velocity some distance y from the nearest surface, κ is the von Kármán constant (generally assumed to be 0.4), u_* is the shear velocity, m is a constant equal to 1/30 for rough surfaces in rough flow and k is the Nikuradse sand roughness factor. The shear velocity was calculated using Eq.6.2:

$$u_* = \sqrt{gRS} \tag{6.2}$$

where *g, R* and *S* are the acceleration due to gravity, the hydraulic radius of the section and the channel slope respectively.

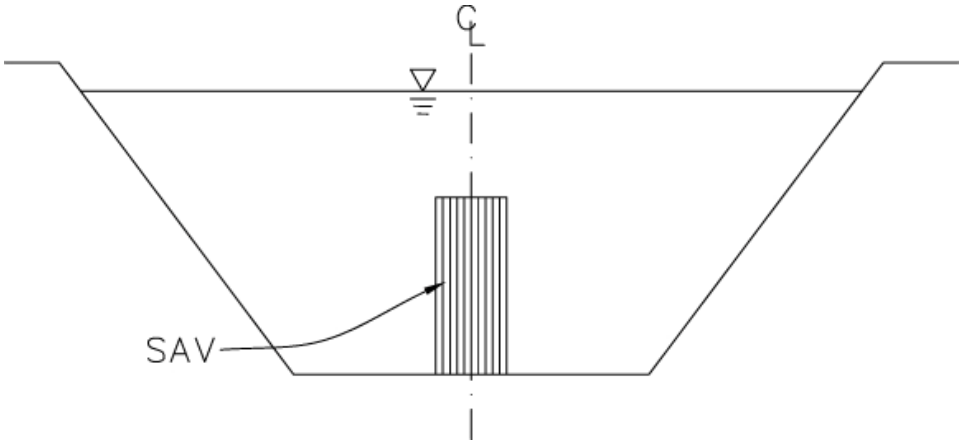

Fig. 6.1. Channel cross-section schematic with central bank of submerged aquatic vegetation

The model integrates Eq.6.1 over the cross-section of the channel to calculate the average velocity (U_{avg}) as shown in Eq.6.3.

$$U_{avg} = \frac{Q}{A} = \frac{1}{A}\int_A u dA \tag{6.3}$$

where *u* is defined by Eq.6.1, *Q* is the total discharge in the section, and *dA* is a differential area. Eq.6.3 is solved in the model using a numerical scheme which defines a rectangular grid over the modeled area, calculates the discharge in each cell and then sums the discharge over the section. Because both cases considered are symmetrical, only half of the section is modeled, as shown in Fig. 6.2.

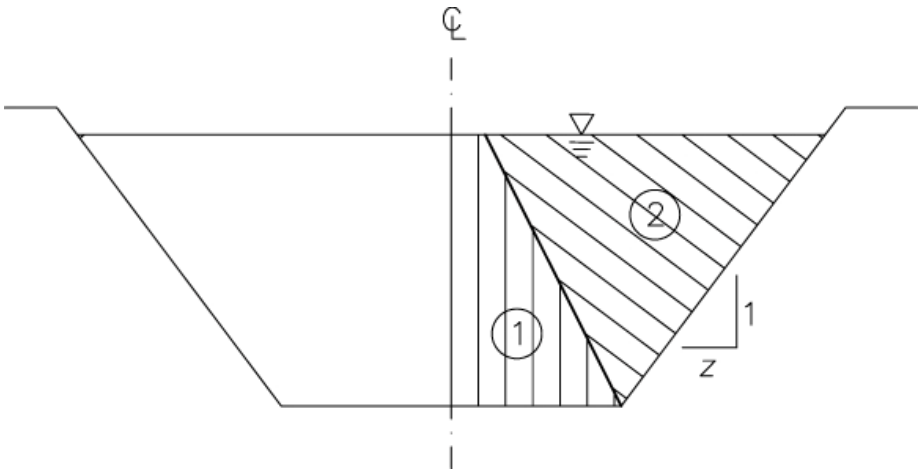

Fig. 6.2. Cross-section showing area subdivisions for model. Used to compare P-v K law to the Chézy method

Each grid element is square and 0.01 meters on a side; the grid size is adjustable in the code, however after some initial testing both cases were run with that grid size. Each cell in the grid is assigned to a region according to a geometric scheme which accounts for the bottom width, side slope and water depth. The dividing line between the two regions in Fig.6.2 bisects the angle between the side of the channel and the bottom of the channel.

The distance from the center of each cell in the grid to the appropriate boundary is calculated and stored. Then a velocity for each cell is calculated using the stored distance and Eq.6.1. The average section velocity computed from this analysis was then compared to that obtained using the Chézy methodology for the same section.

In the first case, the model was used to develop values for *k* (Nikuradse sand roughness coefficients) and relate them to the roughness size *e* that is used to develop the Darcy-Weisbach friction factor *f* used in the Chézy equation.

In the second case, the developed value for *k/e* is used with the P-v K model to evaluate the variation in capacity of a channel, given the addition of a vegetation configuration similar to that shown in Figure 6.1.

CASE 1 – MODEL CALIBRATION (PRANDTL-VON KÁRMÁN TO CHÉZY)

This analysis treats the Chézy method as a baseline methodology. This should not be construed as granting it status as the more accurate method. As discussed previously, the Chézy method is the older and more widely used methodology. This combined with its simplicity is led to its use as the baseline. In default of a significant data collection effort—which was not part of this project—I am not implying that either is more accurate than the other.

The two methodologies used in this analysis are based on different methods of calculating the resistance to flow. The Chézy method (as used herein) is based on Eqs. 2.13 and 2.17 which are repeated here for convenience.

$$U = C\sqrt{RS} \tag{2.13}$$

$$C = \sqrt{\frac{8g}{f}} \tag{2.17}$$

This version of the Chézy method utilizes the Darcy-Weisbach resistance coefficient *f*. For all cases in this analysis the surface is considered to be rough and the flow fully rough. This allows the use of Eq.6.4 to define *f*:

$$\frac{1}{\sqrt{f}} = \frac{2}{2.3}\ln\left(\frac{D}{e}\right) + 1.14 \qquad \text{(Chow 1964)} \tag{6.4}$$

where *f* is ultimately defined as a function of the Moody roughness coefficient *e*.

The P-v K law model based on Eq.6.1 is however, a function of the Nikuradse sand roughness coefficient *k*. Both *k* and *e* are empirical roughness factors which are not a function of flow conditions or of channel configuration.

My purpose in conducting Case 1 was to compare *k* to *e* and develop a relationship for the purposes of this investigation. Defining the relationship between the two independent factors allows me to use them to compare the two methodologies for a range of channel shapes. So in Case 1, I used variations in the cross-section's shape to evaluate the variations of the *k/e* relationship.

I initiated this step by building the numerical model of the channel cross-section, as previously described. Assuming symmetry, the right half of the section was divided into two sub-areas as shown. In area 1 the velocities calculated from the P-v K law are assumed to be a function of their distance from the bottom of the channel. In area 2, the velocities are assumed to be a function of their perpendicular distance from the side wall of the channel. As previously described the model was set to calculate the velocity in the individual cells and then calculate an average velocity for the section. This was then compared with the average velocity calculated using the Chézy method (Eqs.2.13, 2.17 and 6.4).

Equation 6.4 provides *f* as a relatively simple function of the relative roughness *D/e*; however it is applicable for fully rough flow over a rough surface. The model runs in this analysis met this requirement. *D* is four times the hydraulic radius (ASCE 1963) and *e* is the roughness element used in the Moody diagram. The same hydraulic radius and slope were used for both versions.

In the above comparative analysis the Nikuradse sand roughness (*k*) is treated as an unknown. The channel geometry, channel slope and water depth were provided as inputs. The hydraulic radius was calculated using the geometry of the entire section and the value *e* was treated as a known input. Using the average velocity calculated from Chézy, *k* was adjusted until the average velocity from the model matched the Chézy value. This provided a value of *k* which could then be compared to *e* using the factor *k/e*.

The goal for this Case was to develop the factor *k/e* for use in the vegetation modeling. Through the process of this study it had become clear that many factors which are assumed to be constant can actually vary considerably with changes in such parameters as channel geometry, water depth and slope. The main goal for Case 1 then, was to test how the factor *k/e* varied as the channel geometry varied. In essence the goal was to test how sensitive this factor is to changes in channel geometry. The following material provides the results of that sensitivity analysis.

Sensitivity Analysis for *k/e*

In this section, the methodology was used to develop *k/e* using a range of channel parameters. This included testing the relationship for three values of *e*, beginning with the upper end of the range for concrete. Chow (1964) gives roughness values (*e*) for concrete ranging from 0.0003 to 0.003 meters (0.001 to 0.01 feet). I began with the rougher end of this scale and calculated *k* for

a value of *e* equal to 0.003 meters. Values of *k/e* were also tested for *e* values equal to both twice and four times the initial value (0.006 and 0.012 meters).

Figure 6.3 shows the results from the first set of tests, which varied both the channel side slope (*z*) and the channel bottom width (*B*). The water depth (*h*) was set at 1.5 meters for these tests. As Fig. 6.3 shows *k/e* appears to vary very slightly with the channel bottom width. The expanded scale on the y axis in Fig. 6.3 is used to show the variation, however it is not intended to imply that these variations are significant.[19]

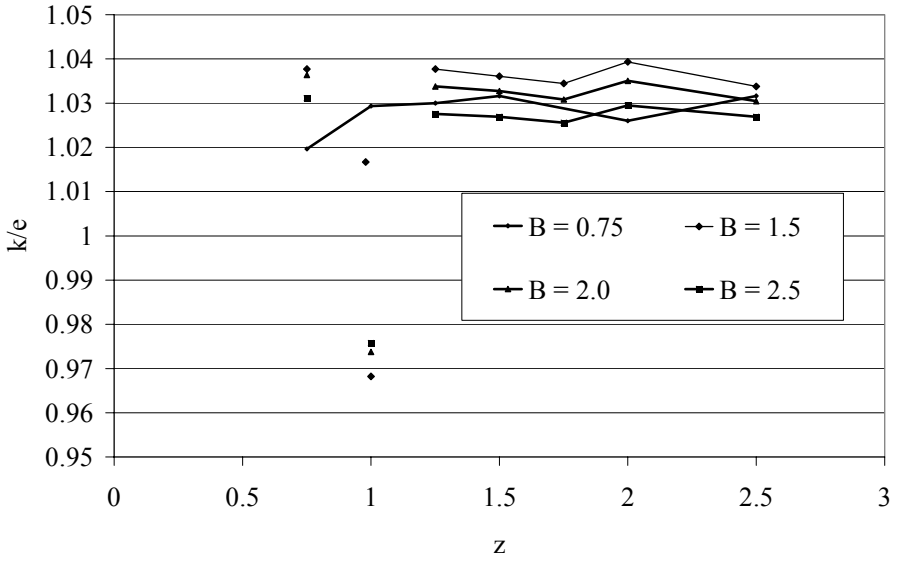

Fig. 6.3. *k/e* sensitivity to channel bottom width and side slope

In Fig. 6.4, *B* is set to 2.5 and *h* is set to 1.5, while *e* and *z* are varied. Fig 6.4 shows that *k/e* is slightly affected by variations in *e*.

[19] The reviewer will note variations around the value for $z = 1.0$. This is an artifact of the rectangular model grid and the fact that $z = 1$ exactly bisects a range of model cells. Closer examination with reduced variations around the value $z = 1$ shows the value for *k/e* first dropping as 1 is neared then passing through the average value to a higher value, then quickly dropping to the average value. And reducing the scale of the model grid reduces the scale of the variation. These values are shown here for completeness, but dropped from later graphs for clarity.

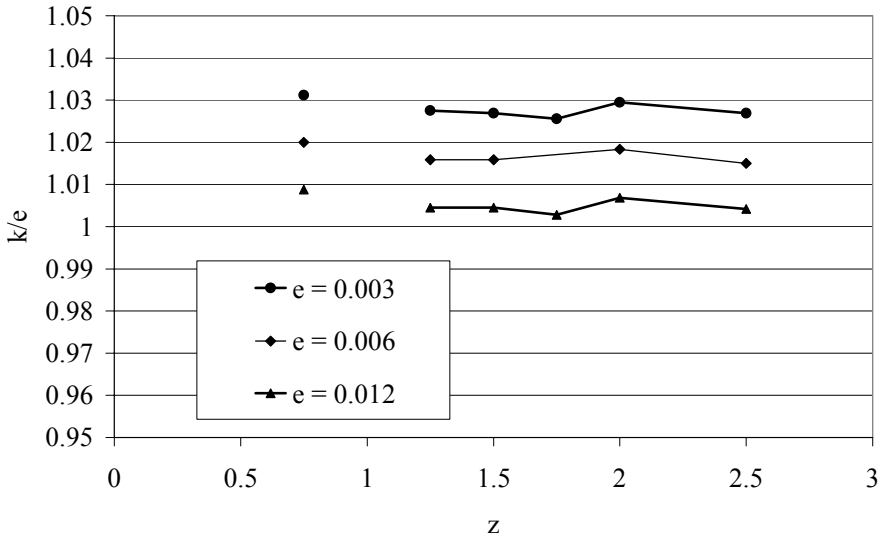

Fig. 6.4. *k/e* sensitivity to channel side slope and roughness height *e*

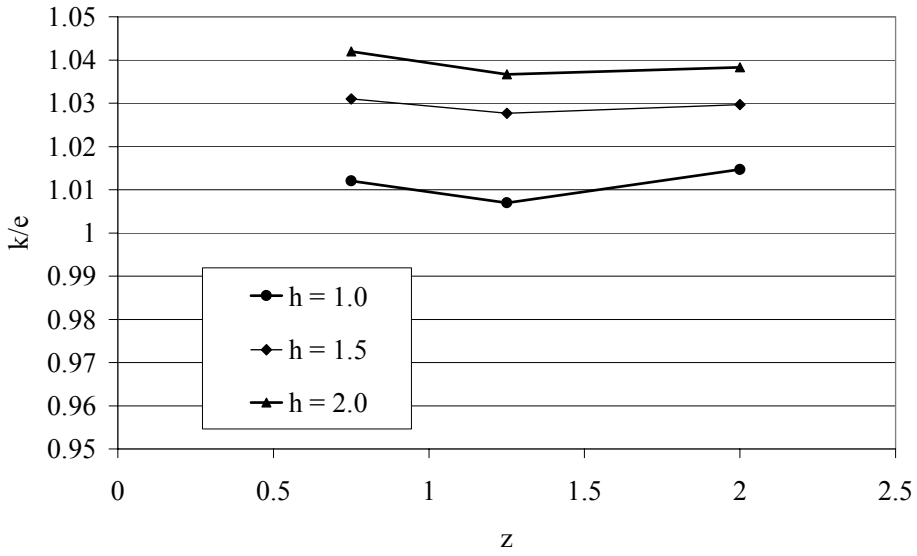

Fig. 6.5. *k/e* sensitivity to water depth and side slope

The results from Figures 6.3 through 6.4 are summarized in Table 6.1. As none of the figures indicated that *k/e* was sensitive to the side slope *z*, that variable is not explicitly shown in this table. However the statistics calculated for the specific value of each variable are for the range of values of *z* shown in the previous figures.

Table 6.1. Comparison of *k/e* values for a range of model variables

Variable	Mean Value of *k/e*	Variance	Std. Dev.
B			
0.75	1.028	2.12E-5	0.0046
1.5	1.037	0.46E-5	0.0021
2	1.033	0.54E-5	0.0023
2.5	1.028	0.41E-5	0.0020
All values of *B*	1.031	2.14E-5	0.0046
e			
0.003	1.028	0.42E-5	0.0020
0.006	1.017	0.44E-5	0.0021
0.012	1.005	0.46E-5	0.0021
All values of *e*	1.017	10.00E-5	0.0100
h			
1.0	1.011	1.51E-5	0.0039
1.5	1.029	0.28E-5	0.0017
2.0	1.039	0.74E-5	0.0027
All values of h	1.027	15.00E-5	0.0125
***k/e* for all variables**	1.026	11.20E-5	0.0106

Figures 6.3 through 6.5 together with Table 6.1 show that there is a measurable relationship between *k/e* and each of the three model variables examined. However if one examines the mean value for all the data (*k/e* = 1.026) and varies it by twice the standard deviation (0.0212) the value of *k/e* would fall within the range of 1.0048 to 1.0472. If each of these values were applied to a roughness value of *e* = 0.003, the total range in value for *k* would be from 0.0030 to 0.0031. As these are empirical roughness factors this is not a significant difference.

Sensitivity Analysis for Shape Factor

Having found *k/e* to be relatively stable, I returned to the sensitivity analysis to evaluate the relationship between the Chézy equation and the P-v K model. Specifically I wanted to test how the relationship varies with the flow parameters used in the later analysis. To demonstrate any

relative differences between the two methodologies, I established a baseline channel section, with dimensions as follows. The bottom width *B* was set to 2.5 meters, the side slope *z* was set to 0.75 (horizontal to 1 vertical), the roughness height *e* was set to 0.003 meters, and the water depth *h* was set to 1.5 meters. The Chézy Equation was modified as shown in Eq.6.5:

$$U_{avg_{P-vK}} = SF * C\sqrt{RS} \tag{6.5}$$

where *SF* is a shape factor as defined in Eq.6.6:

$$SF = \frac{U_{avg_{P-vK}}}{U_{avg_C}} \tag{6.6}$$

and U_{avgC} = the average fluid velocity calculated for the section using the Chézy Equation and $U_{avg\ P\text{-}v\ K}$ = the average fluid velocity calculated using the Prandtl von Kármán universal velocity distribution law.

With the baseline parameters set as defined above, *k* was adjusted until *SF* was equal to exactly 1.000. This required a value of *k* = 0.003073, which required a value of *k/e* that was equal to 1.0243. Having established baseline values for the channel parameters as well as both *k* and *e*, the model was run again varying in turn the: depths, side slopes, bottom widths and roughness values *e*. The results of these comparisons are shown in Figures 6.6 through 6.8.

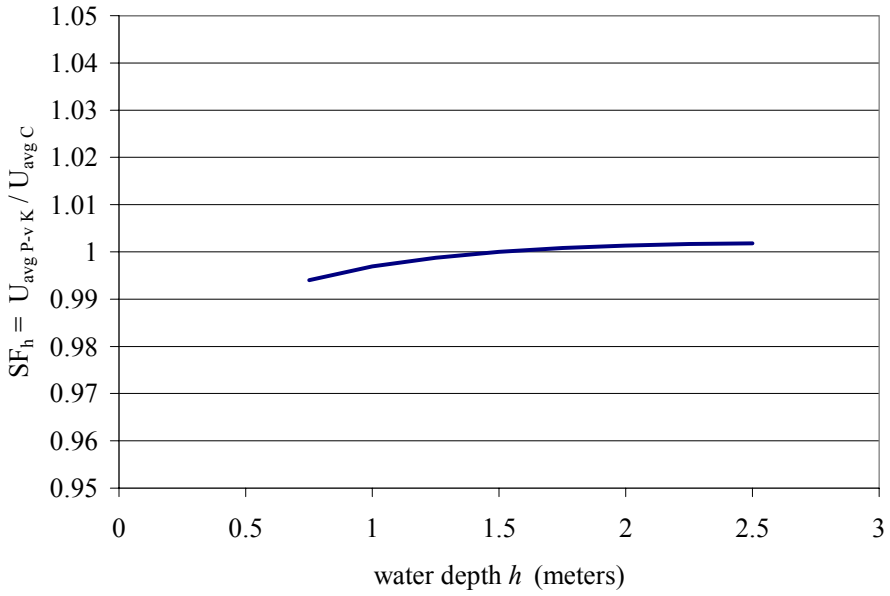

Fig. 6.6. Shape factor as a function of water depth

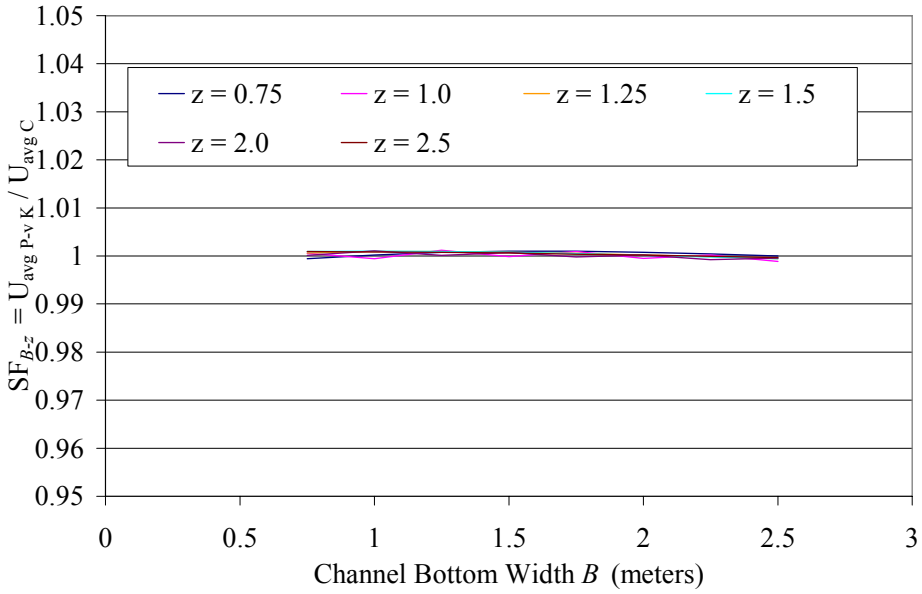

Fig. 6.7. Shape factor as a function of *B* and *z*

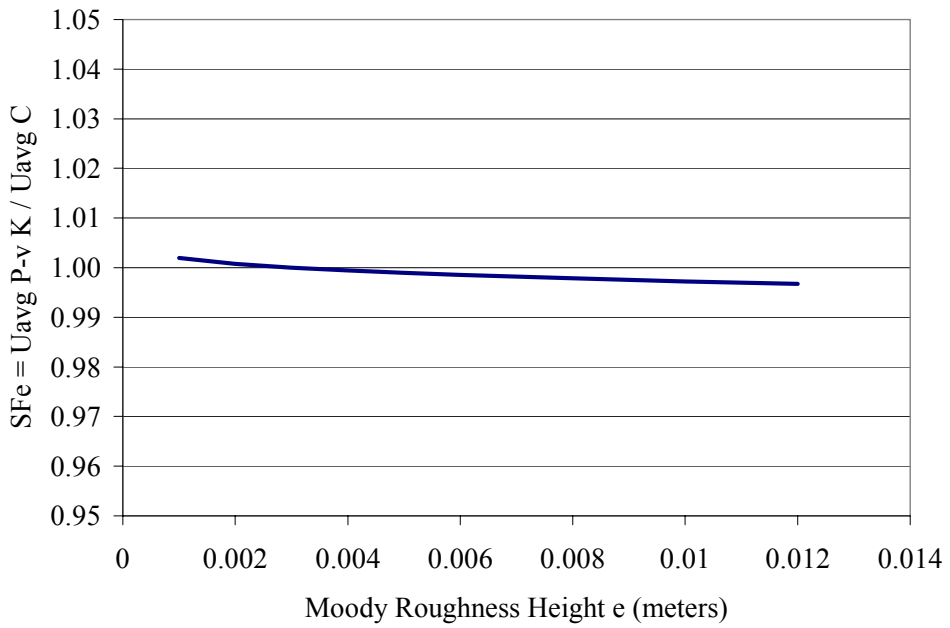

Fig. 6.8. Shape factor as a function of Moody roughness height e

The figures show some sensitivity to the water depth and roughness height, but none for the combined factors of bottom width and side slope. The proposed work in the next section inserts vegetation in the middle of a trapezoidal channel section. In terms of flow parameters this might be expected to have impacts that would be associated with the channel bottom width and the side slopes. Therefore for the purposes of this study each of the shape factors tested above will be considered roughly equivalent to 1.0. That is there is effectively no difference between the two methodologies in terms of resulting average velocity. For the remainder of this study *k/e* is set to the value that resulted in matching velocities for the baseline channel section. That is *k/e* = 1.0243.

CASE 2 – FLOW IN CANALS WITH CENTRAL BANK OF VEGETATION

As in the previous section, I constructed a finite difference model on a rectangular grid, the purpose of which was to provide estimated point velocities throughout the cross-section and thus develop an average velocity. Each cell in the model grid was equal to 0.01 meters on a side.

The model first assigned each cell in the grid to one of the areas shown below in Figure 6.9. Then based on which area the cell was assigned to, the model calculated the distance to the nearest surface. For example all cells in area 3 were assigned distances based on their horizontal distance from the submerged aquatic vegetation. Those in area 4 were assigned distances based on their distance from the bottom of the channel. The radial lines in area 2 depict the scheme for calculating the distance in this area.

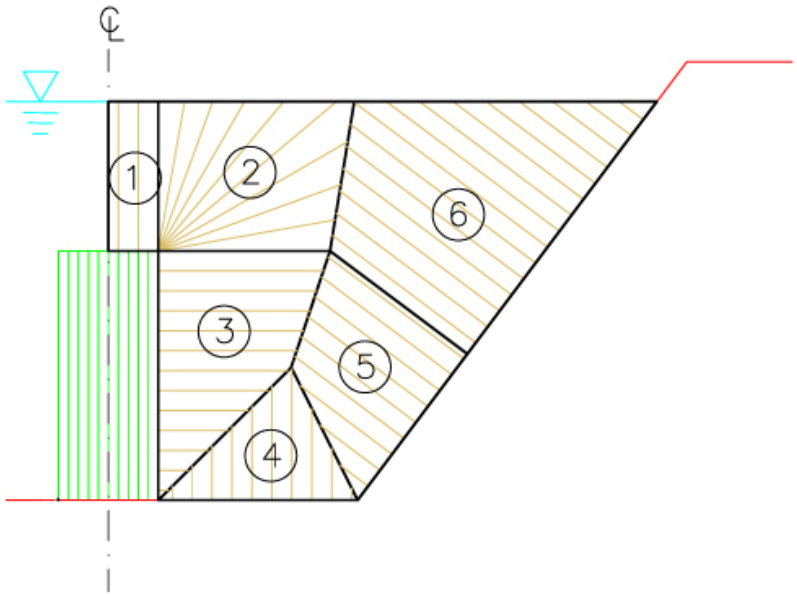

Fig. 6.9. Channel section showing vegetation and modeling subareas. Used to evaluate impacts of submerged aquatic vegetation on flow in channel

The model used the same set of inputs as the model in the previous section, with one exception. This model used the *k/e* ratio that was developed in the previous section; i.e. $k/e = 1.0243$. The bottom width parameter B was set to 2.5 meters and the roughness e was set to 0.003 meters for all the model runs in this section. The primary parameters varied were the width and height of the vegetation in the center. However we also tested using varied values for z and h. The vegetation parameters were tested by first inputting a vegetative width and then running the model for a range of vegetative heights, from 0.8 meters up to the depth of the water. This was

repeated for vegetative widths ranging from 0.5 meters to 2.0 meters. A sample of the results for the values $z = 0.75$ and $h = 1.5$ are shown in Figures 6.10 through 6.12.

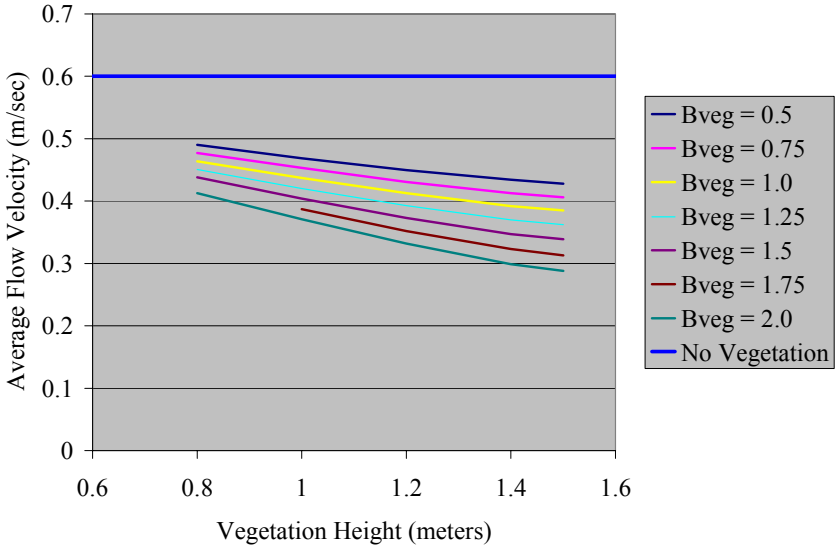

Fig. 6.10. Relative flow velocities for variations in vegetation dimensions. The calculated average velocity with no vegetation was 0.6 meters/sec

B_{veg} represents the width of the vegetation in the flowing section. The x-axis in Figure 6.10 represents the height of the vegetation. As one can see, the lowest and narrowest vegetation results in the flow velocity that is closest to the original (unvegetated) flow. Just as the highest and widest vegetation body results in the lowest velocity. However the data is more easily viewed as a percentage of the original values (cross-sectional area and velocity). This is shown in Figure 6.11.

Figure 6.11 casts the data in terms of percent of impact. The x-axis data values represent the percent of cross-sectional area that remains for open water flow. The y-axis shows the average velocity in the section as a percentage of the flow that would exist if the vegetation were not there. At this point we lose the detail of which points represent which vegetation height. However it is reasonable to presume that the highest point in each line represents the lowest vegetation height.

Figure 6.11 is potentially useful; however it still does not provide the complete picture. As discussed at the beginning of this document, submerged aquatic vegetation does not just reduce the average flow velocity. It also reduces the cross-sectional area available for flow. Figure 6.11 therefore provides the full effect of hydrilla on discharge in a channel.

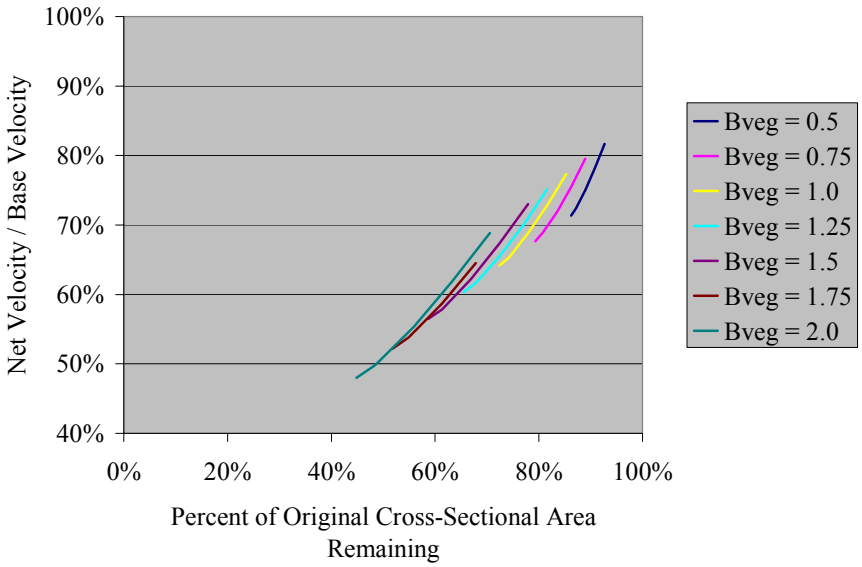

Fig. 6.11. Relative flow velocity as a function of remaining cross-sectional area

As described earlier the upper part of each line corresponds to the lowest vegetation height in each run. I can therefore conduct model runs using the P-v K law combined with the Chézy Equation and calculate values for the flow velocity and total discharge, given a vegetation configuration reasonably close to Figure 6.1. However the nature of the data in Figure 6.12 suggests a simpler approach. I increased the scope of the model runs to include additional combinations of side slopes and water depths and combined the information as point data in Figure 6.13.

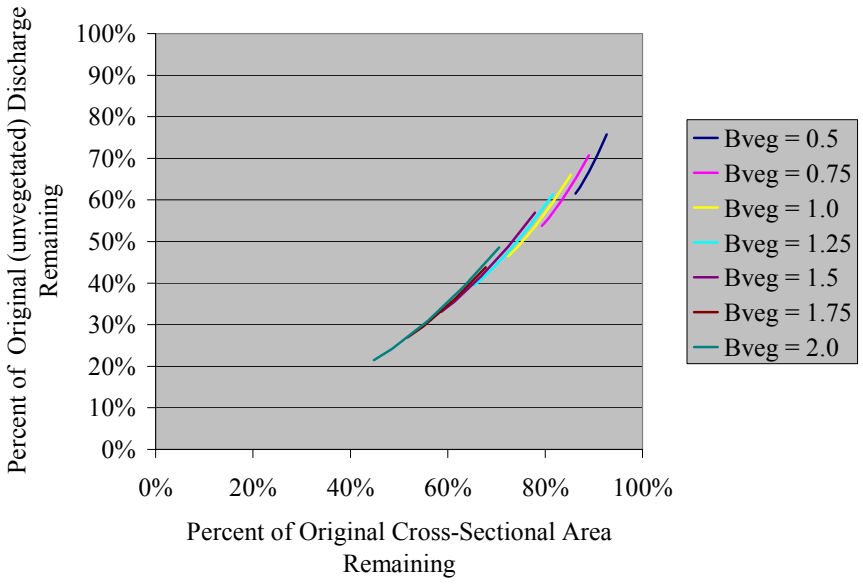

Fig. 6.12. Relative discharge as a function of remaining area

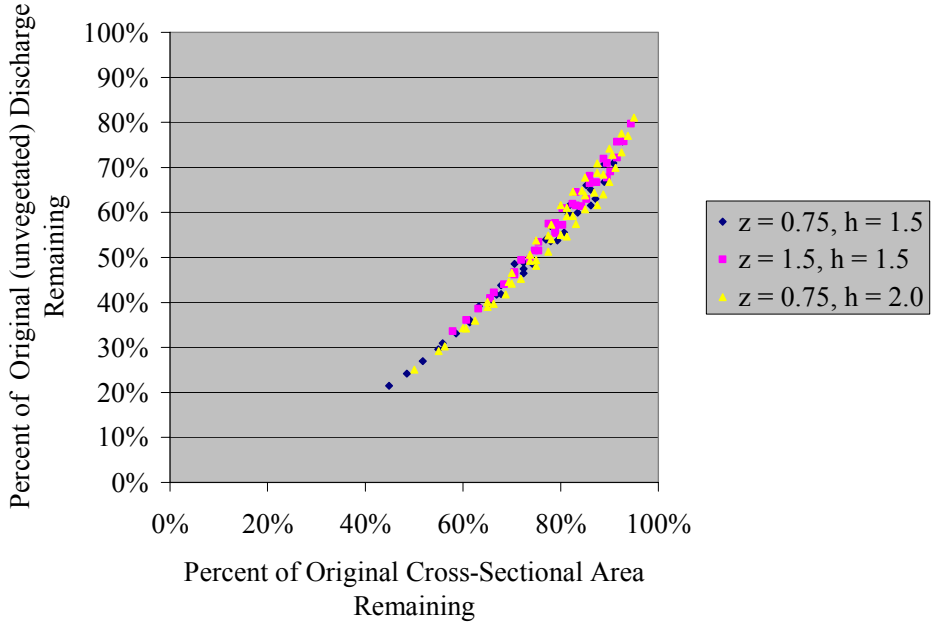

Fig. 6.13. Relative discharge for a range of vegetation and channel configurations

Figure 6.13 shows a relatively tight system of data, which suggests a simple function of the type $y = ax^r$ where again *a* and *r* are fitting parameters. In Figure 6.14 the data has been combined into a single dataset. Equation 6.7 fits this data with an R^2 value equal to 0.98.

$$\frac{Q_{\text{Re}\,maining}}{Q_{Open}} = 0.85\left(\frac{A_{\text{Re}\,maining}}{A_{open}}\right)^{1.76} \tag{6.7}$$

where $Q_{Remaining}$ and Q_{open} are respectively the calculated discharge in the vegetated section and the calculated discharge in the same section with no vegetation. $A_{Remaining}$ and A_{open} are respectively: the remaining cross-sectional area available to flow (open water) in the vegetated section; and the total cross-sectional area of the channel with out vegetation.

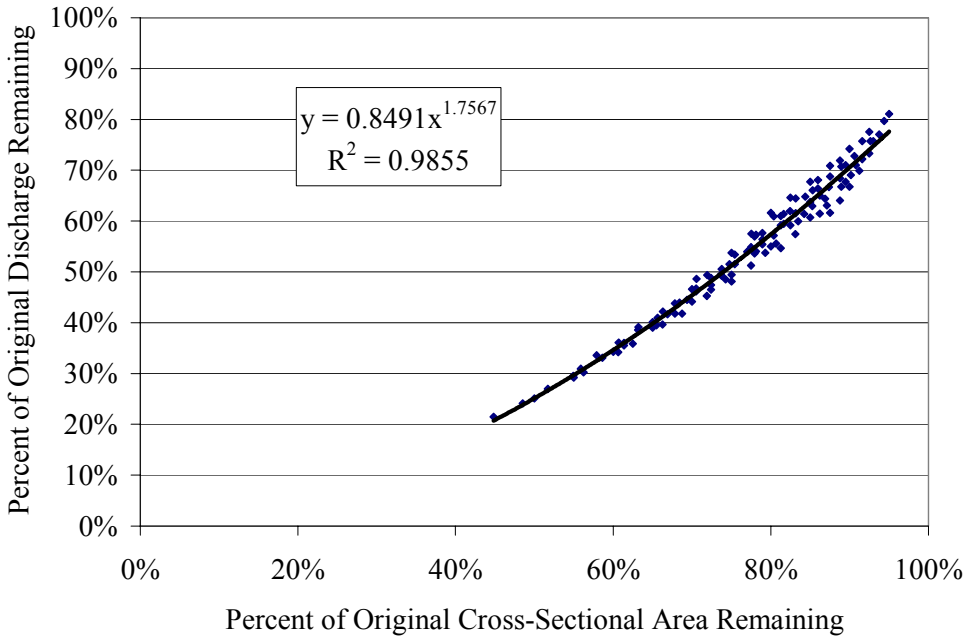

Fig. 6.14. Relative discharge function. Evaluated with a central bank of submerged aquatic vegetation for a range of vegetation and channel configurations

This relationship (Eq.6.7) has been developed with the model setup to simulate a trapezoidal channel with a central mass of vegetation growing from the substrate in the bottom of the canal.

Flow is expected to occur either on both sides of the vegetation or on both sides and over the top. The vegetation is considered impervious and continuous from the substrate to the top of the vegetation.

This relationship has been modeled with the vegetation extending completely to the surface. And it has been modeled with the vegetation height reaching to approximately half the water depth. It appears, at least over the range tested, that the proportionality relationship is valid for a large range of relative vegetation heights and vegetation widths. The tests were run using a channel bottom slope of $S = 0.0001$ and a roughness value of $k \approx e = 0.003$.

It should be noted in Figure 6.14 that as one progresses towards a vegetative condition where 80% or more of the channel cross-section is blocked the data, which represents modeling results, becomes more widely distributed, indicating less confidence in the central function. In addition to this distribution, certain simplifying assumptions become more tenuous as the boundary of the vegetation approaches the boundary of the channel. For general practice this should not be a significant issue. By the time a canal section is 80% or more blocked by vegetation, mathematical flow estimates become redundant.

It is also worth emphasizing that this analysis is based on the assumption of steady state flow and a fully developed flow field. In other words this analysis does not account for entrance type losses associated with the beginning and ending of vegetative masses.

CHAPTER VII

SUMMARY

A number of efforts in this project contributed to the overall conclusions and recommendations. These efforts included field observations, laboratory experiments, field experiments and the analysis.

The field observations helped to characterize the range of aquatic vegetation types as well as the morphology of their presence in the water column. The field work also provided insight into the morphological variations of each plant type. Eventually this phase of the investigation focused on *Hydrilla verticillata*. I found that the vegetation is highly flexible and responds to flow by bending away from it. Although made up of individual stems with small leaves, hydrilla can form significant vegetative masses in the water column, which have major impacts on water flow.

This vegetation also behaves differently at different growth stages. In the early stages of the growing season the vegetation may form a large mass of individually moving stems, which taken together can effectively impact flow capacity. Later in the growing season after the vegetation has topped out it can form large relatively solid masses on the surface wherein the vegetation is tied together by algae and detritus. These masses form a solid impediment to flow and can also impact water quality by blocking light to the lower water column and reducing gas exchange.

The field investigation also showed that the response of hydrilla and other submerged aquatic vegetation to flow can be quite dynamic, with individual strands of vegetation moving radically in response to passing turbulence.

The laboratory experiments established that the vegetation causes significant resistance to flow. When water was forced to flow through the vegetation energy losses were significantly higher than flow through the water column. In fact I established that for a given energy loss per length of channel, flow velocities in open water can be more than 20 times higher than that in the vegetation.

The field experiments established that under certain conditions flowing water in a channel will compress the hydrilla mass until there is virtually no flow in the vegetation and all flows occur in induced channels that were created by the flow through the vegetation.

In the analysis, a model was developed that estimated the structure of the velocity distributions in a channel cross-section, both with vegetation and without. This model was calibrated against the Chézy equation's predictions of flow in a channel and a relationship (k/e) between the Nikuradse roughness factor k and the Moody roughness factor e was developed and tested. This model was used to estimate the structure of the velocity distribution in a vegetated channel and this was ultimately used to develop estimates of the impacts of submerged aquatic vegetation on flow in channels.

A simple equation was developed to estimate the discharge in a flowing channel with submerged aquatic vegetation (specifically *Hydrilla verticillata*) growing along the centerline. The method is based on the percentage of cross-sectional area occupied by the hydrilla and is a function of the calculated discharge which would exist in the absence of the hydrilla.

The overall method assumes a steady state condition for the shape and extent of the vegetation. It assumes that there is no flow in the vegetative mass itself and that the perimeter of the vegetative mass serves as an extension of the wetted perimeter. The method also assumes that the area of the flow section that is within the vegetation is removed from the cross-sectional area. An effective hydraulic radius is calculated using these modifications.

Future work could address the energy losses in the approach to and departure from the vegetative mass. Three dimensional finite element modeling may prove useful, particularly for modeling the approaches to the vegetation from an open (unvegetated) channel. However the models I have identified were not developed for the conditions inherent in vegetated canals. The scale of the cells around the leading edge of the vegetation will need to be relatively small. And the model domain will probably need to extend far enough up the channel to capture significant parts of the backwater curve that will be generated by the vegetation.

Future physical flow work could also expand the scope of this investigation to include a broader range of flow regimes and vegetative conditions. Laser Doppler flow meters could improve both

the morphological detail around the vegetation water interface and provide information on the flow structure within the vegetation.

The bulk of the data collection that this work has been based on was conducted at relatively low Reynolds numbers and with static vegetation. Future work should extend the analysis to non-static vegetative masses and examine the forcing functions that address the waving and interweaving of the vegetative masses. The waving of the vegetation I observed in irrigation canals may be due to something similar to the monami observed in terrestrial forest canopies and in confined submerged vegetation. That is turbulent interchange from the higher energy flows outside of the canopy generating flows within the canopies. Or it may be the result of more active participation or dynamic response/interaction by the vegetation with the flow. Future higher Reynolds number work could also address the relation of large scale turbulence to the lateral waving of the vegetative mass.

And finally the response of the vegetation as a unit, to different levels of flow is worth pursuing. My work indicates that at relatively low flow velocities, the vegetative mass of hydrilla in a channel will compress until there is essentially no flow in the vegetation. At this stage I suspect that there may be a relationship between the relative energy consumption by flow in the vegetation and that of flow in the open water, which governs the response of the vegetation and thus the response of the overall flow.

REFERENCES

ASCE (1963). "Friction Factors in Open Channels." *American Soc. Civ. Eng.Proc. HY* 89(HY 2) 97-143.

Bakhmeteff, B. A. (1936). *The mechanics of turbulent flow*, Princeton University Press, Princeton.

Barfield, B. J., Tollner, E. W., and Hayes, J. C. (1979). "Filtration of sediment by simulated vegetation I. Steady-state flow with homogeneous sediment." *Trans. American Soc. Agric. Eng* 22(3) 540-545,548.

Batchelor, G.K. (1973). *An introduction to fluid dynamics*, Cambridge University Press, Cambridge.

Borovkov, V. S. and Yurchuk, M. (1994) "Hydraulic resistance of vegetated channels." *Hydrotechnical Construction* 28(8) 432-438.

Cajori, F. (1946). *Sir Isaac Newton's mathematical principles of natural philosophy and his system of the world*, University of California Press, Berkeley.

Chow, V. T. (1959). *Open-Channel hydraulics*, 1st Ed., McGraw-Hill, New York.

Chow, V.T. (1964). *Handbook of applied hydrology*, 1st Ed., McGraw-Hill, New York.

Ghisalberti, M. and Nepf, H. M. (2002). "Mixing layers and coherent structures in vegetated aquatic flows." *J. Geophysical Res.* 107(C2) 3-1 – 3-11.

Kouwen, N., Unny, T. E. and Hill, H. M. (1969). "Flow retardance in vegetated channels." *J. Irrig. Drain. Eng.* 95 329-342.

Kouwen, N. and Li, R.M. (1980). "Biomechanics of vegetative channel linings." *J. Hydr. Eng.* 106(HY 6) 1085-1103.

Langeland, K. A. (1996). "*Hydrilla verticillata* (L.F.) Royle (Hydrocharitaceae), 'The perfect aquatic weed'." *Castanea* 61 293-304.

Lewandowski, J.A. (1993). "Vegetation resistance and circulation modeling in a tidal wetland." Doctor of Engineering dissertation, University of California, Berkeley.

Masser, M. P. (2006). Personal Communication, Department of Wildlife and Fisheries Sciences, Texas A&M University, College Station.

Mouret, G. (1921). "Antoine Chézy, histoire d'une formule d'hydraulique." *Annales des Ponts et Chaussées*, 1921-II.

Moustafa, M. M. (1997). "Verification of impermeable barrier depth and effective radius for drain spacing using exact solution of the steady state flow to drains." *Irrig. Drain. Sys.* 11(4) 283-298.

Nepf, H. M. and Vivoni, E. R. (2000). "Flow structure in depth-limited, vegetated flow." *J. Geophysical Res.* 105(C12) 28,547-28,557.

Prandtl, L. (1926). "Über die ausgebildete turbulenz (On fully developed turbulence). *Proc. of the 2d International Congress of Applied Mechanics*, 62-74.

Roberson, J. A. (1970). "Flow in conduits with low roughness concentration." *J. Hydr. Eng.* 96(HY 4) 941-957.

Roberson, J. A. and Crowe, C. T. (1980). *Engineering fluid mechanics*, 2nd Ed., Houghton Mifflin, Boston.

Roig, L. C. (1994). "Hydrodynamic modeling of flows in tidal wetlands." Ph.D. dissertation, University of California, Davis.

Rouse, H. and Ince, S. (1963). *History of hydraulics*, 1st Dover Ed., Dover Publications, New York.

Shepsis, V. (2008). Personal Communication, Coast & Harbor Engineering, Edmonds, WA.

Smart, R. M. and Barko, J. W. (1984). "Culture methodology for experimental investigations involving rooted submersed aquatic plants." *Misc. Paper A-84-6*, USACE Aquatic Plant Control Research Program, Vicksburg.

Strupczewski, W. G. and Szymkiewicz, R. (1996) "Analysis of paradoxes arising from the Chézy formula with constant roughness: I. Depth-discharge curve." *Hydr. Sci. – J. des Sci. Hydrologiques* 41(5) 659-673.

Thompson, G. T. and Roberson, J. A. (1976) "A theory of flow resistance for vegetated channels." *Trans. American Soc. Agric. Eng*. 19(2) 288-293.

Tritton, D.J. (1988). *Physical fluid dynamics*, 2nd Ed., Clarendon Press, Oxford.

USDA (US Department of Agriculture). (2005). "Image: *Spartina alterniflora*.jpg." Available: http://www.google.com/imgres?imgurl=http://upload.wikimedia.org/wikipedia/commons/thumb/7/7d/Spartina_alterniflora.jpg/800px-Spartina_alterniflora.jpg&imgrefurl=http://commons.wikimedia.org/wiki/Image:Spartina_alterniflora.jpg&h=515&w=800&sz=97&tbnid=4ymsjjTmrYcJ:&tbnh=92&tbnw=143&prev=/images%3Fq%3DSpartina%2Balterniflora&hl=en&sa=X&oi=image_result&resnum=1&ct=image&cd=1.

Wu, W., He, Zhiguo and Wang, S. Y. (2006) "Flow conveyance and sediment transport capacity in vegetated channels." *Proc. 7th Int. Conf. on Hydroscience and Engineering.*, 1-14.

Yen, B.C. (2002). "Open channel flow resistance." *J. Hydr. Eng.*, 128(1), 20-39.

APPENDIX A

VEGETATION DENSITY DATA

The photographs in this appendix are records of the vegetation density during flow testing in the greenhouse channel. As the same vegetation was used for multiple phases of testing, it was not feasible to remove the vegetation and weigh it. In addition, the goal of this project is to develop a relatively simple method for estimating vegetative impacts to flow. Therefore visual characterization of the vegetation was selected.

These photos were taken of hydrilla in the greenhouse channel on July 18, 2007 during the energy loss testing.

Photo 1 – Station 6; Water depth is 38 cm. This photo is taken at the channel bottom. Center of photo is approximately 5 cm off of the bottom. Vegetation density is characterized as light. The speckled gray visible behind the vegetation is the far channel wall (channel is 33 cm wide. Scale shown is a carpenter's level and is typically held against the far wall of the channel.	
Photo 2 – Station 6, WD=38cm. This photo is taken at an elevation of approximately 15 cm from the bottom. Vegetation density is characterized as medium.	
Photo 3 – Station 6 WD=38cm. This photo is taken at or near the surface. Vegetation density is characterized as dense.	

Photo 4 – Station 6 WD=38cm. This photo is taken at or near the surface. Vegetation density is characterized as dense. (Duplicate conditions/location to Photo 3)	
Photo 5 – Station 5 WD=39cm. This photo is taken at the bottom. Vegetation is characterized as sparse.	
Photo 8 – Station 5 WD=39cm. This photo is taken approximately 11cm off of the bottom. Vegetation is characterized as sparse.	

Photo 6 – Station 5 WD=39cm. This photo is taken approximately 17cm off of the bottom. The vegetation is characterized as medium.	
Photo 7 – Station 5 WD=39cm. Photo is taken near the surface. Vegetation is characterized as dense.	
Photo 9 – Station 4 WD=41cm. Photo is taken at the bottom. Vegetation is characterized as sparse.	

Photo 10 – Station 4 WD=41cm. Photo is taken at 17cm off of the bottom. Vegetation is characterized as sparse.	
Photo 12 – Station 4 WD=41cm. Photo is taken 14cm above the bottom. Vegetation is characterized as sparse.	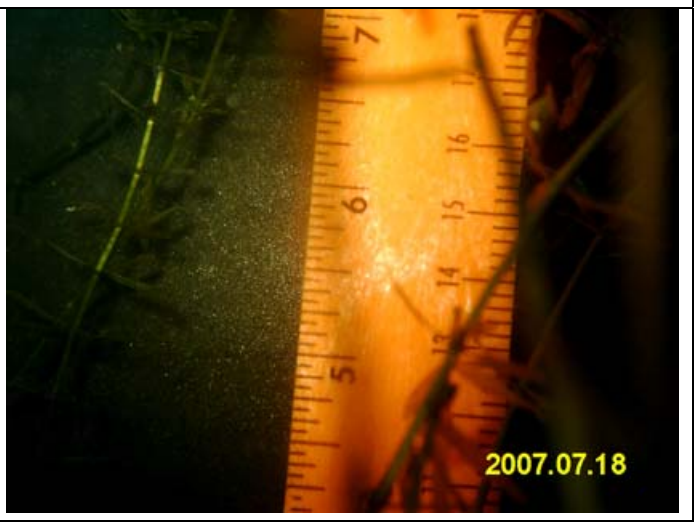
Photo 14 – Station 4 WD=41cm. Photo is taken 20 cm above the bottom. Vegetation is characterized as medium.	

Photo 13 – Station 4 WD=41cm. Photo is taken 23cm above bottom. Vegetation is characterized as light.	
Photo 11 – Station 4 WD=41cm. Photo is taken at surface. Vegetation is characterized as dense.	
Photo 15 – Station 3 WD=38cm. Photo is taken at bottom. Vegetation is characterized as sparse.	

Photo 16 – Station 3 WD=38cm. Photo is taken 14cm above bottom. Vegetation is characterized as sparse.	
Photo 19 – Station 3 WD=38cm. Photo is taken 17cm above bottom. Vegetation is characterized as sparse.	
Photo 17 – Station 3 WD=38cm. Photo is taken 25cm above bottom. Vegetation is characterized as medium.	

Photo 18 – Station 3 WD=38cm. Photo is taken at surface. Vegetation is characterized as dense.	
Photo 24 – Station 2 WD=39cm. Photo is taken at bottom. Vegetation is characterized as sparse.	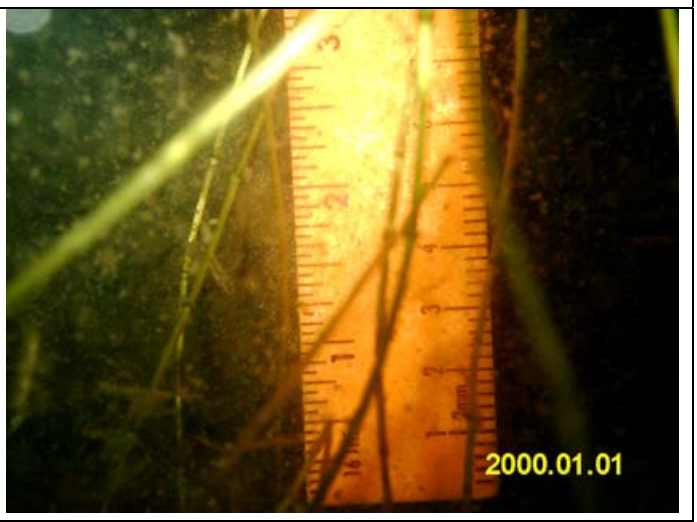
Photo 25 – Station 2 WD=39cm. Photo is taken 13cm above bottom. Vegetation is characterized as sparse.	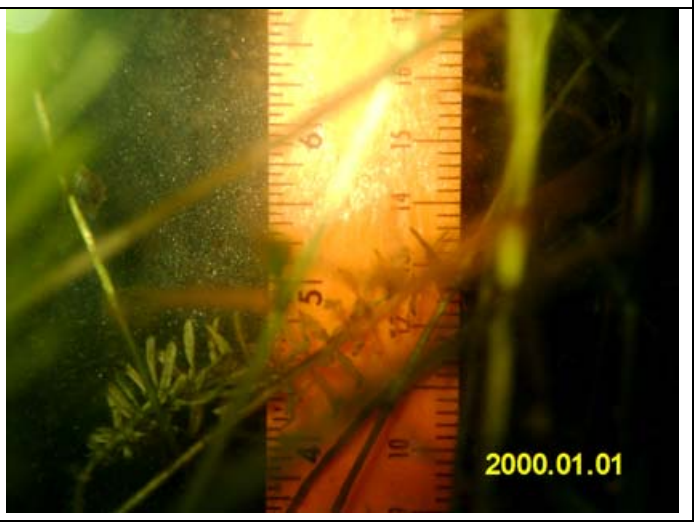

Photo 26 – Station 2 WD=39cm. Photo is taken 29 cm above bottom. Vegetation is characterized as light.	
Photo 27 – Station 2 WD=39cm. Photo is taken at surface. Vegetation is characterized as dense.	
Photo 20 – Station 1 WD=39cm. Photo is taken at bottom. Vegetation is characterized as sparse.	

Photo 21 – Station 1 WD=39cm. Photo is taken 10cm above bottom. Vegetation is characterized as sparse.	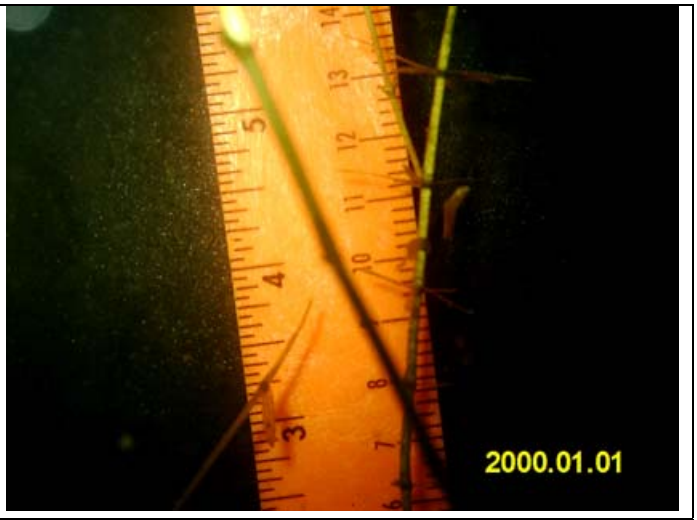
Photo 22 – Station 1 WD=39cm. Photo is taken 22cm above bottom. Vegetation is characterized as sparse.	
Photo 23 – Station 1 WD=39cm. Photo is taken at surface. Vegetation is characterized as sparse.	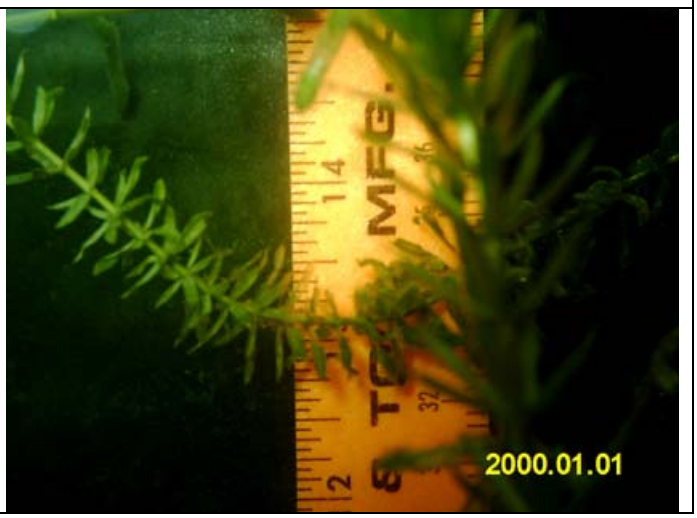

APPENDIX B

MISCELLANEOUS DATA

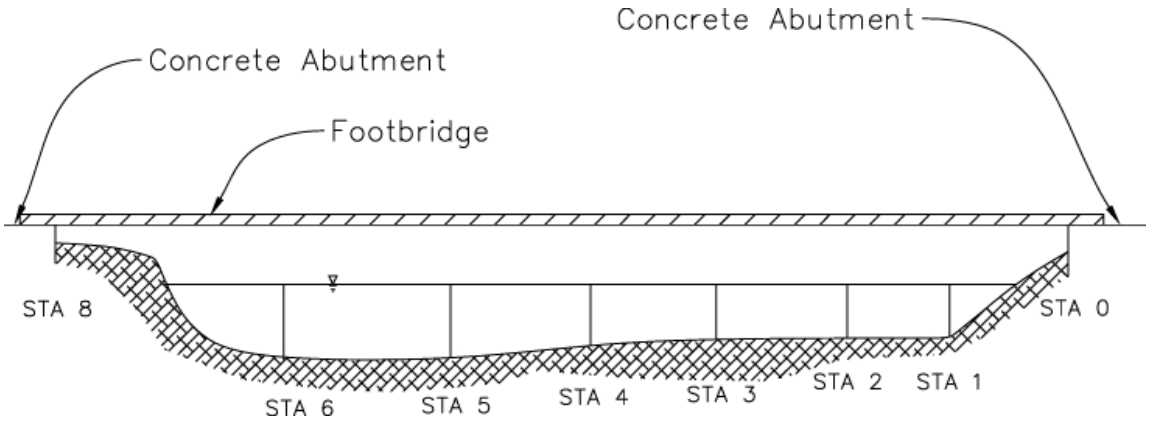

Station	Distance from Sta. 0 (meters)	Depth (meters)	Flow Velocity (m/sec)	Comments
0	0	N/A		
1	1.7	0.76	0.3	
2	3.1	0.76	0.5	
3	5.0	0.76	0.5	
4	6.8	0.84	0.7	no vegetation within 1 m
5	8.7	1.09	0.8	no vegetation within 1 m
6	11.1	1.09	0.4	
8	14.3	N/A		

Fig.B-1. Cross-section of NIC canal in Jamaica

HYDRILLA SAMPLE			
Number	**Weight (gm)**	**Length (cm)**	**Weight/Length (gm/cm)**
1	2.92	81.3	0.036
2	3.96	71.1	0.056
3	2.16	45.7	0.047
4	1.44	30.5	0.047
5	2.02	43.2	0.047
6	1.54	55.9	0.028
7	1.02	30.5	0.033
8	2.68	58.4	0.046
9	1.7	30.5	0.056
10	2.22	33.0	0.067
11	2.22	38.1	0.058
12	1.66	22.9	0.073
13	1.84	43.2	0.043
14	0.96	30.5	0.031
15	1.26	38.1	0.033
16	1.64	40.6	0.040
17	0.32	12.7	0.025
18	2.34	61.0	0.038
19	2.7	71.1	0.038
20	1.46	61.0	0.024
21	2.26	30.5	0.074
22	2.08	27.9	0.074
23	0.44	10.2	0.043
24	3.33	76.2	0.044
25	1.12	17.8	0.063
26	1.52	22.9	0.066
27	0.74	12.7	0.058
28	2.2	53.3	0.041
29	2.02	53.3	0.038
30	0.52	22.9	0.023

Fig.B-2. Data from evaluation of hydrilla stem weight per unit length of stem (Figure 4.9 in text)

	Vegetation Density		
	Light	Dense	Compacted
Flow Vel (cm/sec)	Surface Slope (mm/meter)	(mm/meter)	(mm/meter)
3.8	0.2		
4.6	0.3		
6.5	-0.9		
8.0	1.7		
3.8		1.6	
4.6		1.6	
6.5		2.1	
8.0		3.7	
2.1		0.1	
3.3		0.0	
4.5		0.8	
5.7		1.3	
2.1		0.0	
3.3		0.4	
4.5		1.7	
5.7		1.7	
3.8			2.1
4.6			3.1
6.5			4.0
8.0			5.4
3.8			2.9
4.6			2.2
6.5			4.1
8.0			5.9

Fig.B-2. Data from development of Figure 5.2 in text

Fig 5.5		Fig 5.6		Fig 5.6 (cont	
V (cm/s)	Elev (cm)	V (cm/s)	Elev (cm)	V (cm/s)	Elev (cm)
1.5	9	0.9	1	3.8	10.5
0.8	13	0.8	2	3.8	14
0.7	8	0.9	2	3.8	12.5
1.2	13	0.9	2.5	4.3	15.5
2.7	15	0.5	2.5	5.0	10.5
5.6	16	0.8	6	3.8	11
4.2	16	1.7	8	2.7	15
4.0	15	2.1	7.5	3.8	15.5
4.3	14	2.5	10	7.0	16
3.1	13.5	3.3	10.5	5.0	16
4.4	15	1.9	8	4.0	15
5.0	15	1.4	12	6.9	15
3.9	15	1.6	11	4.4	13.5
5.3	16	3.3	10.5	4.6	15.5
5.9	16	1.8	11.5	1.3	7.5
6.3	15	7.5	15		
1.7	8.5	2.7	14		
3.1	13	2.5	6.5		
2.9	13.5	7.5	14.5		
0.8	12	2.7	11		
2.4	12.5	5.0	14		
0.8	10.5	4.3	14		
1.5	10.5	6.0	15		
1.3	9	6.0	15		
1.3	9.5	7.5	15		
1.1	10.5	4.3	14.5		
1.3	8.5	2.5	11.5		
1.6	8	6.0	14.5		
0.8	6	4.3	13		
1.0	5.5	3.8	11.5		
2.0	4.5	4.3	14		
1.0	3	3.0	13		
0.8	1.5	1.5	15.5		
1.7	2	3.0	15.5		
0.9	3	5.0	13.5		
0.9	0.5	2.0	16		
		5.0	14		
		3.3	15.5		
		4.3	15.5		
		3.0	13.5		

Fig.B-3a. Data from development of figures referenced above

Fig 5.7		Fig 5.7 (cont)		Fig 5.8	
V (cm/s)	**Elev (cm)**	**V (cm/s)**	**Elev (cm)**	**V (cm/s)**	**Elev (cm)**
8.3	15	3.8	6	2.5	4.5
6.3	14	1.8	6.5	3.8	8
3.8	13	1.7	8.5	3.8	4.5
10.0	15	2.5	8.5	2.7	4
5.0	14	3.1	9	1.4	4
3.6	14	2.5	9.5	1.5	2
7.1	14	3.6	9	2.0	1
12.5	14.5	2.5	8	2.5	2
5.6	14	1.4	11	2.8	5
10.0	16	1.7	11	1.3	2.5
7.1	15	2.3	10	1.4	8
8.3	16	2.0	12.5	3.3	6.5
6.3	14.5	4.0	12	2.6	6.5
8.3	13	1.7	12	3.4	0.5
1.9	12.5	9.0	14.5	1.0	3.5
3.1	13.5	7.7	16	0.9	2.5
5.6	15	7.5	14	2.5	6.5
7.1	15	7.5	14	2.1	8
8.3	13.5	4.3	13	0.9	3
5.6	12.5	10.0	16	2.1	4.5
1.7	11.5	7.1	15	2.4	3
2.2	12	4.5	13.5	2.0	2.5
2.9	10	4.3	13.5	1.8	2.5
2.5	9	1.6	11	2.5	3.5
3.3	7.5	5.0	13.5	1.3	2.5
1.8	9	8.3	15.5		
2.5	8	5.0	13		
2.0	5.5				
2.0	2				
3.3	3.5				
2.1	3				
3.3	1.5				
1.7	3.5				
2.9	1.5				
2.5	0.5				
1.7	3.5				
1.2	3.5				
2.2	1.5				
4.3	4				
3.3	4.5				

Fig.B-3b. Data from development of figures referenced above

Fig 5.9		Fig 5.9 (cont)		Fig 5.10	
V (cm/s)	Elev (cm)	V (cm/s)	Elev (cm)	V (cm/s)	Elev (cm)
4.5	14	4.5	11	4.5	13
5.0	12	2.5	11	1.8	11.5
4.8	12	1.7	11.5	2.6	13
4.4	12	4.4	10	3.8	14
3.3	14	1.9	9.5	7.5	11
3.6	13	2.3	12	7.1	11
2.4	15.5	1.7	10.5	3.8	12.5
3.1	12	1.1	9	4.7	11.5
3.6	14.5	1.6	4	4.5	13.5
4.2	13.5	1.1	2	6.3	14
2.9	12	1.7	4	4.5	14
2.7	7	1.6	3	12.5	13
0.9	2	1.1	7	4.8	13
0.8	3	1.2	5	10.0	11
0.8	2	0.8	5	2.8	3
1.0	2	1.6	9	3.2	5
0.9	3	2.9	10	5.9	4
1.1	3	0.7	8	1.9	4
0.7	4	2.3	10	5.0	3
1.0	2	1.4	9	5.9	3.5
1.6	1	3.4	10	5.6	5
1.1	1.5	1.4	9	1.1	3.5
1.4	4.5	3.6	11	0.9	2
1.2	2.5			3.8	3
0.9	3			1.9	2
0.6	2			2.0	0.5
1.0	2.5			2.0	0.5
0.9	3			2.7	4
0.9	2.5			6.4	11
0.7	3			5.0	9
0.5	3.5			7.5	9
0.9	3.5			6.0	9
0.8	4			6.7	9
1.0	3			6.0	10
6.4	14			6.7	8.5
2.2	15			6.7	8
5.3	15			6.0	7.5
3.3	14			1.8	6
3.0	13.5			3.0	9
2.4	11			8.6	9

Fig.B-3c. Data from development of figures referenced above

Fig 5.10 (cont)		Fig 5.10 (cont)		Fig 5.10 (cont)	
V (cm/s)	**Elev (cm)**	**V (cm/s)**	**Elev (cm)**	**V (cm/s)**	**Elev (cm)**
7.5	8.5	3.8	13.5	3.8	14
5.0	8	1.7	14	12.0	16
6.0	7.5	4.3	14	10.0	13
5.0	9	6.7	13	7.5	14
7.5	10	3.0	13	5.0	13
1.6	9.5	3.8	13		
2.0	9.5	6.0	14		
2.7	9	8.6	16		
6.0	9	10.0	16		
2.0	9	4.3	15		
2.1	8	10.9	14		
4.3	8	7.5	14		
5.0	4	4.3	13.5		
5.0	8	4.3	14		
3.8	7	3.0	13		
3.3	7	3.3	14		
3.8	5	4.3	14		
5.0	8	5.0	14.5		
1.9	7.5	5.0	14		
2.7	7.5	7.5	12		
1.8	7.5	6.0	11		
6.0	8	10.0	12		
5.5	7	10.0	12		
3.3	5.5	10.0	13		
3.3	5	6.0	13.5		
3.3	6	5.0	14		
2.0	6	5.0	13.5		
3.3	8	5.0	13.5		
2.0	6	5.0	14		
4.3	7	5.0	13		
3.0	8	5.0	14		
1.2	6	4.3	14		
3.3	6	6.0	14.5		
4.3	12	12.9	16		
5.0	14	5.0	14		
6.0	14	6.0	14		
4.3	13	3.3	14		
3.3	13	15.0	16		
6.0	14	3.8	13		
15.0	15	5.0	13		

Fig.B-3d. Data from development of figures referenced above

VITA

Larry Ralph Demich received his Bachelor of Science degree in civil engineering from Washington State University in 1983. He received the Master of Science degree in applied ocean sciences from the Department of Applied Mechanics and Engineering Sciences at the University of California at San Diego in 1990. He entered the Biological and Agricultural Engineering program at Texas A&M University in 1997 and graduated with the Ph.D. in August 2008.

In the interim between receiving his B.S. degree and returning to school for the M.S. degree Mr. Demich worked as an engineer for the Washington State Department of Transportation and for Washington State Ferries. Subsequent to receiving the M.S. degree, he worked for a number of firms including Makai Ocean Engineering on Oahu, Hartman Associates in Seattle and Moffatt & Nichol Engineers in Long Beach, California. After completing his coursework at Texas A&M University, Mr. Demich returned to the private sector, working for Sverdrup Civil and then Jacobs Civil in the Seattle area. Since 2001, he has operated Demich Engineering in the Seattle area and divided his time between consulting and completing his education. Mr. Demich's research interests include the functioning of hydraulic, sedimentary and ecosystem processes in aquatic systems, both natural and manmade. Mr. Demich holds professional engineering licenses in Washington State and California.

Mr. Demich may be reached at 3033 NE 201st Place, Lake Forest Park, WA 98155. His email address is: larrydemich@demicheng.com. His office phone number is: 206 363 1216.